WL-TR-97-4117

KINETIC MODELING OF FLAME SUPPRESSION

A Report on the MLBT Halon Replacement Initiative, Including the Third Wright Laboratory Symposium on Halon Replacements

Harvey L. Paige
Materials Directorate
WPAFB, OH 45433

George A. Petersson
Wesleyan University
Middletown, CT 06459

Paul Marshall
University of North Texas
Denton, TX 76203

NOVEMBER 1997

FINAL REPORT FOR PERIOD OCTOBER 1993 - SEPTEMBER 1997

MATERIALS DIRECTORATE
AIR FORCE RESEARCH LABORATORY
AIR FORCE MATERIEL COMMAND
WRIGHT-PATTERSON AIR FORCE BASE, OH 45433-7734

NOTICE

USING GOVERNMENT DRAWINGS, SPECIFICATIONS, OR OTHER DATA INCLUDED IN THIS DOCUMENT FOR ANY PURPOSE OTHER THAN GOVERNMENT PROCUREMENT DOES NOT IN ANY WAY OBLIGATE THE US GOVERNMENT. THE FACT THAT THE GOVERNMENT FORMULATED OR SUPPLIED THE DRAWINGS, SPECIFICATIONS, OR OTHER DATA DOES NOT LICENSE THE HOLDER OR ANY OTHER PERSON OR CORPORATION; OR CONVEY ANY RIGHTS OR PERMISSION TO MANUFACTURE, USE, OR SELL ANY PATENTED INVENTION THAT MAY RELATE TO THEM

THIS REPORT IS RELEASABLE TO THE NATIONAL TECHNICAL INFORMATION SERVICE (NTIS). AT NTIS, IT WILL BE AVAILABLE TO THE GENERAL PUBLIC, INCLUDING FOREIGN NATIONS.

THIS TECHNICAL REPORT HAS BEEN REVIEWED AND IS APPROVED FOR PUBLICATION.

HARVEY L. PAIGE
Laboratory Task Manager
Halon Replacement Research Initiative
Safe, Cost-Effective Alternative
Materials and Processes Program

WAYNE E. WARD
Chief
Nonstructural Materials Branch

ROBERT L. RAPSON
Chief
Nonmetallic Materials Division

IF YOUR ADDRESS HAS CHANGED, IF YOU WISH TO BE REMOVED FROM OUR MAILING LIST, OF IF THE ADDRESSEE IS NO LONGER EMPLOYED BY YOUR ORGANIZATION, PLEASE NOTIFY WL/MLBT, BUILDING 654, 2941 P STREET, WRIGHT-PATTERSON AFB OH 45433-7750 TO HELP MAINTAIN A CURRENT MAILING LIST

Do not return copies of this report unless contractual obligaions or notice on a specific document requires its return.

REPORT DOCUMENTATION PAGE

Form Approved
OMB No. 0704-0188

1. AGENCY USE ONLY *(Leave blank)*	2. REPORT DATE	3. REPORT TYPE AND DATES COVERED
	November 1997	Final, From October 1993 to September 1997

4. TITLE AND SUBTITLE
Kinetic Modeling of Flame Suppression: A Report on the MLBT Halon Replacement Initiative, Including the Third Wright Laboratory Symposium on Halon Replacements

5. FUNDING NUMBERS
PE 61102F
PR 2303
TA DW
WU 3F

6. AUTHOR(S)

Harvey L. Paige
Materials Directorate
WPAFB, OH 45433

George A. Petersson
Wesleyan University
Middletown, CT 06459

Paul Marshall
University of North Texas
Denton, TX 76203

7. PERFORMING ORGANIZATION NAME(S) AND ADDRESS(ES)
AFRL/MLBT, Bldg 654
2941 P St, Ste 1
Wright-Patterson AFB, OH 45433-7750

8. PERFORMING ORGANIZATION REPORT NUMBER

9. SPONSORING/MONITORING AGENCY NAME(S) AND ADDRESS(ES)
Materials Directorate
Wright Laboratory
Air Force Materiel Command
Wright-Patterson AFB OH 45433-7734
POC: Harvey L. Page, WL/MLBT, 937-255-9038

10. SPONSORING/MONITORING AGENCY REPORT NUMBER
WL-TR-97-4117

11. SUPPLEMENTARY NOTES

12a. DISTRIBUTION AVAILABILITY STATEMENT
Approved for Public Release; Distribution Unlimited

12b. DISTRIBUTION CODE

13. ABSTRACT *(Maximum 200 words)*

This report documents kinetic modeling work performed under the auspices of the Center for Computational Modeling of Nonstructural Materials, AFRL/MLBT, Wright-Patterson AFB, OH over the period from Ocotber 1993 to September 1997. Many of the results of this work were summarized at the Third Wright Laboratory Symposium on Halon Replacements, held at Wright-Patterson AFB from 22 to 24 July 1997. Included herein is a summary of in-house research and collaborative research with university associates and a review of other selected published work on halon replacements. Also included are abstracts or extended abstracts of presentations at the July Symposium, which brought together leaders in the fields of quantum mechanics, computational chemistry, and kinetic modeling to discuss the present understanding of the reactions of halon and its suggested and potential replacements.

14. SUBJECT TERMS
halon replacements, fluorocarbons, halofluorocarbons, reaction mechanisms, thermodynamics, kinetics, computational chemistry, transition states, flame suppression

15. NUMBER OF PAGES
96

16. PRICE CODE

17. SECURITY CLASSIFICATION OF REPORT	18. SECURITY CLASSIFICATION OF THIS PAGE	19. SECURITY CLASSIFICATION OF ABSTRACT	20. LIMITATION OF ABSTRACT
UNCLASSIFIED	UNCLASSIFIED	UNCLASSIFIED	SAR

Table of Contents

Preceding Page Blank

I. Introduction

Halon compounds such as CF_3Br (halon 1301) and CF_2ClBr (halon 1211) have been employed extensively in fire extinguishers because they exhibit many desirable properties: they are efficient, inexpensive, non-toxic (which is critical to their application in areas which must remain occupied after use such as aircraft cockpits), non-corrosive (and therefore do not damage electronic and other sensitive equipment) and are easily dispersed at the site of the fire. Unfortunately, these halons have an adverse environmental impact. Because of their lack of chemical and photochemical activity in the lower atmosphere, they survive to diffuse into the stratosphere where Br and Cl atoms are released by photolysis and participate in catalytic cycles that destroy ozone:[1,2]

$$X + O_3 \rightarrow XO + O_2 \quad (X = Br, Cl)$$
$$XO + O \rightarrow O_2 + X$$

The Br cycle is particularly efficient, making halons a serious threat to the protective ozone layer. The Montreal Protocol on Substances that Deplete the Ozone Layer ("Montreal Protocol"), is a treaty that was signed in 1987 and ratified by the United States Senate in 1988. The implementation of this treaty, and subsequent Amendments and Adjustments, specifically the Copenhagen Agreement of 1992, banned the production of halons as of 1 January 1994. Even before the halt to production, significant efforts were underway to find alternatives to halons, particularly halon 1301, which had been vital for Air Force applications from computer rooms and chemical storage facilities to engine nacelles and dry bays, and for fuel tank inerting. In the case of the aircraft applications, for which fully satisfactory replacements have not been found, "banked" halons continue to be used. The Air Force has recognized that replacements will be needed for these applications and efforts to find such replacements are continuing.

Fire suppression agents may act in several ways. In a flame, fuel and oxygen react via chain reactions involving highly reactive radical intermediates such as H, OH and O. These radicals are initially formed in an ignition step, for example by dissociation of fuel or oxygen molecules from a spark or high temperatures. The radicals may be lost through recombination reactions such as

$$H + OH \rightarrow H_2O,$$

but the flame is sustained provided the rate of oxidation and radical production (which increase with temperature and concentration) is high enough to replenish the radical pool. Fire suppression mechanisms may be classified as physical or chemical. Physical actions include smothering i.e. separating fuel and air, and cooling and dilution, which can lower the rates of flame reactions to the point that combustion is no longer sustained. All extinguishing agents exhibit some degree of physical action, but halons are particularly effective because of their chemical action, where they interfere with the combustion

chemistry, by accelerating (catalyzing) chain termination reactions. Catalytic activity is a desirable agent property, because small amounts of agent can remove many radicals. The detailed chemical mechanisms are, however, often incompletely understood.

The Air Force Office of Scientific Research (AFOSR) supports long range research on topics of particular interest to the military. Under AFOSR auspices, the personnel and collaborators of the Center for Computational Modeling of Nonstructural Materials at Wright-Patterson Air Force Base have been conducting basic research on the mechanisms of action of halon replacements since 1993. Significant progress has been made, exemplified by the publications listed at the end of Section III of this report. One of the concluding activities of this research effort was the Third Symposium on Halon Replacements which was held at Wright-Patterson AFB in July 1997 to bring together leaders in the field. Based on the symposium, this report summarizes our understanding of halons and potential substitutes, methods for analysis of their action in flames, and recommendations for future focus.

---

1. Molina, M. J., and F. S. Rowland, "Stratospheric sinks for chlorofluoromethanes. Chlorine atom catalyzed destruction of ozone," *Nature*, **249**, 810 (1974).

2. Wayne, R. P., *Chemistry of Atmospheres* , Clarendon Press, Oxford, England (1985) Ch. 4.

II. Background

Fire suppression devices employing halogenated hydrocarbons, especially CCl_4, have been in use since the early 1900s, when inexpensive chlorine from the electrolysis of brine became available. Methyl bromide also entered the fire suppression market by the 1920s and was found to be more effective, but more toxic.[1] The ability of certain chemical species to suppress flames was well known during the Second World War, but it was poorly understood.

> "They [halocarbons] possess also a very valuable property in that they have an inhibitory action on combustion, that is to say the extinctive action is greater than can be accounted for by dilution of oxygen of the atmosphere by their vapours, allowing for the specific heat of the latter."[2]

Parenthetically, it was also known in 1948 that other chemical species were capable of suppressing flames. Included in this category were borates, sulfates, phosphates, silicates, carbonates, and tungstates, and salts of ammonium ion, antimony, bismuth, tin, aluminum, zinc, and iron.[2]

In 1948, the U. S. Army started the search for chemical flame suppressants that would have the effectiveness of carbon tetrachloride and methyl bromide, but with reduced toxicity. These, and related studies, lead to the adoption of halons (primarily 1301 and 1211) for military applications.[1] As the use of these materials grew, concerns about agent and by-product toxicity, and the related questions about appropriate usage scenarios, arose. A 1972 symposium organized by the National Academy of Sciences emphasized appropriate usage of the halons and agent toxicity.[3] A second symposium, in 1975, was organized by Dr. R. G. Gann of the Naval Research Laboratory to investigate the state of knowledge of halon reaction mechanisms.[4]

The earliest explicit Air Force acknowledgment of the environmental consequences of the use of halons appears to be in a Technical Report dated July, 1987, covering work from August, 1985 to August, 1986.[5] By 1987, the Air Force had concluded that the use of halons would need to be curtailed and provided support for inclusion of halons in the controls to be set forth in the Montreal Protocol.[6]

In 1988, an article by an Air Force officer and a contractor set forth the extant situation, including problems, with existing halons and outlined possible solutions to the problems. This paper, reprinted as a part of a Technical Report[7], detailed many of the limitations of existing and probable replacements. A number of other issues also surfaced, such as global warming potentials, that are now frequently discussed. Since that 1988 report, a search of the Defense Technical Information Center (DTIC) database shows a total of 74 Air Force-sponsored technical reports published on various aspects of halon, with five

additional reports in various stages of editing. There are also 20 Army-sponsored reports, 21 from the Navy, 10 from the Federal Aviation Administration, and 2 sponsored by DARPA. Many of these, especially before 1990, did not acknowledge the environmental problems associated with halon. More recently, nearly all such reports are found to be driven by environmental and health considerations. There are, in addition, a large number of papers, reports, and books in the open literature detailing environmental and health concerns related to fire suppression by halon or its proposed replacements.

The Air Force was the lead agency in a joint Air Force, Army, Federal Aviation Administration and Navy effort established in October of 1993 to find a near-term replacement for halon 1301. A Small Business Innovative Research (SBIR) effort considered six hundred potential suppression agents. The list was narrowed to ten compounds for further testing, all of which were fluorocarbon-based.[8,9] A more widely-circulated publication from the National Institute of Standards and Technology (NIST) lists 103 substances, 35 of which were not fluorocarbon-based.[10] The information in these two reports was the basis for a final list of 12 substances which would be subjects of additional laboratory and large scale testing. This work, in turn, resulted in the list being reduced to four potential agents, and then to a single compound. The "Halon Replacement Program for Aviation" has now published reports detailing the operational parameters that most influence flame extinguishment in dry bays[9] and engine nacelles[11]. These parameters were monitored in extensive large-scale tests that selected HFC-125, C_2F_5H, as the extinguishant for dry bay[12] and engine nacelle[13] fire protection. This compound, like most of the replacement agents tested, is primarily a physically-acting agent. Thus, in addition to its limited flame inhibition capability, there is a weight and volume penalty associated with its use. The magnitude of this penalty will be better understood upon publication of the Phase III reports of the project.[14]

A recent report by the National Research Council stated as a key finding: "It is unlikely that a drop-in replacement agent will be discovered that will exhibit all of the beneficial properties of halon 1301 and not also exhibit a significant environmental impact."[15] The near-term replacement, HFC-125, while not capable of causing ozone depletion, has an environmental impact by virtue of its global warming potential. With an atmospheric lifetime estimated to be 36 years, and strong absorption bands in the 8 to 12 mm spectral window, large quantities of C_2F_5H in the atmosphere are undesirable.[16] Another of the four agents tested, CF_3I (halon13001) exhibits similar effectiveness to CF_3Br (halon 1301), with zero ozone depletion and global warming potentials. Its disadvantageous impact is in the human environment. It has exhibited moderate to high toxicity, mutagenicity potential, and cardiac sensitization in canine subjects,[17] so it is not presently being considered by the DoD Halon Alternatives working Group. In some applications powders such as $NaHCO_3$ (sodium bicarbonate) and water mists are effective halon substitutes. For aircraft applications, they are too "dirty" (leaving damaging deposits on surfaces) or heavy, or both.

Thus, in spite of massive efforts, the goal of a suitable replacement has eluded all workers. In the recent book on halon replacements, it is stated that "...the research and testing community has evaluated all of the obvious and some of the not so obvious replacement compounds and has found that all of them are lacking for one reason or another...."[18] It is in this context that the research described in Section III of this report was undertaken.

---

1. Ford, C. L., pp. 1 ff, in *Halogenated Fire Suppressants*, R. G. Gann, Ed., American Chemical Society, Washington, D. C. (1975).

2. Cameron, A. M., *Chemistry in Relation to Fire Risk and Fire Extinction*, Sir Issac Pitman and Sons, Ltd., London, England, (1948).

3. "An Appraisal of Halogenated Fire Extinguishing Agents," W. J. Christian and R. C. Wants, Eds., National Academy of Sciences, Washington, D. C. (1972).

4. Gann, R. G., Ed., *Halogenated Fire Suppressants*, American Chemical Society, Washington, D. C. (1975).

5. Tapscott, R. E., and E. T. Morehouse, Jr., "Next-Generation Fire Extinguishing Agents, Phase I -- Suppression Concepts," ESL Technical Report 87-03 (DTIC No. AD-A192 279) (1987).

6. Anderson, S. O., K. L. Metchis, and R. Rubenstein, p.10, in *Halon Replacements*, A. W. Miziolek and W. Tsang, Eds., American Chemical Society, Washington, D. C. (1995).

7. Anderson, S. O., M. J. Ryan, J. L. Walker, R. E. Tapscott, and E. T. Morehouse, Jr., "Halons, Stratospheric Ozone, and the U. S. Air Force," ASC Technical Report 94-9251 (DTIC No. AD B192 467) (1988)

8. Zallen, D. M., "Halon Replacements Study," WL Technical Report 94-5032 (DTIC No. AD-B194 978) (1994).

9. Poole, B. A., and J. A. Wheeler, "Halon Replacement Program for Aviation, Dry Bay Application Phase II, WL-TR-97-3075 and WL-TR-97-3076.

10. Pitts, W. M., M. R. Nyden, R. G. Gann, W. G. Mallard, and W. Tsang, "Construction of an Exploratory List of Chemicals to Initiate the Search for Halon Alternatives," NIST Technical Note 1279 and NTIS PB91-107508, National Technical Information Service, Springfield, VA (1990).

11. WL Technical Report 95-3077 (In Preparation).

12. WL Technical Report 97-3075 (In Preparation).

13. WL Technical Report 97-3076 (In Preparation).

14. WL Technical Report 97-3066 and SURVIAC Technical Report 97-028 (In Preparation).

15. *Fire Suppression Substitutes and Alternatives to Halon for U. S. Navy Applications,* National Research Council, Washington, D. C. (1997).

16. Wuebbles, D. J., P. S. Connell, and K. O. Patten, p.69, in *Halon Replacements*, A. W. Miziolek and W. Tsang, Eds., American Chemical Society, Washington, D. C. (1995).

17. Tapscott, R. E., S. R. Skaggs, and D. Dierdorf, pp. 152-154, in *Halon Replacements*, A. W. Miziolek and W. Tsang, Eds., American Chemical Society, Washington, D. C. (1995).

18. Miziolek, A. W., W. Tsang, and J. T. Herron, p. 2 in *Halon Replacements*, A. W. Miziolek and W. Tsang, Eds., American Chemical Society, Washington, D. C. (1995).

III. Halon Related Studies at the Center for Computational Modeling of Nonstructural Materials

The Center and associated external collaborators have attacked the problem of finding halon replacements at several levels. As outlined below, these efforts include development of new methods for accurate thermochemical predictions and the analysis of potential energy surfaces to determine reactivity via quantum mechanical computations, experimental measurements of thermochemistry and kinetics, and development of global reaction mechanisms for the action of catalytic flame suppressants.

III. A. Thermochemistry

The thermochemistry and reaction kinetics of halogenated hydrocarbons have been investigated by *ab initio* methods in order to improve our understanding of their flame chemistry and likely roles in flame suppression. Bond additivity corrections at the G2, G2(MP2), CBS-4, and CBS-Q levels of theory were developed for fluorinated and chlorinated C_1 and C_2 species, including saturated and unsaturated compounds. The resulting enthalpies of formation are in excellent agreement with experimental values.

III. A. 1. *Ab Initio* Calculations

Advances in computational methods and computer hardware have made possible the accurate *ab initio* calculation of molecular energies including electron correlation for small and medium-size molecules. The accurate description of molecular wave functions requires the convergence of both the one-particle expansion (basis set) and the *n*-particle expansion (correlation energy). Currently available configuration interaction and coupled-cluster methods allow inclusion of the most important terms in the *n*-particle expansion, leaving basis set truncation as the primary source of error in the accurate calculation of molecular energies.

The slow convergence of the correlation energy with the one-electron basis set expansion has provided the motivation for several attempts to extrapolate to the complete basis set limit.[1-8] Such extrapolations require a well defined sequence of basis sets, and a model for the convergence of the resulting sequence of approximations to the correlation energy. The various extrapolation schemes that have been proposed differ in the method used to obtain a well defined sequence of one-electron basis sets. The complete basis set (CBS) extrapolations described in this report employ the asymptotic convergence of pair natural orbital (PNO) expansions.

A series of papers[3-5] demonstrated the N^{-1} asymptotic convergence of second-order pair correlation energies[9] calculated with the leading N pair natural orbitals:[10]

$$\lim_{N\to\infty} e_{ij}^{(2)}(N) = e_{ij}^{(2)}(\infty) + (25/512)|S|_{ij}^{2}\left(N+\delta_{ij}\right)^{-1} \qquad (1)$$

and the modification necessary to extrapolate infinite-order (*e.g.* QCISD) pair energies:

$$\lim_{N\to\infty} e_{ij}^{(\infty)}(N) = e_{ij}^{(\infty)}(\infty) + \left(\sum_{\mu=1}^{N} C_{\mu_{ij}}\right)^{2}\left[e_{ij}^{(2)}(N) - e_{ij}^{(2)}(\infty)\right] \qquad (2)$$

where the $C_{\mu_{ij}}$'s are obtained from the first-order wave function, $\psi^{(1)}$, after diagonalization of the coefficient matrix over virtual orbital pairs, $C_{ab}^{(1)}$, for each occupied pair *ij*:

$$\psi_{ij}^{(1)}(N) = C_0\Phi_0 + \sum_{a=a'=2}^{N} C_{aa',ij}^{(1)}\Phi_{ij}^{aa'} \qquad (3)$$

The interference factor, $\left(\Sigma\, C_\mu\right)^2$, is the square of the trace of the first-order wave function. This interference effect accounts for the rapid convergence with basis set associated with the slow convergence with order of perturbation theory in species such as a beryllium atom that have HOMO - LUMO near degeneracies.[5]

These asymptotic results were subsequently[11-15] used to develop practical methods for extrapolating finite basis set calculations to obtain estimates of the complete basis set (CBS) limit. The precise CBS extrapolation algorithm that has been implemented in the commercially available computer program Gaussian 94 has been described in detail.[16-18] The extrapolated CBS energy is size-consistent and will approach the exact energy as the basis set employed in the numerical calculations is systematically improved.

A *theoretical model chemistry* is a complete algorithm for the calculation of the energy of any molecular system.[19] It cannot involve subjective decisions in its application. It must be size consistent so that the energy of every molecular species is uniquely defined. A model chemistry is useful if for some class of molecules it is the most accurate calculation we can afford to do. A simple model chemistry employs the same basis set for each of the energy components (*i.e.* geometry, zero-point vibrational energy, and each component of the electronic energy: SCF, MP2, MP3, *etc.*).[9, 20, 21] A compound model chemistry employs different basis sets for each of the energy components. The earliest examples used a low level of correlation energy and a small basis set for the geometry and ZPE, since these calculations require multiple gradient and curvature calculations.[22-28] The electronic energy is then determined with a higher level of correlation energy and a larger basis set: Energy[Method(1)]//Geometry [Method(2)]. A popular example is the MP2/6-31G**//UHF/3-21G* compound model.[29]

The accurate calculation of molecular energies requires convergence of both the one-particle (basis set) expansion and the n-particle (CI, perturbation, or coupled-cluster) expansion. However, the order-by-order contributions to chemical energies, and thus the number of significant figures required, generally decrease with increasing order of perturbation theory. Concomitant with the decreasing contributions, the computational demands increase rapidly for the higher-orders of perturbation theory[30]. These two complementary trends combine to dictate that efficient computational models should employ smaller basis sets for the higher-orders of perturbation theory.

Once the treatment of the higher-order terms has been selected, we require procedures for the geometry, zero-point energy, SCF energy, and MP2 energy that are compatible with the higher-order treatment in both accuracy and speed. The general approach for both the CBS-n and G2 models[17, 31-34] is to first determine the geometry and ZPE at a low level of theory, and then perform a high level single point electronic energy calculation at this geometry using large basis sets for the SCF calculation, medium basis sets for the MP2 calculation, and small basis sets for the higher-order calculations. The components of each model have been selected to be balanced so that no single component dominates either the computer time or the error. The CBS-n models employ the above asymptotic extrapolation to reduce the error from truncation of the basis sets used to calculate the correlation energy. The compound model single point energy is evaluated at a geometry determined at a lower level of theory (*e.g.* CBS-4//UHF/3-21G or G2//MP2/6-31G*),[17, 31-34] which we shall reexamine when we consider transition states.

Any chemical process can be viewed as a combination of adding or removing electrons and making or breaking chemical bonds. We can therefore evaluate the reliability of any model chemistry by calibrating the accuracy for electron affinities (EA's), ionization potentials (IP's), and atomization energies S D_0's. Proton affinities (PA's) must also be included since the neutral molecules that would give a protonated species after loss of an electron are often unstable. We have elected to use the "G2 test set" introduced by Curtiss, Raghavachari, and Pople.[34] This test set of 147 atoms, molecules, and ions provides 125 chemical energy differences of all four types and includes a wide range of molecular structure.

The CBS-QCI/APNO model shows the best performance with this test set of any general theoretical model proposed to date, with a mean absolute deviation (MAD) from experiment of 0.53 kcal/mol. Of the models defined for both the first- and second-row elements, the CBS-Q model gives the greatest accuracy (MAD = 1.01 kcal/mol), followed by G2 theory (MAD = 1.21 kcal/mol), G2(MP2) theory (MAD = 1.59 kcal/mol), and finally the CBS-4 model (MAD = 1.98 kcal/mol). All are at or under the accuracy of ~2 kcal/mol required for meaningful thermochemical predictions.

Each of the CBS models has a range of molecular size for which it is the most accurate computational model currently available. Absolute computer times are of course dependent on the particular versions of the hardware and software used, but the relative times are of more general significance. The CBS-4, CBS-Q, and CBS-QCI/APNO models form a convenient sequence of cost-effective models, each successive member of which reduces both the RMS error and the maximum accessible molecular size by a factor-of-two. We recommend this sequence as a standard set of tools for the study of chemical problems, using the highest level model that is practical for each application.

Data comparing a wide variety of thermochemical models have been given by Foresman and Frisch.[30] We repeat a small subset of their results in Table I below to illustrate several elementary, but important points. First, we note that *ab initio* calculations are not necessarily *good* calculations. Even with large basis sets, Hartree-Fock calculations are inferior to the better semiempirical calculations.[35] Electron correlation is important for thermochemistry.

Using the same level of theory for the geometry, zero-point vibrational energy, and electronic energy, as in MP2/6-311+G(2d,p), provides a model that is inferior to the fourth-order CBS-4 compound thermochemical model in *both* speed and accuracy. To develop faster models, we are inclined to employ gradient corrected density functional methods[36] such as Becke's three parameter exchange functional[37] with the Lee, Yang, and Parr correlation functional.[38] The 6-31+G(d,p) basis set gives good results at modest cost, and continues our CBS-QCI/APNO, CBS-Q, CBS-4 sequence with an additional doubling of the error while extending the range (with HF/3-21G* geometries and ZPEs) to molecules twice as large. Such calculations probably represent the limiting speed for useful thermochemical predictions. Local DFT methods as presently formulated (*e.g.* SVWN5)[39] offer no advantage in accuracy over semiempirical methods.

Ideally, a computational model chemistry should not only provide chemical energy differences, but it should also provide a realistic estimate of the uncertainty. The 125 examples in the G2 test set have been used to determine the approximate shapes of the distribution functions for the errors from the CBS-4, CBS-Q, G2(MP2), G2, and CBS-QCI/APNO models. The results[17] are quite striking - none of the six models shows a statistically significant deviation from a Gaussian distribution function, indicating that the RMS errors for the G2 test set can be used in the same way that experimental uncertainties are used to assess reliability. Nevertheless, the possibility of relatively large errors in cases with high symmetry (or in large molecules) should be recognized for any computational model chemistry. The largest errors uncovered to date[17] for the CBS-4, G2(MP2), and G2 models are all more than four standard deviations measured with the G2 test set. On the other hand errors in individual bond dissociation energies are generally smaller than errors

Table I. Summary of error measurements (kcal/mol) for the G2 test set of 125 chemical energy differences.

Type	Model Chemistry	MAD	Max. Error
ab initio	CBS-QCI/APNO	0.5	1.5
	CBS-Q	1.0	3.8
	G2	1.2	5.1
	G2(MP2)	1.6	6.2
	CBS-4	2.0	7.0
	MP2/6-311+G(2d,p)	8.9	39.2
	HF/6-311+G(2d,p)	46.1	173.8
DFT	Becke3LYP/6-311+G(3df,2df,2p)	2.7	12.5
	Becke3LYP/6-31+G(d,p)//HF/3-21G*	3.9	33.9
	SVWN5/6-311+G(2d,p)	18.1	81.0
Semiempirical	AM1	18.8	95.5

in atomization energies.[40]

Within an isoelectronic sequence, errors can be sufficiently constant to permit empirical corrections. For example, the CBS-4 model consistently overestimates singlet-triplet gaps in carbenes by ~1 kcal/mol.

III. A. 2. Bond Additivity Corrections

An isodesmic reaction conserves the number of bonds of each order between each pair of atom types. For example, the reaction:

$$H_2C{=}C{=}CH_2 + CH_4 \rightarrow 2\ H_2C{=}CH_2 \qquad (4)$$

preserves two carbon-carbon double bonds and eight C-H bonds. If the error in the calculated bond energy were constant for each type of bond and these errors were exactly additive, then the calculated enthalpy change for an isodesmic reaction would be exact. In our example, if the heats of formation of ethylene and methane are known more accurately than the heat of formation of allene, then the calculated enthalpy change for equation (4) can be used to determine the heat of formation of allene.

Alternatively, we can determine the error, Δ_{ij}, in each bond *ij* and add these *bond additivity corrections* (BAC's) to obtain the total correction to the heat of formation:

$$\Delta_f H(BAC) = \sum_{ij} n_{ij} \Delta_{ij} \qquad (5)$$

n_{ij} is the number of bonds *ij*. Such isodesmic bond additivity corrections have already been used to advantage in correcting G2 and CBS-n heats of formation for halocarbons,[41] and Melius has made detailed studies[42, 43] of the behavior of more general BACs. Corrections for such systematic errors will become more important as it becomes possible to apply *ab initio* models to larger and larger molecules. Table II illustrates the potential power of such methods in an ideal case. To achieve comparable results in general we will have to understand the effects on BACs of such variables as hybridization, bond order, and charge.

Table II. Convergence of the calculated heat of formation of propane (an ideal example) with and without isodesmic bond additivity corrections.[a]

Method	$\Delta_f H^o_0$ (kcal/mol)	
	Without BAC	With BAC
UHF/3-21G	233.5	-18.4
MP3/6-31G*	56.8	-19.2
B3LYP/6-311+G(2df,p)	-14.2	-18.2
CBS-4	-22.8	-19.2
G2(MP2)	-18.7	-19.3
G2	-19.2	-19.4
CBS-Q	-20.1	-19.4
CBS-QCI/APNO	-22.1	-19.2
Experiment	-19.5 ±0.1	

[a] Using BAC_{C-H} from CH_4 and BAC_{C-C} from C_2H_6.

In order to test the capabilities of the currently utilized high level "compound methods" to calculate accurate enthalpies of halocarbons, the G2, G2(MP2), CBS-Q and CBS-4 methods were applied[44] to a series of 15 halomethanes including methane, the four fluoromethanes, the four chloromethanes and the six compounds containing both chlorine and fluorine. The computed enthalpies exhibit substantial deviations from experiment, with RMS errors of about 17 kJ mol^{-1}. These deviations are systematic, with almost all calculated enthalpies lying lower than reported experimental values, as evidenced by large negative mean deviations. These results are in sharp contrast to many earlier investigations of non-halogenated organic species; e.g. RMS deviations from experimental enthalpies for the "G2 test set" were typically 4-9 kJ mol^{-1} for these methods (*vide supra*).

To explore the distribution of errors in these series in greater detail, it is instructive to plot the deviation from experiment, [$\Delta_f H^\circ$(calc) - $\Delta_f H^\circ$(expt)], as a function of one type of carbon-halogen bond while holding the number of the other C-X bond types constant, e.g. a plot of error versus n_{CF} (number of CF bonds) in the series CH_3Cl, CH_2FCl, CHF_2Cl, CF_3Cl. This plot is displayed for the CBS-Q method in Fig. 1 (one finds similar trends using the other methods). One observes quite clearly that the negative error increases monotonically with increasing number of either C-F or C-Cl bonds; the trend is "roughly" linear with the number of C-X bonds.

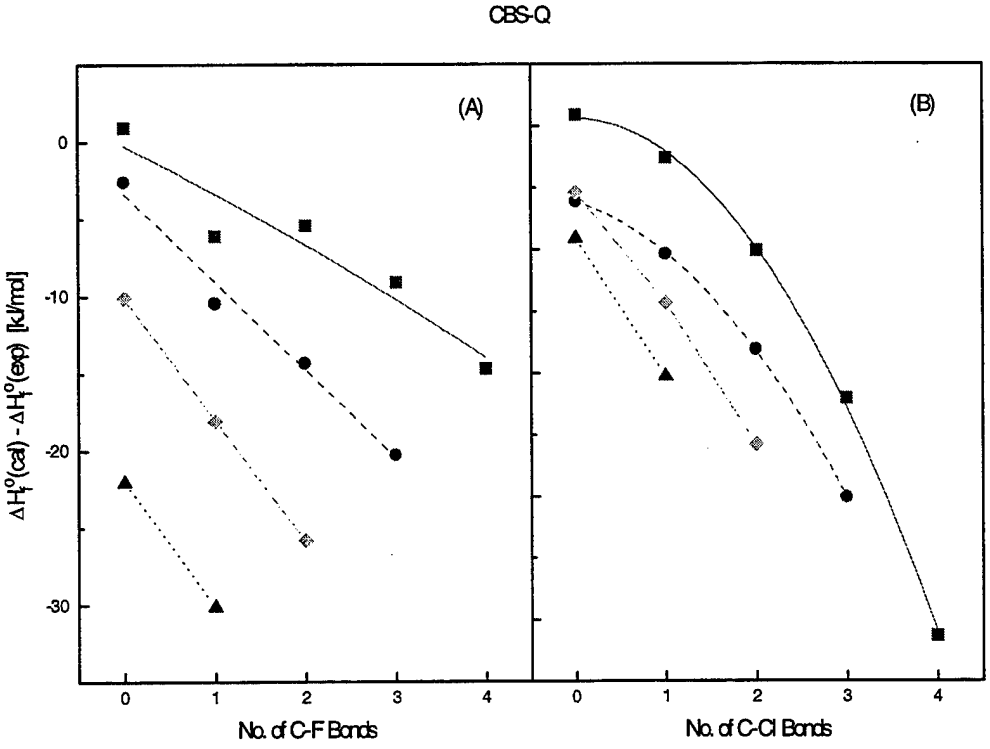

Fig. 1. Chlorofluoromethanes: Deviations of $\Delta_f H^\circ$[CBS-Q] from experiment: (**A**) Plotted as a function of the number of C-F bonds: ■ 0 C-Cl bonds; ● 1 C-Cl bond; ◆ 2 C-Cl bonds; ▲ C-Cl bonds. (**B**) Plotted as a function of the number of C-Cl bonds: ■ 0 C-F bonds; ● 1 C-F bond; ◆ 2 C-F bonds; ▲ 3 C-F bonds.

Linear regression was used to fit equation (5) to the experimental data on the series of 15 chlorofluoromethanes. This provided values for the BAC corrected enthalpies of formation for all four *ab initio* methods. The BAC corrected enthalpies of formation are in extremely good agreement with experiment. The residual RMS deviations of about 3 kJ mol^{-1} are almost an order of magnitude lower than errors in the uncorrected enthalpies and, indeed,

lies significantly below the RMS experimental uncertainty of 7 kJ mol^{-1}. The BAC's have also removed the systematic underprediction of the enthalpies of formation, as revealed by extremely small average errors in the corrected results. Hence, **BAC corrections** for the G2 and CBS-Q methods were successfully employed to predict highly accurate enthalpies of formation in the chlorofluoromethanes. Similar improvements were also obtained with the G2(MP2) and CBS-4 methods.[44] We note briefly that, as discussed at length in the paper based upon this work,[44] the curvature exhibited in Fig. 1B and the increasingly negative slopes of the lines in Fig. 1A are manifestations of "heavy atom" interactions between the C-F and C-Cl bonds.

Next, the G2, G2(MP2), CBS-Q and CBS-4 quantum mechanical protocols were utilized to compute the enthalpies of formation of C2 fluorocarbons. The deviations between *ab initio* and experimental enthalpies for fluoroethanes are plotted (for the G2 and CBS-Q methods only) in Fig. 2. One observes that the G2 enthalpies exhibit large negative deviations from experiment. Furthermore, from Fig. 2, one sees that these negative errors are systematic with an approximately linear dependence upon the number of C-F bonds in the molecule.

Since the deviations are linearly dependent upon n_{CF}, one may, in principle, again apply the BAC correction to obtain corrected results. Furthermore, because of the close similarity of the fluoroethanes (C2's) to the fluoromethanes (C1's) in the earlier work, it would be reasonable to expect that the same C-F BAC parameter should also correct the systematic errors found in this study. It was found that transferring the C-F BAC to fluoroethanes yields a substantial decrease in RMS deviations in the C2's but that not all of the negative systematic error has been removed by the bond additivity correction. While the problem could be remedied by refitting to minimize the RMS residuals in the fluoroethanes, this yields a larger value for Δ_{CF}, which would overcorrect enthalpies in the C1's. Further, it is physically unrealistic that the error due to a C-F bond should differ in the two series.

In order to explore the source of the remaining systematic errors in the fluoroethanes, we referred to the results of our earlier investigation of the chlorofluoromethanes.[44] In that work, it was discussed at some length how trends and curvature in plots of $\Delta_f H^o$(calc) - $\Delta_f H^o$(expt) vs. $n_{C\text{-}F}$ (at fixed $n_{C\text{-}Cl}$) and vs. $n_{C\text{-}Cl}$ (at fixed $n_{C\text{-}F}$) provided definitive evidence of "heavy atom" interactions. In the earlier work, it was decided not to include heavy atom interactions since the RMS residuals using linearly independent BAC's were already below the experimental uncertainties in the chlorofluoromethanes. In contrast, for the fluoroethanes, the comparatively large residual errors and negative average deviations indicate that the introduction of a heavy atom interaction parameter is necessary in this series to account for enhanced errors due to the presence of a second carbon atom attached to the carbon containing the C-C bond. As detailed in our work,[45] an interaction parameter, f_c, was incorporated into the BAC equation (5) and its value optimized (holding Δ_{CF} constant at the value determined for the CFC's) to minimize the RMS deviation from experiment in the fluoroethanes. The removal of systematic error is demonstrated in Fig. 2, in which it is seen that errors in the BAC corrected enthalpies of formation are clustered about $\Delta_f H^o$(calc) - $\Delta_f H^o$(expt) = 0.

We have since extended our studies to the fluoroethylenes ($C_2H_xF_{4-x}$, x=0-4) and fluoroacetylenes ($C_2H_xF_{2-x}$, x=0-2) using the G2 and G2(MP2) methods.[46] It was decided to use the very same parameter values, Δ_{CF} and f_C, used in the fluoroethanes. Systematic errors in the calculated enthalpies are almost completely removed by application of the BAC and interaction parameter. It is very satisfying to find that, for both methods, the RMS deviations in BAC corrected enthalpies of the fluoroethylenes are lower than RMS uncertainties in the experimental data. Similar improvements were found with BAC corrected enthalpies of formation of fluoroacetylenes.

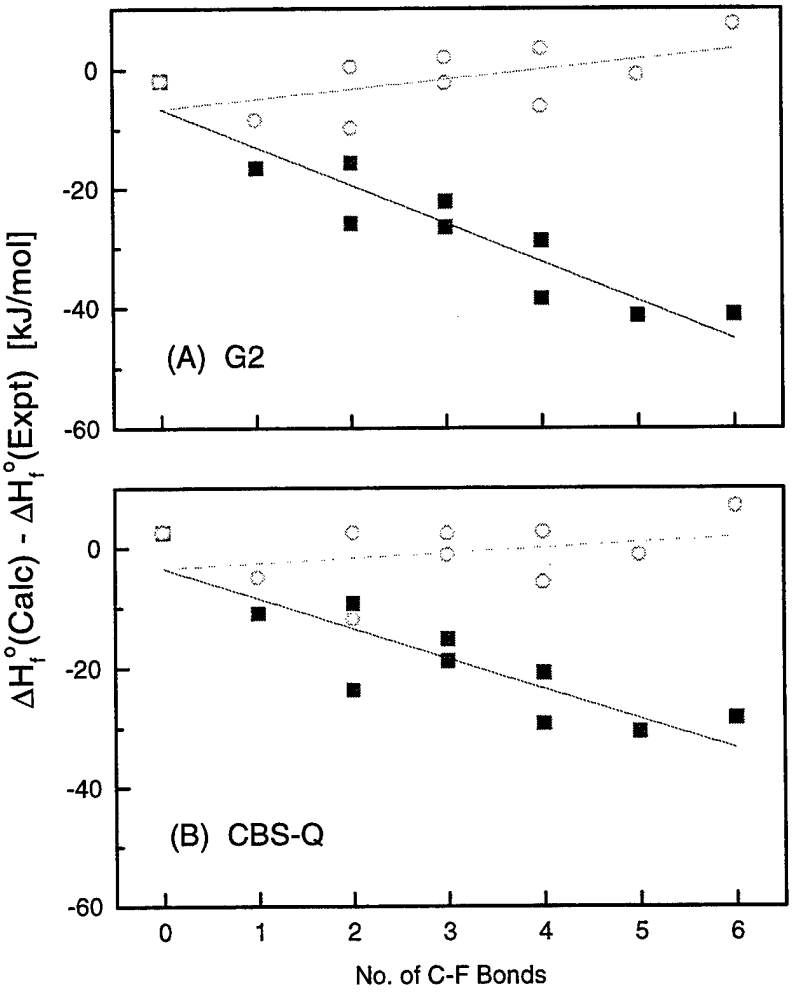

Fig. 2. Fluoroethanes: Deviations of $\Delta_f H^o$ from experiment as a function of the number of C-F bonds. ■ uncorrected; ○ BAC corrected. **(A)** G2 **(B)** CBS-Q.

C-H bond strengths of large polyfluoroalkanes, including the agents CH_3CHF_2 and CH_3CHFCF_3, were analyzed by combination of MP2/6-311+G(3df,2p) *ab initio* energies

with isodesmic reactions.[47] The results for C1 and C2 species were in good accord with experimental data, and predictions were made or C3 and C4 compounds. The strongest predicted C-H bonds are $(CF_3)C$-H and $(CF_3)_2CH$-H, both with bond dissociation enthalpies of about 450 kJ/mol, which are up to about 45 kJ/mol higher than the hydrocarbon analogs.[47]

III. A. 3. Experimental Thermochemistry

As part of the halon project at Wright Patterson, the kinetics of:

$$CF_3I + OH \rightarrow CF_3 + IOH$$

has been assessed in both directions. The activation energy, E_a, of the forward rate constant was determined via flash-photolysis resonance fluorescence (see section II.B.3) while the activation energy for the reverse rate constant, E_a', was derived from the *ab initio* PES. The difference E_a-E_a' is the reaction enthalpy ΔH, and thus yields $\Delta_f H$(IOH). The value obtained was in good accord with *ab initio* estimates.

III. B. Elementary Reaction Rates

The absolute rates of chemical reactions present a formidable challenge to theoretical predictions. An elementary bimolecular chemical reaction:

$$R_1 + R_2 \rightarrow P_1 + P_2 \qquad (9)$$

proceeds at a rate that is proportional to the concentrations of the reactants and the specific rate constant, $k_{rate}(T)$:

$$\frac{dP_1}{dt} = \frac{dP_2}{dt} = -\frac{dR_1}{dt} = -\frac{dR_2}{dt} = k_{rate}(T)\, R_1\, R_2 \qquad (10)$$

It is now over one hundred years since Arrhenius published the seminal article[51] on the variation of the rate constant with absolute temperature:

$$k_{rate}(T) = A\, e^{-\Delta E_a / RT} \qquad (11)$$

The principal difficulty for theoretical predictions lies in the extreme sensitivity of $k_{rate}(T)$ to small errors in the activation energy, ΔE_a, which can be interpreted as the difference in energy between the "transition state" and the reactants. An error of only 1.4 kcal/mol in ΔE_a leads to an error of an order-of-magnitude in $k_{rate}(T)$ at room temperature.

III. B. 1. Potential Energy Surfaces

The geometry and energy of a stable molecule can often be measured experimentally to greater accuracy than is currently available computationally. However, transition states cannot generally be isolated for experimental study, and thus are obvious targets for computational studies. The development of analytical gradient and curvature methods[22-28] has made possible the rigorous determination of transition states within a given level of correlation energy and basis set (*e.g.* MP2/6-31G*).[29]

The potential energy surface (PES) for a typical bimolecular chemical reaction such as:

$$H_2 + OH \rightarrow H + H_2O \qquad (6)$$

includes valleys (leading to the reactants and products) connected at the transition state (TS), which is a first-order saddle point (*i.e.* a stationary point with exactly one negative force constant). The reaction path or intrinsic reaction coordinate (IRC) is defined[48,49] as the path beginning in the direction of negative curvature away from the TS and following the gradient of the PES to the reactants and products.

If we move in a direction perpendicular to the reaction path, we find a potential energy curve (or surface) corresponding to a stable reactant or product molecule if we are far from the TS. Even around the TS, the variation of the PES perpendicular to the IRC is very similar to the PES for a stable molecule. Transition States differ from stable molecules in that they possess one negative force constant which defines the reaction coordinate. Calculated energies along the coordinates with positive force constants behave very much like their counterparts in stable molecules. However, the energy changes along the reaction coordinate are much more difficult to predict. It is the variation of the energy along this coordinate that is very sensitive to (and thus requires the inclusion of) the correlation energy.

UHF calculations give notoriously bad results for transition states. For example, the UHF/3-21G energy profile for the transfer of a hydrogen atom from H_2 to OH is endothermic rather than exothermic and consequently places the transition state too close to the products.[50] One might erroneously conclude that such calculations provide no useful information about the reaction path. Fortunately, this is not the case. Although the variation of the energy along the reaction path is very poorly described by the UHF/3-21G method, the variation of the energy perpendicular to the reaction path is very nicely described by the UHF/3-21G method, just as in stable molecules. The UHF/3-21G reaction path very closely approximates the MP2/6-31G* reaction path.[50] However, the energy variation along this path, and hence the position of the UHF/3-21G transition state, is incorrect. Nevertheless, the UHF/3-21G reaction path passes through (or near) the MP2/6-31G* transition state. Hence, if we calculate the MP2/6-31G* energy along the UHF/3-21G reaction path, we obtain an energy profile that differs trivially from the MP2/6-31G*

energy profile along the MP2/6-31G* reaction path.[50] This is rather remarkable for the H_2 + OH reaction, given the very poor UHF/3-21G//UHF/3-21G energy profile.

Based on these observations, we have proposed[50] the *"IRCMax" transition state method*, in which we select the maximum of the high-level Energy[Method(1)] along the low-level IRC obtained from the Geom[Method(2)] calculations. The IRCMax transition state extension of the compound models takes advantage of the enormous improvement (from one to two orders-of-magnitude) in computational speed[30] achieved by using low-level, Geom[Method(2)], IRC calculations. We then perform several single point higher level, Energy[Method(1)], calculations along the Geom[Method(2)] reaction path to locate the Energy[Method(1)] transition state, that is, the maximum of Energy[Method(1)] along the Geom[Method(2)] IRC. Calculations at three points bracketing the transition state are sufficient to permit a parabolic fit to determine the transition state geometry and the activation energy.

Since we determine the maximum of Energy[Method(1)] along a path from reactants to products, the IRCMax method gives a rigorous upper bound to the high-level Method(1) transition state energy. In addition, when applied to the compound CBS and G2 models, the IRCMax method reduces to the normal treatment of bimolecular reactants and products, Energy[Method(1)]//Geom[Method(2)]. Thus the IRCMax method can be viewed as an extension of these compound models to transition states. The results demonstrate the numerical superiority of this IRCMax method, Max{Energy[Method(1)]}//IRC{Geom[Method(2)]}, over conventional Energy[Method(1)]//Geom[Method(2)] calculations.

The saddle point on the PES is independent of mass and thus invariant to isotopic substitution, but the IRC is determined in mass weighted coordinates and thus varies slightly with isotopic substitution. The IRCMax TS geometry will therefore show a small artificial isotope shift perpendicular to the IRC. However, this effect is much smaller than the real isotope shift parallel to the IRC resulting from variations in the ZPE along the IRC. The latter effect is included in the IRCMax search for the variational TS.

III. B. 2. Absolute Rate Theory

More than sixty years ago, Eyring proposed[52] the use of statistical mechanics to evaluate the preexponential factor, A, in equation (11) using partition functions, Q, and the "collision velocity", k_BT/h:

$$A\ (T) = \frac{Q^{\ddagger}(T)}{Q_{R_1}(T)\,Q_{R_2}(T)} \bullet \frac{k_B T}{h} \qquad (12)$$

thereby accounting for the small temperature variations in A. The evaluation of the translational, vibrational, and rotational partition functions:

$$Q_{translation} = V\left(2\pi M k_B T\right)^{3/2}/h^3 \tag{13}$$

$$Q_{rotation} = 2\pi\left(4\pi/\sigma\right)\prod_j\left(2\pi I_j k_B T\right)^{1/2}/h \tag{14}$$

$$Q_{vibration} = \prod_j\left(1-e^{-h\nu_j/k_B T}\right)^{-1} \tag{15}$$

$$Q_{electronic} = \sum_j e^{-\Delta E_j/k_B T} \tag{16}$$

$$Q_{total} = Q_{electronic}\, Q_{vibration}\, Q_{rotation}\, Q_{translation} \tag{17}$$

requires only a knowledge of the mass (for $Q_{translation}$), geometry (for the moments of inertia, I_j, in $Q_{rotation}$), vibrational frequencies (n_j for $Q_{vibration}$), and DE of any low-lying electronic states for the reactants and transition state ($Q_{electronic}$).

The electronic, vibrational, and rotational energy levels can often be determined from experiment for the reactants, but not for the transition state. The use of *ab initio* quantum mechanical methods to evaluate the required electronic, vibrational, and rotational energy levels is therefore of considerable practical importance.

Eyring presumed that motion along the path from reactants to products could be treated classically. However, if the reduced mass for this motion is finite, the quantum mechanical wave packet can tunnel through the barrier, $V(R)$, rather than climb over the top. The probability of reactants with energy, E, tunneling through such a barrier is determined by the initial and final wave amplitudes:

$$\kappa(E) = \left|\frac{\psi\left[R_f(E), E\right]}{\psi\left[R_i(E), E\right]}\right|^2 \tag{18}$$

Eckart introduced[53] a simple mathematical form for the potential energy function, $V(R)$:

$$V(R) = \frac{\Delta E_{reaction}}{e^{2\pi R/L}+1} + \frac{\left(\sqrt{\Delta E^{\ddagger}_{forward}} + \sqrt{\Delta E^{\ddagger}_{reverse}}\right)^2}{e^{2\pi R/L}+2+e^{-2\pi R/L}} \tag{19}$$

for which he determined the exact transmission probability, $k(E)$. This transmission probability must then be weighted by the Boltzmann distribution function. The final expression for the rate constant is therefore:

$$k_{rate}(T) = \frac{Q^{\ddagger}(T)}{Q_{R_1}(T)\,Q_{R_2}(T)} \bullet \frac{k_B T}{h} \int_0^{\infty} \kappa(E)\, e^{-E / k_B T}\, dE \qquad (20)$$

Truhlar and Kuppermann introduced[48] the correct definition of the reaction path, R, in mass weighted coordinates and were the first to recognize the importance of including in $V(R)$, the quantum mechanical zero-point vibrational energy for all normal modes that are orthogonal to R. The challenge we face is to accurately determine all the quantities required to evaluate equation (20).

III. B. 3. Experimental Rate Constants

Elementary reactions of radicals are studied in a flash-photolysis resonance fluorescence apparatus. Radicals are generated by pulsed flashlamp or excimer laser photolysis of precursor molecules, and allowed to react with a large excess of second reagent under pseudo-first-order conditions. The radical concentration in a zone at the center of the reactor is monitored as a function of time with microsecond resolution by resonance fluorescence spectroscopy. Because the reaction time scale is short compared to diffusion of reactive species from the zone to the walls of the reactor, the zone acts as an effectively wall-less reactor and heterogeneous chemistry is eliminated. The temperature can be varied up to about 900 K. Use of low radical concentrations reduces any secondary chemistry and isolates individual reactions from interefering processes. Halon-related studies which have been completed include measurement of the rate constants for CF_3I reactions with the flame species H, OH and O, CF_3Br with H and the iodoalkanes CH_3I, CD_3I, C_2H_5I, CH_3CHICH_3 and $(CH_3)_3CI$.[54,55] Examples of the data obtained are shown in Fig. 3. These data fill gaps in the kinetic data base for combustion modeling, and help assess the reliability of the computational methods described above.

III. C. Overall Mechanistic Studies

A reaction scheme for the inhibition of hydrogen-oxygen flames by CF_3I was constructed from new experiments and computations carried out by the Center for Computational Modeling of Nonstructural Materials, combined with existing literature information. The mechanism is a subset of the reactions to be considered in inhibition of hydrocarbon flames, and was tested against measured flame concentration profiles by Andrew McIlroy at Sandia National Laboratory.[56] The analysis revealed catalytic removal of atomic hydrogen by CF_3I early in the combustion process.

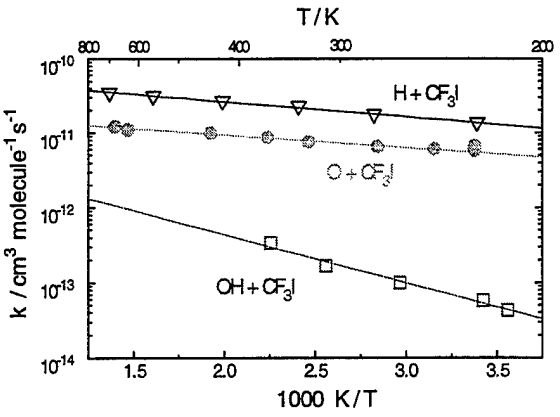

Fig. 3. Arrhenius plots of the measured rate constants for CF_3I reactions with the combustion radicals H, O and OH.

III. D. Bibliography

1. Schwartz, C. *Phys. Rev.* **1962**, *126*, 1015.
2. Schwartz, C. in *Methods in Computational Physics*, **1963**, Alder, B.; Fernbach, S.; Rotenberg, M. Eds., *Vol. 2*, Academic, New York.
3. Nyden, M. R.; Petersson, G. A. *J. Chem. Phys.* **1981**, *75*, 1843.
4. Petersson, G. A.; Nyden, M. R. *J. Chem. Phys.* **1981**, *75*, 3423.
5. Petersson, G. A.; Licht, S. L. *J. Chem. Phys.* **1981**, *75*, 4556.
6. Brown, F. B.; Truhlar, D. G. *Chem. Phys. Lett.* **1985**, *117*, 307.
7. Dunning Jr., T. H. *J. Chem. Phys.* **1989**, *90*, 1007.
8. Siegbahn, P. E. M.; Blomberg, M. R. A.; Svensson, M. *Chem. Phys. Lett.* **1994**, *223*, 35.
9. Møller, C.; Plesset, M. S. *Phys. Rev.* **1934**, *46*, 618.
10. Löwdin, P. O. *Phys. Rev.* **1955**, *97*, 1474.
11. Petersson, G. A.; Yee, A. K.; Bennett, A. *J. Chem. Phys.* **1985**, *83*, 5105.
12. Petersson, G. A.; Braunstein, M. *J. Chem. Phys.* **1985**, *83*, 5129.
13. Petersson, G. A.; Bennett, A; Tensfeldt, T. A.; Al-Laham, M. A.; Shirley, W. A.; Mantzaris, J. *J. Chem. Phys.* **1988**, *89*, 2193.
14. Petersson, G. A.; Al-Laham, M. A.; *J. Chem. Phys.* **1991**, *94*, 6081.
15. Petersson, G. A.; Tensfeldt, T. G.; Montgomery Jr., J. A. *J. Chem. Phys.* **1991**, *94*, 6091.
16. Montgomery, J. A., Jr.; Ochterski, J. W.; Petersson, G. A. *J. Chem. Phys.* **1994**, *101*, 5900.
17. Ochterski, J. W.; Petersson, G. A.; Montgomery, J. A., Jr. *J. Chem. Phys.* **1996**, *104*, 2598.

18. Frisch, M. J.; Trucks, G. W.; Schlegel, H. B.; Gill, P. M. W.; Johnson, B. G.; Robb, M. A.; Cheeseman, J. R.; Keith, T.; Petersson, G. A.; Montgomery, J. A., Jr., Raghavachari, K.; Al-Laham, M. A.; Zakrzewski, V. G.; Ortiz, J. V.; Foresman, J. B.; Peng, C. Y.; Ayala, P. Y.; Chen, W.; Wong, M. W.; Andres, J. L.; Replogle, E. S.; Gomperts, R.; Martin, R. L.; Fox, D. J.; Binkley, J. S.; Defrees, D. J.; Baker, J.; Stewart, J. P.; Head-Gordon, M.; Gonzalez, C.; Pople, J. A. *Gaussian94*, Revision B.3: Gaussian, Inc.: Pittsburgh PA, **1995**.
19. Pople, J. A. in *Energy, Structure and Reactivity*, **1973**, Smith, D. W; McRae, W. B. Eds., p 51, Wiley, N. Y.
20. Roothaan, C. C. J. *Rev. Mod. Phys.* **1951**, *23*, 69.
21. Pople, J. A.; Nesbet, R. K. J. Chem. Phys. **1959**, *22*, 571.
22. Peng, C.; Schlegel, H. B. I*srael J. Chem.* **1993**, *33*, 449.
23. Handy, N. C.; Schaefer, H. F., III, *J. Chem. Phys.* **1984**, *81*, 5031.
24. Pople, J. A.; Krishnan, R.; Schlegel, H. B.; Binkley, J. S. *Int. J. Quant. Chem. Symp* **1979**, *13*, 325.
25. Schlegel, H. B. *J. Comp. Chem.* **1982**, *3*, 214.
26. Head-Gordon, M.; Head-Gordon, T. *Chem. Phys. Lett.* **1994**, *220*, 122.
27. Frisch, M. J.; Head-Gordon, M.; Pople, J. A. *Chem. Phys. Lett.* **1990**, *166*, 275.
28. Frisch, M. J.; Head-Gordon, M.; Pople, J. A. *Chem. Phys. Lett.* **1990**, *166*, 281.
29. Hehre, W. J.; Radom, L.; Schleyer, P. v. R.; Pople, J. A. *Ab Initio Molecular Orbital Theory*; **1986**, John Wiley & Sons: New York.
30. Foresman, J. B.; Frisch, A. *Exploring Chemistry with Electronic Structure Methods*, Second Edition, 1996, Gaussian, Inc., Pittsburgh, PA.
31. Pople, J. A.; Head-Gordon, M.; Fox, D. J.; Raghavachari, K.; Curtiss, L. A. *J. Chem. Phys.* **1989**, *90*, 5622.
32. Curtiss, L. A.; Jones, C.; Trucks, G. W.; Raghavachari, K.; Pople, J. A. *J. Chem. Phys.* **1990**, *93*, 2537.
33. Curtiss, L. A.; Raghavachari, K.; Trucks, G. W.; Pople, J. A. *J. Chem. Phys.* **1991**, *94*, 7221.
34. Curtiss, L. A.; Raghavachari, K.; Pople, J. A. *J. Chem. Phys.* **1993**, *98*, 1293.
35. Dewar, M. J. S.; Zoebisch, E. G.; Healy, E. F. *J. Am. Chem. Soc.* **1985**, *107*, 3902.
36. Becke, A. D. *J. Chem. Phys.* **1993**, *98*, 5648.
37. Becke, A. D. *Phys. Rev. A* **1988** *38*, 3098.
38. Lee, C; Yang, W.; Parr, R. G. *Phys. Rev. B* **1988**, *37*, 785.
39. Vosko, S. H.; Wilk, L.; Nusair, M. *Canadian J. Phys.* **1980**, *58*, 1200.
40. Ochterski, J. W.; Petersson, G. A.; Wiberg, K. B. *J. Am. Chem. Soc.* **1995**, *117*, 11299.
41. Berry, R. J.; Burgess, D. R. F., Jr.; Nyden, M. R.; Zachariah, M. R.; Schwartz, M. *J. Phys. Chem.* **1995**, *99*, 17145.
42. Ho, P.; Melius, C. F. *J. Phys. Chem.* **1990**, *94*, 5120.
43. Allendorf, M. D.; Melius, C. F. *J. Phys. Chem.* **1993**, *97*, 72.

44. Berry, R. J.; Burgess, D. R., Jr.; Nyden, M. R.; Zachariah, M. R.; Melius, C. F.; Schwartz, M. *J. Phys. Chem.* **1996**, *100*, 7405.
45. Berry, R. J.; Ehlers, C. J.; Burgess, D. R., Jr.; Zachariah, M. R.; Nyden, M. R.; Schwartz, M. *J. Mol. Struct. (Theochem)*, in press.
46. Berry, R. J.; Schwartz, M. *Structural Chem.*, in press.
47. Marshall, P.; Schwartz, M. *J. Phys. Chem. A* **1997**, *101*, 2906.
48. Truhlar, D. G.; Kuppermann, A. *J. Am. Chem. Soc.* **1971**, *93*, 1840.
49. Gonzalez, C.; Schlegel, H. B. *J. Phys. Chem.* **1989**, *90*, 2154.
50. Malick, D. K.; Petersson, G. A.; Montgomery, J. A., Jr. manuscript in preparation.
51. Arrhenius, S. *Z. Physikal. Chem.* **1889**, *4*, 226.
52. Eyring, H. *J. Chem. Phys.* **1935**, *3*, 107.
53. Eckart, C. *Phys. Rev.* **1930**, *35*, 1303.
54. Marshall, P.; Misra, A.; Berry, R. J. *Chem. Phys. Lett.* **1997**, *265*, 48.
55. Yuan, J.; Wells, L.; Marshall, P. *J. Phys. Chem. A* **1997**, *101*, 3542.
56. Marshall, P.; Misra, A., Yuan, J.; Berry, R.; McIlroy, A. *Halon Options Technical Working Conference Proceedings* **1997**, 262.

III. E. Publication List (1995-1997)

Center for Computational Modeling of Nonstructural Materials

AFRL/MLBT

1. R. J. Berry and P. Marshall, "A Computational Study of the Reaction Kinetics of Methyl Radicals with Trifluorohalomethanes," *Int. J. Chem. Kin.*, submitted.

2. R. J. Berry and M. Schwartz, "Halon Thermochemistry: *Ab Initio* Calculations of the Enthalpies of Formation of Fluoroethylenes and Fluoroacetylenes," *Structural Chemistry*, accepted.

3. A. Misra, R. J. Berry, and P. Marshall, "Potential Energy Surfaces for the Reaction of O-atoms with CH_3I: Implications for Thermochemistry and Kinetics," *J. Phys. Chem.*, **A 101**, 7420, 1997.

4. A. Misra and P. Marshall, "Computational Studies of the Isomers of ClIO and $ClIO_2$: Implications for the Stratospheric Chemistry of Iodine," *J. Chem. Soc., Faraday Trans.*, **93**(18), 3301, 1997.

5. G. Petersson, "Complete Basis Set Thermochemistry and Kinetics" in "Computational Thermochemistry: Prediction and Estimation of Molecular Thermodynamics," K. Irikura, and D. Frurip (Eds.), ACS Symposium Series, American Chemical Society, Washington, D. C., in press.

6. R. J. Berry, M. Schwartz, and P. Marshall, "*Ab Initio* Calculations for Kinetic Modeling of Halocarbons" in "Computational Thermochemistry: Prediction and Estimation of Molecular Thermodynamics," K. Irikura, and D. Frurip (Eds.), ACS Symposium Series, American Chemical Society, Washington, D. C., in press.

7. R. J. Berry, C. J. Ehlers, D. R. Burgess, Jr., M. R. Zachariah, M. R. Nyden, and M. Schwartz, "Halon Thermochemistry: *Ab Initio* Calculations of the Enthalpies of Formation of Fluoroethanes," *J. Mol. Struct. (Theochem)*, in press.

8. T. D. Fang, P. H. Taylor, B. Dellinger, C. J. Ehlers, and R. J. Berry, "Kinetics of the OH - CH_3-CF_2Cl Reaction over an Extended Temperature Range," *J. Phys. Chem.*, **A 101**, 5758, 1997.

9. J. Yuan, L. Wells, and P. Marshall, "Kinetic Studies of the Reactions of Atomic Hydrogen with Iodoalkanes," *J. Phys. Chem.*, **A 101**, 3542, 1997.

10. P. Marshall and M. Schwartz, "A Computational Study of C-H Bond Strengths in Polyfluoroalkanes," *J. Phys. Chem.*, **A 101**, 2906, 1997.

11. R. J. Berry, C. J. Ehlers, D. R. Burgess, Jr., M. R. Zachariah, and P. Marshall, "A Computational Study of the Reactions of Atomic Hydrogen with Fluoromethanes: Kinetics and Product Channels," *Chem. Phys. Lett.*, **269**, 107, 1997.

12. P. Marshall, A. Misra, and R. J. Berry, "Computational Studies of the Reactions of CH_3I with H and OH," *Chem. Phys. Lett.*, **265**, 48, 1997.

13. P. H. Taylor, M. S. Rahman, M. Arif, B. Dellinger, and P. Marshall, "Kinetic and Mechanistic Studies of the Reaction of Hydroxyl Radicals with Acetaldehyde Over an Extended Temperature Range," *26th Symposium (International) on Combustion*, The Combustion Institute: Pittsburgh, PA, 1996; pp 497-504.

14. H. L. Paige, R. J. Berry, M. Schwartz, P. Marshall, D. R. F. Burgess and M. R. Nyden, "*Ab Initio* Calculations and Kinetics Modeling of Halon and Halon Replacements," *Proceedings of the Halon Options Technical Working Conference*, 259, 1996.

15. R. J. Berry, D. R. Burgess, Jr., M. R. Nyden, M. R. Zachariah, C. F. Melius, and M. Schwartz, "Halon Thermochemistry: Calculated Enthalpies of Formation of Chlorofluoromethanes," *J. Phys. Chem.*, **100**, 7405, 1996.

16. R. J. Berry, D. R. Burgess, Jr., M. R. Nyden, M. R. Zachariah, and M. Schwartz, "Halon Thermochemistry: *Ab Initio* Calculations of the Enthalpies of Formation of Fluoromethanes," *J. Phys. Chem.*, **99**, 17145, 1995.

17. C. L. Stanton, R. J. Berry, and M. Schwartz, "Molecular Geometry and the Rotational Potential Surface in Perfluoro(isopropyl methyl ether)," *J. Phys. Chem.*, **99**, 3473, 1995.

IV. Symposium

The Third Symposium on Halon Replacements, "Kinetic Modeling of Flame Suppression" was held at the Wright Laboratory, Wright-Patterson AFB from 22 to 24 July 1997. It brought together leaders in the field to summarize the understanding of halons and potential replacements, including methods for analysis of their action in flames, and to make recommendations for the future focus of our search for viable halon replacements.

IV. A. Overview and Purposes

The symposium was organized around several themes:

- New developments in the *ab initio* theory of absolute rates for elementary reactions.
- Calibration of these new methods by comparison to the best available experimental data.
- Applications of these new methods to the critical reactions in flame chemistry and fire suppression.
- Experimental determination of previously unknown rates for critical reactions in flame chemistry and fire suppression.
- Use of both sets of rate constants to develop comprehensive computer models for the overall mechanism of flames and fire suppression.
- The application of these computer models together with empirical data to search for new fire suppressants.
- The testing of these new fire suppressants to determine their suitability as potential replacements for Halon 1301.

IV. B. Program

July 22; Tuesday Morning

8:00-8:05; Introductions; Harvey Paige
8:05-8:15; Welcome; Col. Donald R. Kitchen, Acting Director, Materials Directorate

Session A. Chair: Paul Marshall

A1. 8:15-9:00; H. Bernhard Schlegel, Wayne State University
Exploring Potential Energy Surfaces for Chemical Reactions Using Ab Initio Molecular Orbital Theory

A2. 9:00-9:45; Joseph Durant, Sandia National Lab
Evaluation of Transition State Properties by Density Functional Theory

9:45-10:15 Break

A3. 10:15-11:00; George Petersson, Wesleyan University
Complete Basis Set Reaction Rates

A4. 11:00-11:45; Martin Schwartz, University of North Texas
Rate Constant Predictions for Hydrogen Abstraction Reactions

11:45-1:30 Lunch

July 22; Tuesday Afternoon

Session B. Chair: Rajiv Berry

B1. 1:30-2:15; Robert P. Salmon, Edward R. Ritter, Villanova University
Mechanism for Perfluoroisobutene Production during Fluorocarbon Pyrolysis

B2. 2:15-3:00; Donald Burgess, Michael Zachariah, NIST
The Use of BAC-MP4 Calculations in the Development of a Chemical Kinetic Mechanism for Fluorinated Hydrocarbons

3:00-3:30 Break

B3. 3:30-4:15; Phillip Westmoreland, University of Massachusetts
Modeling Thermochemistry and Transition States for CF_3CHFCF_3

B4. 4:15-5:00; Karl Irikura, Wing Tsang, NIST
Ab Initio Kinetics of the Thermal Dehydrohalogenation of Alkyl Halides

July 23; Wednesday Morning

Session C. Chair: Martin Schwartz

C1. 8:00-8:45; Jerzy Jodowski, Marie-Thérèse Rayez, Jean-Claude Rayez, University of Bordeaux, France *A Theoretical Study of the Two-Channel Hydrogen Abstraction by Cl and Br Atoms and Reverse Reactions*

C2. 8:45-9:30; L. Truett, H. Thermann, D. Trees, K. Seshadri, University of California, San Diego *Inhibition of Hydrogen-Air Diffusion Flames by Bromotrifluoromethane*

9:30-10:00 Break

C3. 10:00-10:45; Peter Haaland, Huntington Research and Engineering *Labile Bromine Fire Suppressants*

C4. 10:45-11:30; Joseph Bozzelli, New Jersey Institute of Technology *Reactions of Bromine Species Leading to Inhibition in H_2 and CH_4 Oxidation*

11:30-1:30 Lunch

July 23; Wednesday Afternoon

Session D. Chair: Joseph Bozzelli

D1. 1:30-2:15; Frédérique Battin-Leclerc, University of Nancy, France *Investigations on the Inhibiting Effect of CF_3I and Some Fluorinated Hydrocarbons*

D2. 2:15-3:00; Rajiv Berry, Materials Directorate, Air Force Research Lab *Kinetics and Unusual Products of the Reactions of Oxygen Atoms with Alkyl Iodides*

3:00-3:30 Break

D3. 3:30-4:15; Paul Marshall, University of North Texas *The Kinetics of Elementary Reactions of CF_3Br and CF_3I with H, OH, O and CH_3 Radicals: Experiments, Ab Initio Calculations and Implications for Combustion Chemistry*

D4. 4:15-5:00; Andrew McIlroy, Sandia National Lab *Kinetic Modeling of Hydrogen Combustion Suppression by CF_3I*

6:30 Dinner

July 24; Thursday Morning

Session E. Chair: George Petersson

E1. 8:00-8:45; Marc Rumminger, Greg Linteris, Dirk Reinelt, Valeri Babushok, NIST
Numerical Modeling Results for Iron-Pentacarbonyl Inhibited Flames

E2. 8:45-9:30; Valeri Babushok, NIST
Chemical Limits to Flame Inhibition: Effectiveness of Metallic Flame Suppressants

9:30-10:00 Break

E3. 10:00-10:45; Thanh Nguyen Truong, University of Utah
Predicting Kinetics, Dynamics and Mechanisms of Gas-Phase Polyatomic Reactions from First Principles: Practical Ab Initio Direct Dynamics Methodology

E4. 10:45-11:30; Guy-Marie Côme, University of Nancy, France
Computer tools for complex reactions modelling

11:30-1:30 Lunch

July 24; Thursday Afternoon

1:30-3:00; Discussion

3:00-3:30 Break

3:30-4:30; Theresa Windus, talk on ASC-MSRC supercomputer center and/or visit to the Engine Nacelle Test Facility or the Dry Bay Test Facility

IV. C. Extended Abstracts

The following abstracts were supplied by the authors of the papers. For convenience in contacting authors, names, addresses, and e-mail addresses are provided.

Exploring Potential Energy Surfaces for Chemical Reactions Using Ab Initio Molecular Orbital Calculations

H. Bernhard Schlegel

Department of Chemistry, Wayne State University, Detroit, Michigan, 48202
tel: (313) 577-2562; fax: (313) 577-8822
email: hbs@sun.chem.wayne.edu

This talk covers a number of recent developments in ab initio molecular orbital calculations that may be relevant to the study of halon replacements: improved geometry optimization using redundant internal coordinates,[1-3] a combined method for finding transition states and reaction paths,[5-7] a more accurate approach for calculating projected frequencies along the reaction path,[8] an automatic method for identifying internal rotors from normal mode analysis and better approximations for partition functions for hindered rotors,[9] problems related to spin contamination in calculations on radicals[10-13] and the use of the Marcus relation to analyze barrier heights for radical abstraction reactions.[14,15]

Geometry optimization is a key step in any study of potential energy surfaces. The efficiency of a geometry optimization depends both on the algorithm used and on the coordinates employed.[2,3] A coordinate system that is very well suited to describe the structure and bonding of a molecule can be constructed from all bonds, all valence angles between bonded atoms and all dihedral angles between bonded atoms. However, such a coordinate system often has more than the requisit 3N-6 coordinates. Redundancies in the coordinates are removed by using a projector based on the generalized inverse of the G matrix; constraints on individual coordinates can be added to this projector. For minimizations, redundant internal coordinates provide substantial improvements in optimization efficiency over cartesian and non-redundant internal coordinates, especially for flexible and polycyclic systems.[1] Transition structure searches are also improved when redundant coordinates are used[1] and when the initial steps are guided by the quadratic synchronous transit approach.[4]

Mapping out a reaction mechanism involves finding the transition state and following the reaction path connecting it to reactants and products.[2,6] Transition states can be significantly more difficult to locate than minima and reaction paths can be expensive to follow.[2,6] We have developed an efficient algorithm for determining the transition state, minima and reaction path in a single procedure.[5] Starting with an approximate path represented by N points, the path is iteratively relaxed until one of the N points reached the transition state, the endpoints optimize to minima and the remaining points converged to a second order approximation of the steepest descent path.[7] The method appears to be more reliable than conventional transition state optimization algorithms, and requires only energies and gradients, but not second derivative calculations. The procedure has been applied to a number of model reactions. In most cases, the reaction mechanism can be

described well using 5 to 7 points to represent the transition state, the minima and the path. The computational cost of relaxing the path is less than or comparable to the cost of standard techniques for finding the transition state and the minima, determining the transition vector and following the reaction path on both sides of the transition state.

Some of the factors affecting the accuracy of following reaction paths and calculating projected frequencies perpendicular to the reaction path have been examined.[8] The S_N2 reaction of Cl^- with CH_3Cl computed at the HF/6-31G* level of theory has been used as a test case. The symmetric C-H stretching mode couples strongly to the reaction path, and the projected frequency of this mode is very sensitive to the numerical accuracy of the path following and frequency projection methods. The transition state geometry must be converged very tightly so that the path steps in the correct direction. For second order implicit algorithms for following reaction paths,[7] improved accuracy can be obtained by computing the tangent used for path following and frequency projection from the displacement along the path rather than from the gradient. An even greater increase in accuracy can be achieved by employing the Hessian, used to compute the frequencies, to take a Newton-Raphson step to improve the convergence of the reaction path following. Taken together, these techniques yield a 1 - 3 order of magnitude decrease in the errors in the projected frequencies along the reaction path.

A procedure has been developed to automatically identify the normal modes of vibration that correspond to internal rotations and to compute corrections to the partition function.[9] The rigid-rotor internal rotation modes are obtained by fixing the stretching, bending and out-of-plane motions and solving the vibrational problem for the constrained system. The normal modes corresponding to internal rotations are identified by comparing them with the constrained modes. The composition of the rotating groups and the moments of inertia can then be determined from the structure and connectivity of the molecule; the potential periodicity, the symmetry numbers for the rotating groups and the well multiplicity are obtained using empirical rules and simple calculations, and can be altered by user input. An improved analytical approximation to the partition function for a one dimensional hindered rotor has been developed. The treatment has been generalized to give an approximation for multiple internal rotors.

Radicals are often calculated by spin unrestricted methods such as UHF, UMPn, UQCI and UCC. However, such calculation can have contamination from unwanted spin states.[10-12] This occurs most frequently in conjugated radicals and in transition states. The value of S^2 can be an important diagnostic tool for judging the quality of such calculations.[10-12] Spin projection methods can be used to remove contributions from unwanted spin states. The bond dissociation potentials for

$HF \rightarrow H + F$

and $CH_4 \rightarrow CH_3 + H$

have been considered as examples. Spin projection should not be used for Hartree-Fock or density funtional methods, since it leads the serious distortions of the potential energy curves.[13] Spin projection should be used for Møller-Plesset perturbation theory, and yields results comparable to higher levels of theory. Coupled cluster (CCSD), quadratic configuration (QCISD) and Bueckner (BD) methods are much less affected by spin contamination, and can be used without projection if bonds are not stretched beyond twice their equilibrium values.[12]

Marcus theory can be quite useful in correlating data for large series of reactions. Hydrogen abstraction reactions

$CH_3X + \cdot CH_2Y \rightarrow \cdot CH_2X + CH_3Y$,[14]

$CH_3X + \cdot Y \rightarrow \cdot CH_2X + HY$[15]

and $HX + \cdot Y \rightarrow \cdot X + HY$[15] (X,Y = H, F, Cl, OH, SH, NH_2, CH_3, CN)

have been studied using ab initio molecular orbital theory. The Marcus relation can be used to estimate the barrier heights of the cross reactions based on the intrinsic barriers for the identity reactions and the heats of reaction for the cross reactions. The barrier heights are predicted quite well for ca 90% of the reaction. For the exceptions, charge transfer states are suspected of contributing to the transition states.

1. Peng, C.; Ayala, P. Y.; Schlegel, H. B.; Frisch, M. J.; Using redundant internal coordinates to optimize equilibrium geometries and transition states. *J. Comput. Chem.* **1996**, *17*, 49-56.

2. Schlegel, H. B. Geometry optimization on potential energy surfaces. in *Modern Electronic Structure Theory* Yarkony, D. R., ed., World Scientific Publishing, **1995**, 459-500.

3. Schlegel, H. B.; Geometry Optimization, in *Encyclopedia of Computational Chemistry*, (Wiley), **1998**.

4. Peng, C.; Schlegel, H. B.; Combining synchronous transit and quasi-newton methods for finding transition states. *Israeli J. Chem.* **1994**, *33*, 449-54.

5. Ayala, P. Y.; Schlegel, H. B.; A combined method for determining reaction paths, minima and transition state geometries. *J. Chem. Phys.* **1997**, *107*, 375-384.

6. Schlegel, H. B.; Reaction Paths, in *Encyclopedia of Computational Chemistry*, (Wiley), **1998**.

7. Gonzalez, C.; Schlegel, H. B.; An improved algorithm for reaction path following. *J. Chem. Phys.* **1989**, *90*, 2154-2161; Gonzalez, C.; Schlegel, H. B.; Reaction Path Following in Mass-Weighted Internal Coordinates. *J. Phys. Chem.*, **1990**, *94*, 5523-5527; Gonzalez, C.; Schlegel, H. B.; Improved algorithms for reaction path following: Higher order implicit algorithms. *J. Chem. Phys.* **1991**,*95*, 5853-5860.

8. Baboul, A. G.; Schlegel, H. B.; Improved Method for Calculating Projected Frequencies along a Reaction Path. *J. Chem. Phys.* (accepted).

9. Ayala, P. Y.; Schlegel, H. B.; Identification and Treatment of Internal Rotation in Normal Mode Vibrational Analysis. *J. Chem. Phys.* (submitted).

10. Schlegel, H. B.; Spin Contamination, in *Encyclopedia of Computational Chemistry*, (Wiley), **1998**.

11. Schlegel, H. B.; Potential energy curves using unrestricted Møller-Plesset perturbation theory with spin annihilation. *J. Chem. Phys.*, **1986**, *84*, 4530-4534; Schlegel, H. B.; Møller-Plesset perturbation theory with spin projection. *J. Phys. Chem.* **1988**, *92*, 3075-3078.

12. Chen, W.; Schlegel, H. B.; Evaluation of S^2 for post-SCF methods and spin projection of UMPn energies. *J. Chem. Phys.* **1994**, *101*, 5957-68.

13. Wittbrodt, J. M.; Schlegel, H. B.; Some reasons not to use spin projected density functional theory. *J. Chem. Phys.* **1996**, *105*, 6574-77.

14. Fox, G. L.; Schlegel, H. B.; An ab initio study of hydrogen atom abstractions from substituted methanes by substituted methyl radicals. *J. Phys. Chem.* **1992**, *96*, 298-302.

15. Fox, G. L.; Ayala, P. Y.; Schlegel, H. B.; unpublished results.

Evaluation of Transition State Properties by Density Functional Theory

Joseph L. Durant

Combustion Research Facility, Sandia National Laboratories, Livermore, CA 94551
tel: (510) 294-3343; fax: (510) 294-2276
email: jdurant@ca.sandia.gov

The past several years have seen an explosion in interest in Density Functional Theory (DFT) within the chemical physics community. The DFT method has very favorable scaling behavior with system size, behaving similarly to HF methods. Indeed, there are now a number of algorithms which, for large systems exhibit linear scaling of compute time with system size. Additionally, the algorithms used to compute DFT energies, like those used in HF calculations, are easily parallelized, allowing efficient use of present high performance computing platforms. However, unlike HF, the DFT method includes electron-electron correlation energy. This obviates the need for more computationally expensive (and difficult to parallelize) post-SCF calculations to recover the correlation energy, and means that, in principle, DFT can provide the exact electronic energy for much larger systems than can be treated by more conventional post-SCF methods.

Hohenberg and Kohn have proven that there exists a density functional which relates the electron density to the exact energy for the ground state of any multi-electron system. Unfortunately, they do not tell us what that functional is, or how to approach its performance in a systematic way. As a result, considerable effort has been devoted to construction of new functionals and evaluation of their performance. Typically evaluation is done for species at their equilibrium geometries. However, there has been much less attention paid to the performance of these functionals for transition states.

We have therefore evaluated the performance of five popular DFT functionals, BH&HLYP, B39W91, B3P86, B3LYP and BLYP in characterizing a set of "well known" transition states. We calculated geometries, real and imaginary frequencies and classical barrier heights for these transition states. We have also characterized the effects of increasing basis set size by performing calculations.

We find BH&HLYP performs best in calculating classical barrier heights. The other functionals gave rise to surfaces which were too attractive, and systematically underpredicted barrier heights. The BLYP functional was the one "pure" DFT functional considered in this work. It gave rise to barrierless surface for the

$O + HCl \rightarrow OH + Cl$,

$F + H_2 \rightarrow HF + H$

and $N + O_2 \rightarrow NO + O$

transition states. This poor performance highlights the need for inclusion of HF exchange into the functional, resulting in "hybrid functionals." All the functionals perform reasonably well predicting geometries, and the BH&HLYP, B3PW91 and B3P86 functionals have similar performance in predicting vibrational frequencies. In examining the effect of basis set size we find essentially no systematic improvement in performance with increase in basis set size, from 6-31G(d) to 6-311G(3df, 2p).

This work was sponsored by the U.S. Department of Energy, Office of Basic Energy Sciences, Division of Chemical Sciences.

Complete Basis Set Reaction Rates

George Petersson

Hall-Atwater Laboratories of Chemistry, Wesleyan University, Middletown CT 06459
tel: (860) 685-2508; fax: (860) 685-2211
email: gpetersson@wesleyan.edu

The slow convergence of the correlation energy with the one-electron basis set expansion has provided the motivation for several attempts to extrapolate to the complete basis set limit.[1-8] In a series of papers,[3-5] we demonstrated the N^{-1} asymptotic convergence of second-order pair correlation energies[9] calculated with the leading N pair natural orbitals.[10] Subsequently,[11-15] we used these asymptotic results to develop practical methods for extrapolating finite basis set calculations to obtain estimates of the complete basis set (CBS) limit. The essential idea is conveyed by a graph of $e_{ij}(N)$ as a function of $(\Sigma C_\mu)^2(N+\delta_{ij})^{-1}$, where the C_μ 's are obtained from the first-order wave function, $\psi^{(1)} = \sum C_\mu \Phi_\mu$. As $N \rightarrow \infty$, $(N+\delta_{ij})^{-1}$ approaches zero, so the intercept is the CBS limit, $e_{ij}(\infty)$. Note that only certain closed-shell sets of pair natural orbitals (denoted by filled red circles in the figure) are useful for the extrapolation. The precise CBS extrapolation algorithm that has been implemented in the commercially available computer program[18] Gaussian 94 has been described in detail elsewhere.[16-19] The extrapolated CBS energy is size-consistent and will approach the exact energy as the basis set employed in the calculations is systematically improved.

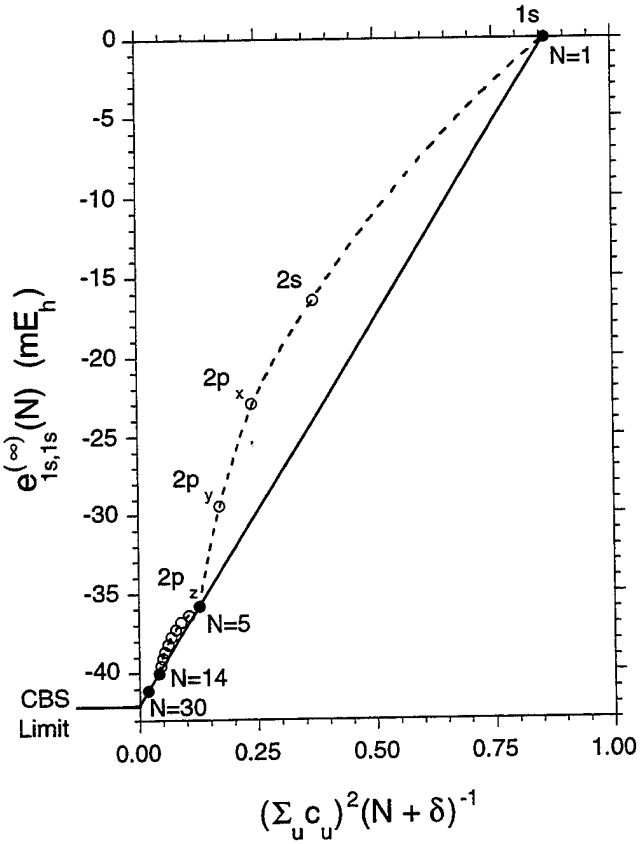

The accurate calculation of molecular energies requires convergence of both the one-particle (basis set) expansion and the n-particle (CI, perturbation, or coupled-cluster) expansion. However, the order-by- order contributions to chemical energies, and thus the number of significant figures required, generally decrease with increasing order of perturbation theory. The general approach for our CBS-n models is therefore to first determine the geometry and ZPE at a low level of theory, and then perform a high level single point electronic energy calculation at this geometry using large basis sets for the SCF calculation, medium basis sets for the MP2 calculation, and small basis sets for the higher-order

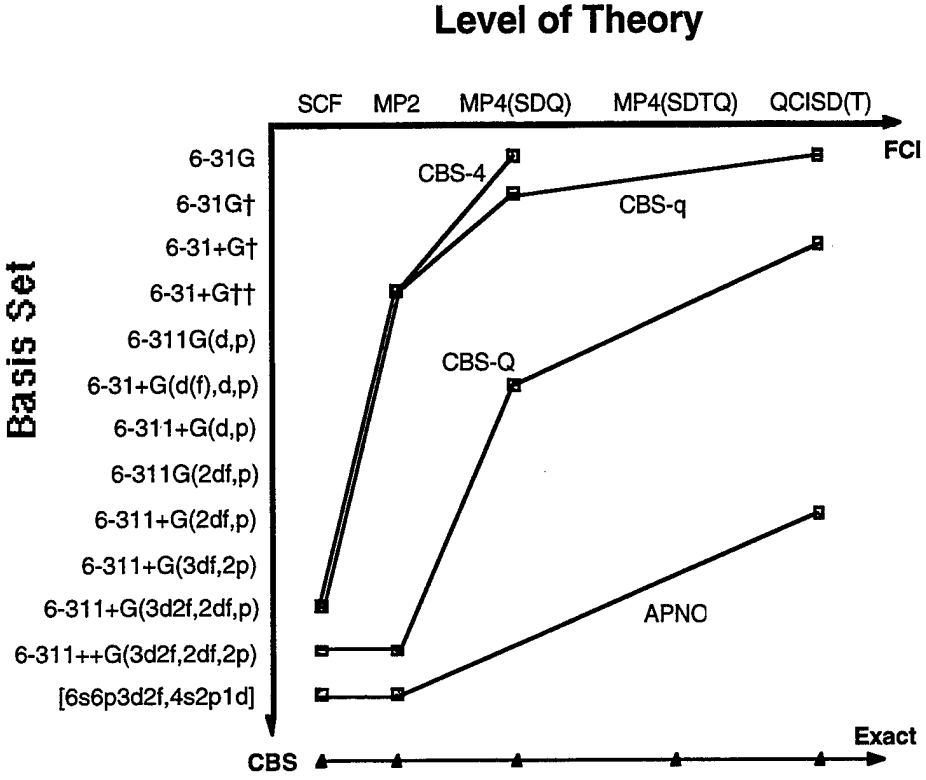

calculations through order n. The components of each model have been selected to be balanced so that no single component dominates either the computer time or the error. The CBS-n models employ the above asymptotic extrapolation to reduce the error from truncation of the basis sets used to calculate the correlation energy. The compound model single point energy is evaluated at a geometry determined at a lower level of theory (*e.g.* CBS-4//UHF/3-21G),[17] which we shall reexamine when we consider transition states. Our sequence of cost effective computational models are denoted CBS-4, CBS-Q, and CBS-QCI/APNO. The RMS errors for the 125 chemical energy differences of the G2 test set[20] are 2.5, 1.3, and 0.7 kcal/mol respectively.

The absolute rates of chemical reactions present a formidable challenge to theoretical predictions. The principal difficulty for theoretical predictions lies in the extreme sensitivity of $k_{rate}(T)$ to small errors in the activation energy, $\Delta E^{\ddagger}$, which can be interpreted as the difference in energy between the "transition state" and the reactants.[21] An error of only 1.4

kcal/mol in $\Delta E^{\ddagger}$ leads to an error of an order-of-magnitude in $k_{rate}(T)$ at room temperature.

The development of analytical gradient and curvature methods[22-28] has made possible the rigorous determination of transition states within a given level of correlation energy and basis set (*e.g.* MP2/6-31G*).[29] The potential energy surface (PES) for a typical bimolecular chemical reaction includes valleys (leading to the reactants and products) connected at the transition state (TS), which is a first-order saddle point (*i.e.* a stationary point with exactly one negative force constant). The reaction path or intrinsic reaction coordinate (IRC) is defined[30,31] as the path beginning in the direction of negative curvature away from the TS and following the gradient of the PES to the reactants and products.

If we move in a direction perpendicular to the reaction path, we find a potential energy curve (or surface) corresponding to a stable reactant or product molecule if we are far from the TS. Even around the TS, the variation of the PES perpendicular to the IRC is very similar to the PES for a stable molecule. Transition States differ from stable molecules in that they possess one negative force constant which defines the reaction coordinate.

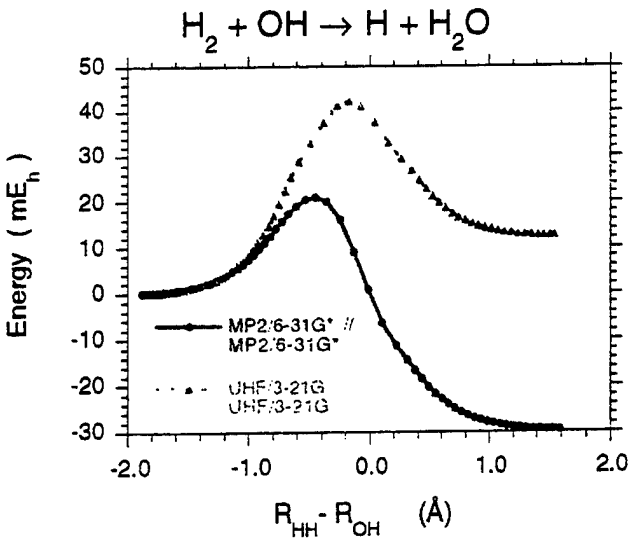

Calculated energies along the coordinates with positive force constants behave very much like their counterparts in stable molecules. However, the energy changes along the reaction coordinate are much more difficult to predict. It is the variation of the energy along this coordinate that is very sensitive to (and thus requires the inclusion of) the correlation energy, as demonstrated by the figure to the left. Based on these observations, we have developed[32] the *"IRCMax" transition state method*, in which we select the [Method(1)] (*e.g.* MP2/6-31G* in the figure below) along the low-level IRC obtained from the Geom[Method(2)] (*e.g.* UHF/3-21G in the figure below) calculations. The IRCMax transition state extension of the compound models takes advantage of the enormous improvement (from one to two orders-of-magnitude) in computational speed[19] achieved

by using the low-level, Geom[Method(2)] (*e.g.* UHF/3-21G in our example), IRC calculations. We then perform several single point higher level, Energy[Method(1)] (*e.g.* MP2/6-31G* in our example), calculations along the Geom[Method(2)] reaction path to locate the Energy[Method(1)] transition state, that is, the maximum of Energy[Method(1)] along the Geom[Method(2)] IRC. Calculations at three points bracketing the transition state are sufficient to permit a parabolic fit and the activation energy.

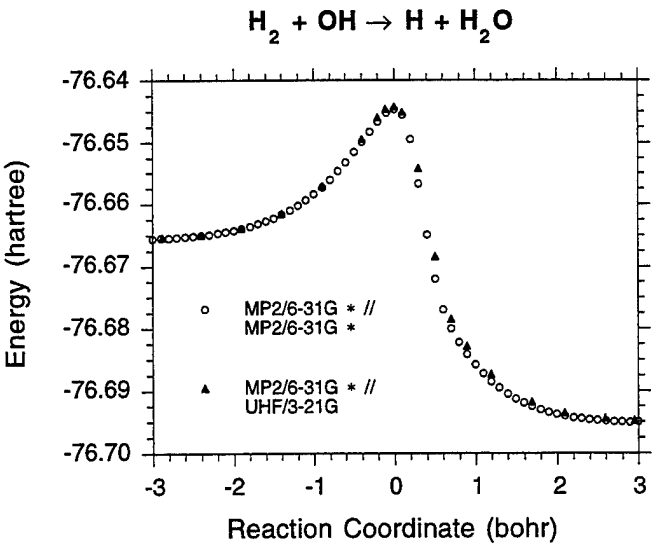

Since we determine the maximum of Energy[Method(1)] along a path from reactants to products, the IRCMax method gives a rigorous upper bound to the high-level Method(1) transition state energy. In addition, when applied to the compound CBS and G2 models, the IRCMax method reduces to the normal treatment of bimolecular reactants and products, Energy[Method(1)]//Geom[Method(2)]. Thus the IRCMax method can be viewed as an extension of these compound models to transition states. The results presented demonstrate the numerical superiority of this IRCMax method, Max{Energy[Method(1)]}// IRC{Geom[Method(2)]}, over conventional Energy[Method(1)]//Geom[Method(2)] calculations. Errors in transition state geometries are reduced by as much as a factor of five and errors in barrier heights are reduced by as much as a factor of ten.[32]

More than sixty years ago, Eyring proposed[33] the use of statistical mechanics to evaluate the absolute rate constant:

$$k_{rate}(T) = \frac{Q^{\ddagger}(T)}{Q_{R_1}(T)\,Q_{R_2}(T)} \bullet \frac{k_B T}{h} \int_0^{\infty} \kappa(E)\, e^{-E / k_B T}\, dE \qquad (1)$$

Truhlar and Kuppermann introduced[30] the correct definition of the reaction path, R, in mass weighted coordinates and were the first to recognize the importance of including in $V(R)$, the quantum mechanical zero-point vibrational energy for all normal modes that are orthogonal to R. Changes in zero-point energies along the reaction paths for the exothermic reactions can increase the barrier height (by 0.6 kcal/mol for H_2 + OH) or decrease the barrier height (by 0.4 kcal/mol for H_2 + F) depending on the stiffness of the bending force

constant. Accurate rate constants can only be obtained if we include the ZPE in our determination of the IRCMax transition state geometry and energy. Our final algorithm is thus an adaptation of Truhlar's "zero curvature variational transition state theory" (ZC-VTST)[34] to our CBS models[16-18] through use of the IRCMax technique.[32]

The challenge we face is to accurately determine all the quantities required to evaluate Eq.(1). We have selected five hydrogen abstraction reactions for the initial test of our methodology. The barrier heights for these reactions range from 1.3 kcal/mol (H_2 + F) to 20.6 kcal/mol (H_2O + H). We include temperatures from 250 K to 2500 K. The rate constants range from 10^{-18} up to 10^{-10} cm^3 / molecule sec. If we include variations of the zero-point energy along the reaction path (*i.e.* variational transition state theory),[34] all absolute rate constants obtained from our CBS-QCI/APNO model are within the uncertainty of the experiments.[35] The

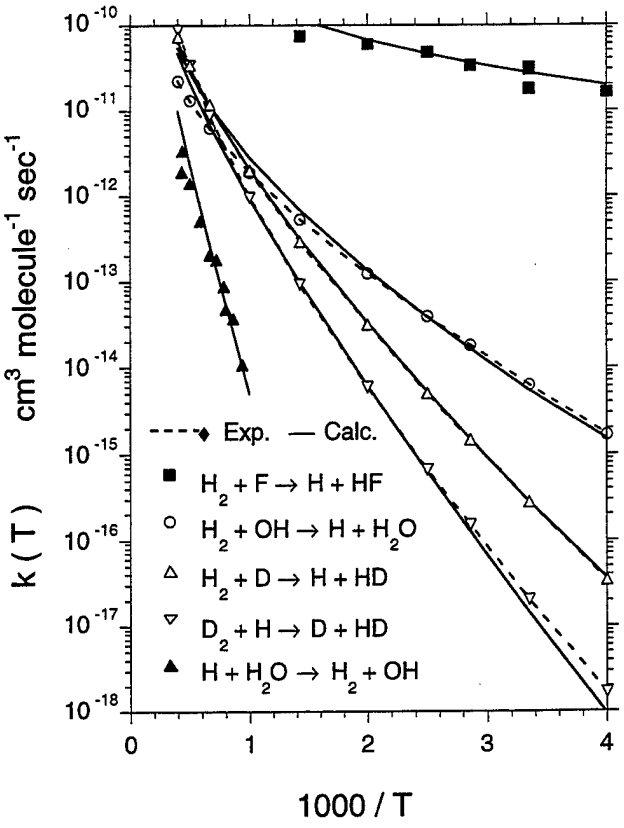

dashed curves and open symbols for H_2 + OH, H_2 + D, and D_2 + H represent the least-squares fits of smooth curves to large experimental data sets in an attempt to reduce the noise level in the experimental data.[35] The close agreement with theory suggests that this attempt was successful.

The problem of predicting absolute rates for a wide range of gas phase chemical reactions has in principle been solved. We have made contact with experiment, demonstrating that in favorable circumstances a sufficiently accurate evaluation of Eq.(1) can provide absolute rate constants within the uncertainty of experimental rates. However, much remains to be done. We must systematically determine the minimum level of calculation necessary to maintain the accuracy of each part of these calculations. Nevertheless, the use of the IRCMax method with the G2 and CBS-Q computational models is giving immediate improvements in our ability to solve practical problems.

Acknowledgments

The complete basis set extrapolation was developed in collaboration with Marc R. Nyden, Thomas G. Tensfeldt, and Mohammed A. Al-Laham. The CBS-4, CBS-Q, and CBS-QCI/APNO models were developed in collaboration with Joseph W. Ochterski and John A. Montgomery, Jr. The IRCMax method was developed in collaboration with John A. Montgomery, Jr. and David Malick. The absolute rate calculations were a collaborative effort with Paul Marshall. We are grateful to the Air Force Office of Scientific Research, the Petroleum Research Fund, and Gaussian. Inc. for their continued support of this research.

References

1. Schwartz, C. *Phys. Rev.* **1962**, *126*, 1015.
2. Schwartz, C. In *Methods in Computational Physics*; Alder, B.; Fernbach, S.; Rotenberg, M., Eds., Academic: New York, 1963, Vol. 2.
3. Nyden, M. R.; Petersson, G. A. *J. Chem. Phys.* **1981**, *75*, 1843.
4. Petersson, G. A.; Nyden, M. R. *J. Chem. Phys.* **1981**, *75*, 3423.
5. Petersson, G. A.; Licht, S. L. *J. Chem. Phys.* **1981**, *75*, 4556.
6. Brown, F. B.; Truhlar, D. G. *Chem. Phys. Lett.* **1985**, *117*, 307.
7. Dunning, T. H., Jr. *J. Chem. Phys.* **1989**, *90*, 1007.
8. Siegbahn, P. E. M.; Blomberg, M. R. A.; Svensson, M. *Chem. Phys. Lett.* **1994**, *223*, 35.
9. Møller, C.; Plesset, M. S. *Phys. Rev.* **1934**, *46*, 618.
10. Löwdin, P. O. *Phys. Rev.* **1955**, *97*, 1474.
11. Petersson, G. A.; Yee, A. K.; Bennett, A. *J. Chem. Phys.* **1985**, *83*, 5105.
12. Petersson, G. A.; Braunstein, M. *J. Chem. Phys.* **1985**, *83*, 5129.
13. Petersson, G. A.; Bennett, A; Tensfeldt, T. A.; Al-Laham, M. A.; Shirley, W. A.; Mantzaris, J. *J. Chem. Phys.* **1988**, *89*, 2193.
14. Petersson, G. A.; Al-Laham, M. A.; *J. Chem. Phys.* **1991**, *94*, 6081.
15. Petersson, G. A.; Tensfeldt, T. G.; Montgomery, J. A., Jr. *J. Chem. Phys.* **1991**, *94*, 6091.
16. Montgomery, J. A., Jr.; Ochterski, J. W.; Petersson, G. A. *J. Chem. Phys.* **1994**, *101*, 5900.
17. Ochterski, J. W.; Petersson, G. A.; Montgomery, J. A., Jr. *J. Chem. Phys.* **1996**, *104*, 2598.
18. Frisch, M. J.; Trucks, G. W.; Schlegel, H. B.; Gill, P. M. W.; Johnson, B. G.; Robb, M. A.; Cheeseman, J. R.; Keith, T.; Petersson, G. A.; Montgomery, J. A., Jr., Raghavachari, K.; Al-Laham, M. A.; Zakrzewski, V. G.; Ortiz, J. V.; Foresman, J. B.; Peng, C. Y.; Ayala, P. Y.; Chen, W.; Wong, M. W.; Andres, J. L.; Replogle, E. S.; Gomperts, R.; Martin, R. L.; Fox, D. J.; Binkley, J. S.; Defrees, D. J.; Baker, J.;

Stewart, J. P.; Head-Gordon, M.; Gonzalez, C.; Pople, J. A. *Gaussian94*, Revision B.3: Gaussian, Inc.: Pittsburgh PA, **1995**.
19. Foresman, J. B.; Frisch, A. *Exploring Chemistry with Electronic Structure Methods*, 2nd ed.; Gaussian, Inc.: Pittsburgh, PA., 1996.
20. Curtiss, L. A.; Raghavachari, K.; Pople, J. A. *J. Chem. Phys.* **1993**, *98*, 1293.
21. Arrhenius, S. *Z. Phys. Chem.* **1889**, *4*, 226.
22. Peng, C.; Schlegel, H. B. *Israel J. Chem.* **1993**, *33*, 449.
23. Handy, N. C.; Schaefer, H. F., III, *J. Chem. Phys.* **1984**, *81*, 5031.
24. Pople, J. A.; Krishnan, R.; Schlegel, H. B.; Binkley, J. S. *Int. J. Quant. Chem. Symp.* **1979**, *13*, 325.
25. Schlegel, H. B. *J. Comput. Chem.* **1982**, *3*, 214.
26. Head-Gordon, M.; Head-Gordon, T. *Chem. Phys. Lett.* **1994**, *220*, 122.
27. Frisch, M. J.; Head-Gordon, M.; Pople, J. A. *Chem. Phys. Lett.* **1990**, *166*, 275.
28. Frisch, M. J.; Head-Gordon, M.; Pople, J. A. *Chem. Phys. Lett.* **1990**, *166*, 281.
29. Hehre, W. J.; Radom, L.; Schleyer, P. v. R.; Pople, J. A. *Ab Initio Molecular Orbital Theory*; John Wiley & Sons: New York, 1986.
30. Truhlar, D. G.; Kuppermann, A. *J. Am. Chem. Soc.* **1971**, *93*, 1840.
31. Gonzalez, C.; Schlegel, H. B. *J. Phys. Chem.* **1989**, *90*, 2154.
32. Malick, D. K.; Petersson, G. A.; Montgomery, J. A., Jr. submitted.
33. Eyring, H. *J. Chem. Phys.* **1935**, *3*, 107.
34. Truhlar, D. G. *J. Chem. Phys.* **1970**, *53*, 2041.
35. NIST Chemical Kinetics Database, version 6.0.

Rate Constant Predictions for Hydrogen Abstraction from Halomethanes

Martin Schwartz,[a] Paul Marshall,[a] and Rajiv J. Berry[b]

[a]*Department of Chemistry, University of North Texas, Denton, TX 76203*
tel: (940) 565-3542; fax: (940) 565-4318
email: marty@unt.edu

[b]*WL/MLBT, Wright-Patterson AFB, OH 45433*

Partially hydrogenated fluorocarbons and chlorofluorocarbons have been proposed as potential replacements for the halon (bromofluorocarbon) fire suppressants, which have been banned from further manufacture due to their high ozone depletion potentials.

Evaluation of the efficacy of these compounds to serve as alternative fire suppressants can, in principle, be greatly aided via high temperature computational kinetic modeling of the interactions of HFCs and CFCs and their decomposition products with the species present in hydrocarbon fires. The reliability of this modeling is critically dependent upon the accuracy of estimated rate constants for the various reactions involving these species under combustion conditions ($\geq$2000 K). Unfortunately, the required kinetic data are often unavailable or else have been obtained only at temperatures below 1000 K.

One of the most important species responsible for flame propagation is the hydroxyl radical, which can also act to initiate decomposition of halomethanes via proton abstraction:

$$CH_xF_yCl_z + OH \rightarrow CH_{x-1}F_yCl_z + H_2O \qquad [1]$$

We have utilized *ab initio* quantum mechanics and Canonical Transition State Theory (TST) to calculate the rate constants for proton abstraction from the ten members of this series at temperatures ranging from 250 K to 2000 K, using the equation:

$$k_{TST} = \Gamma \frac{k_B T}{h} \frac{Q_{TS}}{Q_{Rct}} e^{-\frac{E_o^{\ddagger}}{RT}} \qquad [2]$$

In this equation, $E_o^{\ddagger}$ is the classical forward energy barrier, Q_{TS} and Q_{Rct} are the statistical mechanical partition functions of the transition state and reactants, and Γ represents the tunneling factor, which is expected to be important in proton transfer reactions.

Initial procedures utilized G2 energies calculated for the reactants, products and for the MP2/6-31G(d) transition state to determine the forward and reverse energy barriers, together with the HF/6-31G(d) imaginary frequency (ω_i) [required for the calculation of Γ] to determine k_{TST} via Eq. (2). Values of the calculated rate constant were found to be more than an order of magnitude greater than experiment. Even after the classical barrier height (often found to be the major source of error in rate constant calculations) was adjusted to effect agreement between k_{TST} and k_{exp} at 298 K, it was observed that the curvature of the Arrhenius plot of the temperature dependence of calculated rate constants was substantially greater than found for the measured rate constants.

In order to ascertain the sources of error in k_{TST}, G2 energies were determined at various points along the MP2/6-31G(d) Intrinsic Reaction Coordinate (IRC). It was found that (a) the maximum in the G2 potential energy surface (PES) was somewhat greater than the G2 energy evaluated at the MP2 transition state, and (b) the breadth of the higher level PES was substantially greater than that predicted using the HF/6-31G(d) imaginary frequency. In order to correct these errors, the G2 energies along the IRC were fit by a semi-empirical Eckart potential function to extract a better value for the barrier and for the imaginary frequency. Significantly, it was found that the value of ω_i determined by this fit was, typically, a factor of 2.5 lower than the HF frequency [e.g. for the CH_4 + OH reaction, ω_i(Fit) = 1165 cm^{-1} vs. ω_i(HF) = 2836 cm^{-1}].

When the fitted energy barrier and imaginary frequency were utilized to determine k_{TST}, it was found that computed rate constants were somewhat lower than experiment. However, this time, following a relatively small adjustment in the barrier height [$\Delta E_o^{\ddagger} = -4.0 \pm 2.0$ kJ/mol] to require that $k_{TST} = k_{exp}$ at 298 K, the computed and experimental rate constants were in almost perfect agreement with experiment for all 10 reactions at all temperatures where experimental data are available.

Mechanism for Perfluoroisobutene Production during Fluorocarbon Pyrolysis

Robert P. Salmon and Edward R. Ritter

Department of Chemical Engineering, Villanova University, Villanova PA 19085
tel: (610) 519-4948; fax: (610) 519-7354
email: eritter@ucis.vill.edu

This work presents results of an experimental study which focuses on the formation of perfluoroisobutene (i-C_4F_8). Experiments were carried out at atmospheric pressure in a quartz flow tube reactor over the temperature range of 823K to 1273K and an initial reactant feed concentration of 2% with the balance nitrogen. Reactants studied include chlorodifluoromethane (CHF_2Cl), 1,1,1,2-tetrafluoro-2-chloroethane (CF_3CHFCl), trifluoromethane (CHF_3), perfluoropropene (C_3F_6), and mixtures of these species. Effluent gas concentrations were obtained using a water cooled gas sampling probe, and analysis of products was performed via on line gas chromatography with flame ionization detection and gas chromatography with mass selective detection. C_3F_6 pyrolysis produced more than 22% i-C_4F_8 yield, while mixtures with CHF_2Cl and CHF_3 resulted in i-C_4F_8 yields of 13% and 28%, respectively. The pyrolysis of CF_3CHFCl resulted in slightly greater than 6% i- C_4F_8 yield, and CHF_2Cl decomposition produced up to 6% i-C_4F_8 yield, while CHF_2Cl/CF_3CHFCl copyrolysis produced 8% yield of i-C_4F_8. These results suggest that the addition of a difluoromethylene (^{1}:CF_2) source increases i-C_4F_8 production. This is consistent with the major pathway to i-C_4F_8 production being C_3F_6 isomerization to singlet perfluorodimethylcarbene (^{1}:$C(CF_3)_2$) and subsequent collisional stabilization to the triplet carbene (^{3}:$C(CF_3)_2$) followed by ^{1}:CF_2 addition. This work focuses on an experimental study and detailed modeling is beyond the scope of this work.

EXPERIMENTAL: This experimental study was carried out in a tubular flow reactor. Experiments were performed with dilute (2%) mixtures of various chlorinated and fluorinated hydrocarbons with the balance nitrogen. A detailed description of the experimental apparatus is presented elsewhere (DiFelice and Ritter, 1996) and will be briefly summarized here. The apparatus consisted of a 2.0 cm id quartz tube and a six zone electrically heated tube furnace. Each zone was 7.6 cm (3 inches) long, for a total furnace length of 45.7 cm (18 inches). All experiments were performed isobarically near 1 atmosphere. The entire apparatus was enclosed in a Plexiglas structure vented to the hood system in order to prevent any possible exposure to i-C_4F_8. The reactor effluent was sent to a series of two scrubbers filled with a saturated aqueous calcium hydroxide solution to fix any free fluoride as insoluble calcium fluoride (CaF_2). Gaseous scrubber effluent was vented 10 feet into the fume hood duct. Analytical capabilities consisted of on-line gas chromatography with flame ionization detection (GC/FID) and gas chromatography with mass selective detection (GC/MS). Inlet gas samples were drawn through a bypass line

and reactor effluent gas samples were drawn through a stainless-steel water-cooled gas-sampling probe moved axially to vary reaction time. Reactant and stable products were quantified using a GOW MAC model 750 P gas chromatograph (GC) with dual flame ionization detectors(FIDs). Gas chromatographic separations were carried out using a packed column Graphpac 60/80 mesh with 5% Fluorocol (Supelco). Product identification was performed with a Hewlett Packard 5890 Series II gas chromatograph equipped with a 5972 Series mass selective detector. A Carbograph 1 capillary column (30 m X 0.25mm ID, Alltech) was used under cryogenic temperature conditions to achieve separation of fluorinated and chlorinated hydrocarbon mixtures.

RESULTS: *Copyrolysis of C_3F_6 and CHF_3 in Nitrogen Bath Gas*

In separate studies, 2% mixtures of CHF_3 and C_3F_6 in nitrogen were pyrolyzed and the concentrations of major products and perfluoroisobutene were measured. Both reactants were observed to form sizable amounts of i-C_4F_8. To further investigate the chemistry, CHF_3 was copyrolyzed with C_3F_6. We have studied the decomposition of 2% CHF_3/2% C_3F_6 mixtures from 1023K to 1223K at 2 seconds reaction time. It was found that for temperatures below 1173K, more than 95% of the carbon fed to the reactor is accounted for as gas phase product. Above this temperature the carbon balance begins to decrease to 85% at 1223K. The conversion of C_3F_6 appears to decrease slightly as a result of the addition of CHF_3, however, it was observed that CHF_3 decomposes to form C_3F_6 as a reaction product. The major product at the lower temperatures is C_2F_4, however, i-C_4F_8 formation increases substantially as the temperature is increased. It accounts for almost 30% of the initial carbon fed to system at 1223K and 2 seconds reaction time. Other products include C_4F_6 and C_4F_8 (perfluoro-2-butene).

DISCUSSION: *Reaction Pathways to i-C_4F_8 via CHF_3 and C_3F_6*

Based on the results of this study it is suggested that one possible mechanism to i-C_4F_8 formation is as follows. Trifluoromethane (CHF_3) decomposes via HF elimination to form difluoromethylene (Schug and Wagner, 1979).

$$CHF_3 \rightarrow {}^1{:}CF_2 + HF$$

Perfluoropropene (C_3F_6) can undergo a 1,2 fluorine shift to form perfluorodimethylcarbene (Buravtsev et al, 1989 and Zaitsev et al, 1990).

$$C_3F_6 \rightarrow {}^1{:}C(CF_3)_2$$

Preliminary MP4 calculations performed at this lab using the Gaussian 94 computer code (Frisch et al, 1995) suggest an upper limit activation energy (E_a) of 74.3 kcal/mol for this isomerization. The singlet-triplet splitting of this carbene has been reported as -17.8

kcal/mol, (Dixon, 1986) where a negative indicates a ground state triplet. Therefore, once formed, this singlet carbene can be collisionally stabilized to form the triplet,

$$^1{:}C(CF_3)_2 + M \rightarrow {}^3{:}C(CF_3)_2 + M$$

where M indicates a third body.

In singlet carbenes the two electrons on the carbon have opposite spin and are paired. These are designated with a superscript ^{1} as in $^1{:}CH_2$ (singlet methylene). Triplet carbenes, on the other hand, have electrons with the same spin and remain unpaired. These are designated with a ^{3} as in $^3{:}CH_2$ (triplet methylene).

Perfluoropropene can also undergo carbon-carbon bond rupture to form perfluoromethylcarbene and difluoromethylene.

$$C_3F_6 \rightarrow {}^1{:}CFCF_3 + {}^1{:}CF_2 \qquad \Delta H_r^\circ = 103.5 \text{ kcal/mol}$$

This reaction has an estimated $E_a = 106$ kcal/mol based on $\Delta H + RT_m$ which is significantly higher than that of C_3F_6 isomerization. This suggests that isomerization to $^1{:}C(CF_2)_3$ is a favorable pathway. Once $^3{:}C(CF_3)_2$ is formed, it is essentially trapped because of the large energy barrier for isomerization back to C_3F_6. Holmes and Rakestraw (1992) state the barrier for rearrangement of triplet carbenes is very high. They reference studies that give the E_a for a 1,2- hydrogen shift for both triplet CH_3CH and triplet $CH_2{=}C$ greater than 50 kcal/mol. Energy requirements for fluorine migration are expected to be larger than hydrogen migration.

A QRRK analysis was performed on C_3F_6 decomposition and isomerization and shows that isomerization to $^1{:}C(CF_3)_2$ is dominant across the temperature range 1123K - 1223K. The net rate of $^3{:}C(CF_3)_2$ formation is the sum of the rate of formation of $^3{:}C(CF_3)_2$ and $^1{:}C(CF_3)_2$, because $^1{:}C(CF_3)_2$ is an excited state and would be collisionally stabilized to $^3{:}C(CF_3)_2$, not $^1{:}C(CF_3)_2$. This suggests that i-C_4F_8 formation is limited by $^1{:}CF_2$, which accounts for the dramatic increase in i-C_4F_8 when C_3F_6 is copyrolyzed with a $^1{:}CF_2$ source. At high temperatures (1250K) the rate of dissociation is comparable to $^3{:}C(CF_3)_2$ formation.

Once perfluorodimethylcarbene is formed, difluoromethylene can then combine with triplet perfluorodimethylcarbene to form a triplet perfluoroisobutene diradical. This can then be collisionally stabilized to perfluoroisobutene. Difluoromethylene can also combine with singlet perfluorodimethylcarbene to give perfluoroisobutene directly.

$$^1{:}CF_2 + {}^3{:}C(CF_3)_2 \rightarrow i\text{-}C_4F_8\,(t)$$
$$i\text{-}C_4F_8\,(t) + M \rightarrow i\text{-}C_4F_8 + M$$
$$^1{:}CF2 + {}^1{:}C(CF_3)_2 \rightarrow i\text{-}C_4F_8$$

The energy requirements for these combinations appear to be rather small. Triplet carbenes are diradicals, therefore an estimate for the E_a for $^1{:}CF_2$ combination with $^3{:}C(CF_3)_2$ can be obtained from Burgess et. al. (1995) who give an E_a = 5.2 kcal/mol for $^1{:}CF_2$ combination with $.CHF_2$. This reaction mechanism appears to be the most likely reaction pathway to i-C_4F_8. A discussion of other potential pathways will also be presented.

REFERENCES:

Buravtsev, N.N.; Grigor'ev A. S.; Kolbanovskii Y. A.,(1989), *Kinet. Cata.*, 30, 386.

Burgess D.R.F.; Zachariah, M.R.; Tsang, W.; Westmoreland, P.R., (1995) NIST Technical Note 1412.

DiFelice, J.J.; Ritter, E.R., (1996), *Combst. Sci. Tech.*, 116-117, 5-30.

Dixon, David A., (1986), *J. Phys. Chem.*, 90, 54.

Frisch, M.J.; Trucks, G.W.; Schlegel, H.B.; Gill, M.W.; Johnson, B.G.; Robb, M.A.; Cheeseman, J.R.; Keith, T.; Petersson, G.A.; Montgomery, J.A.; Raghavachari, K; Al-Laham, M.A.; Zakrzewski, V.G.; Ortiz, J.V.; Foresman, J.B.; Cioslowski, J.; Stefanov, B.B.; Nanayakkara, A.; Challacombe, M.; Peng, C.Y.; Ayala, P.Y.; Chen, W; Wong, M.W.; Andres, J.L.; Replogle, E.S.; Gomperts, R; Martin, R.L.; Fox, D.J.; Binkley, J.S.; Defrees, D.J.; Baker, J.; Stewart, J.P.; Head-Gordon, M.; Gonzalez, C.; Pople, J.A., (1995), Gaussian 94, Revision E.1, Gaussian Inc., Pittsburgh, PA.

Holmes, B.E. and Rakestraw, D.J., (1992), *J. Phys. Chem.*, 96, 2210.

Schug, K.P.; Wagner, H.; Zabel, F., (1979), *Ber. Bunsenges. Phys. Chem.*, 83, 167.

Zaitsev, S.A.; Kushina, L.I.; Fedurtsa, M.U.; Shchemelev, G.V.; Kushina, I.D.; Barabanov, V.G., (1990), *Ukr.Khim. Zh,* (Russ. Ed.), 56(8), 893-894.

The Use of BAC-MP4 Calculations in the Development of a Chemical Kinetic Mechanism for Fluorinated Hydrocarbons

Donald R. Burgess, Jr. and Michael R. Zachariah

Process Measurements DivisionReacting Flows Group, Physics B312, National Institute of Standards and Technology, Gaithersburg, MD 20899
tel: (301) 975-2614; fax: (301) 869-5924
email: dburgess@nist.gov

Development of a comprehensive reaction set that describes the destruction of fluorinated hydrocarbons and their influence on hydrocarbon flame chemistry involves many different procedures. There exists in the literature much experimentally-derived thermochemical data for fluorocarbon species and rate constants for relevant reactions. However, there is a lot of data that does not exist or is incomplete (for example, rate constants only at room temperature), especially for radicals. Consequently, in order to have a complete reaction set, thermochemical and chemical kinetic data must be estimated by analogy to other species and reactions using bond dissociation energies (BDE), Evans-Polanyi relationships, and the like. Given a rate constant at one temperature and some knowledge of the transition state, one can estimate/calculate the temperature dependence of a given reaction using RRK methods. In some cases, no experimental data or good analogy exists and, consequently, one must employ ab initio procedures to calculate thermochemical and chemical kinetic data in order to complete the reaction set. We report on our use of HF/6-31G(d)//MP4/6-31G(d,p) calculations to determine the structures and energies of fluorinated hydrocarbon molecules and transition states. A Bond-Additivity-Correction (BAC) procedure was used to provide chemically accurate energies (<10 kJ/mol). The utility of these calculations will be discussed and comparisons with experimental data will be provided.

Assembling a Reaction Mechanism for CF_3CHFCF_3 in Flames

Phillip R. Westmoreland

Chemical Engineering; University of Massachusetts Amherst, 159 Goessmann, Box 33110; Amherst MA 01003-3110
tel: (413) 545-1750; fax: (413) 545-1647
westm@ecs.umass.edu; http://www.ecs.umass.edu/che/westmoreland.html

A mechanism and parameter set have been developed for CF_3CHFCF_3 (Fig. 1), which is being investigated as a Halon 1301 replacement by experiments and flame modeling. A set of reactions proposed based on principles developed in earlier work at NIST on C_1 and C_2 fluoroalkanes.[1] Unfortunately, the only literature data available on the mechanism's parameters are $\Delta_f H^\circ_{298}(CF_2{=}CFCF_3)$, $\Delta_f H^\circ_{298}(CF_3\text{-}CO\text{-}CF_3)$, and limited kinetics, so the BAC-MP4 method[2] is used for predictions of thermochemistry and high-pressure-limit kinetics.

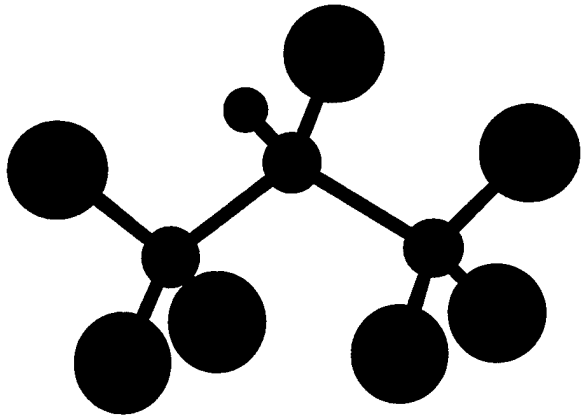

Fig. 1. Geometry of CF_3CHFCF_3 (FM-200, HFC-227ea or heptafluoropropane).

Use of CF_3CHFCF_3 was proposed by the Navy as a possible CF_3 source, based on CF_3's suppressant ability. Westbrook pioneered in mechanistic modeling of

---

[1]D. R. Burgess, M. R. Zachariah, W. Tsang, and P. R. Westmoreland, *Thermochemical and Chemical Kinetic Data for Fluorinated Hydrocarbons*, National Institute of Standards and Technology Technical Note 1412 (1995)

[2]M. R. Zachariah, P. R. Westmoreland, D. R. F. Burgess, Jr., W. Tsang, and C. F. Melius, "BAC-MP4 Predictions of Thermochemical Data for C_1 and C_2 Stable and Radical Hydrofluorocarbons and Oxidized Hydrofluorocarbons," *J. Phys. Chem.*, **100**, 8737-8747 (1996).

CF_3Br suppression chemistry.[3] His CF_3Br modeling indicated that bromine suppressed flames by removing H atoms catalytically:

$$H + HBr \rightarrow H_2 + Br$$
$$H + Br \rightarrow HBr$$

The fluorocarbon part of the molecule removed H atoms, making CF_3Br superior to CH_3Br or HBr.

The NIST (1995) modeling tested C_1 and C_2 HFC's but also clarified CF_3's role in trapping flame radicals. O and OH react with CF_3 to form unreactive CF_2=O. It slowly reacts by $H+CF_2=O \rightarrow H_2+CFO$, and although CFO is structurally like CHO, it decompose slowly. In contrast to CF_3, CHF_2 reacts with O and OH to form CHF=O, which is more reactive because of its abstractable H. High heat capacity also helps, but CF_4 is less effective than CF_3 because it is nearly inert.

Reaction classification. Understanding hydrocarbon flame chemistry provides a basis for composing the mechanism. Most important is that only two types of reactions are important in hydrofluorocarbon combustion:

- Abstraction inherently has pressure-independent rate constants. In hydrofluorocarbon flames, only abstraction of H needs to be considered because F is held so strongly. Transition-state theory is sufficient to predict rate constants, adding tunneling at lower temperatures.[4]
- Association may have pressure-dependent rate constants, depending on the pressure and product channel. The reason is that this type of reaction is "chemically activated" – chemical energy of the newly formed bond is released into rovibrational energy, which can be dissipated by breaking a bond or by collisional stabilization. For many association events, no adduct may be detectable because decomposition and/or isomerization dominates stabilization of the chemically activated adduct. Pressure dependence may then either be classical falloff or inverses falloff, where an association/decomposition channel is pressure-independent at low pressures. Common types of association in flames are radical-radical combination, radical addition to pi bonds, and carbene insertion. Prediction requires not only the reactant, transition-state, and intermediate structural and thermochemical parameters, but also a quantum reaction theory such as Bimolecular Quantum RRK,[5] RRKM,[6] or Master Equation theory.[7]

---

[3]C. K. Westbrook, *Combustion Science and Technology*, **34**, 201 (1983).
[4]K. J. Laidler, *Chemical Kinetics, 3rd Ed.*, Harper & Row, 1987.
[5]A. M. Dean, *J. Phys. Chem.*, 89:4600 (1985).
[6]P. J. Robinson, K. A. Holbrook, "Unimolecular Reactions," Wiley-Interscience, London, 1972.
[7]R. G. Gilbert, S. C. Smith, "Theory of Unimolecular and Recombination Reactions," Blackwell Scientific, Oxford, 1990.

Association includes thermal activated decomposition by the principle of microscopic reversibility. Radical decomposition by beta-scission is quite important. However, molecules do not usually decompose in flames but rather react with radicals.

In hydrofluorocarbon chemistry, 1,2- and 1,1-HF eliminations are quite important in the context of chemically activated reactions. This behavior is in contrast to hydrocarbon flames, in which molecular elimination is much less important. Consider CF_3CHFCF_3 itself. Activation energies calculated here by the BAC-MP4 method are 80.2 kcal/mol for HF elimination to make perfluoropropene, compared to 96.7 kcal/mol for C-C fission, 103.9 kcal/mol for C-H fission, and 119.9 kcal/mol for C-F fission. Thus, reaction of H with perfluoroisopropyl forms chemically activated CF_3CHFCF_3, which is not stabilized at flame temperatures but rather decomposes immediately to CF_2=$CFCF_3$ + HF.

Results. Based on the above considerations, a mechanism was proposed for the C_3 chemistry in CF_3CHFCF_3. A minimum set of parameters was developed with BAC-MP4 and quantum reaction-theory calculations, combined with the NIST C_1 and C_2 fluoroalkane set,[1] and will be tested by flame modeling with the results compared to laboratory data.

As shown in Fig. 2, CF_3CHFCF_3 probably reacts mainly by abstraction of its one H atom. For the present set, only H, O, and OH were considered as abstractors. Thermal 1,2-elimination of HF could occur, as described above, and it is included in the set; however, this elimination should be more important to the chemically activated H+C_3F_7 reaction.

Other C_3F_7 reactions include beta-scission of F and combinations with O and OH. Note that decomposition to CF_3 + C_2F_4, assumed in some other studies, would not be possible from the isopropyl radical. Instead, these products could form only from an n-propyl radical. O and OH + C_3F_7 yield chemically activated adducts, forming perfluoro-ethanal (perfluoro-acetaldehyde) and an isopropyl. Combination with O_2 could occur, but the resulting peroxyl radical was assumed to revert to reactants, giving no net reaction.

Perfluoropropene was assumed to react primarily by radical additions of H, O, and OH to the pi bond. Addition to the end carbon was analyzed, but reversion to reactants seems most likely. Addition to the center carbon gives chemically activated adducts which can then decompose by beta-scissions. The lowest-energy decomposition channel of the propene forms CF_2 + $CFCF_3$, but this channel should be too slow to compete with the radical additions.

The only thermochemistry predicted here that can be compared to data is $\Delta_f H^\circ_{298}$ for CF_2=$CFCF_3$. Its literature value is -269.0 kcal/mol (1125.5 kJ/mol), while the BAC-MP4 value is -273.4 kcal/mol (1143.9 kJ/mol).

Abstraction of the secondary H in CF_3CHFCF_3 is slower than in propane. One reason is that the H is held slightly more strongly in the fluoroalkane. The BAC-MP4 calculations give 103.9 kcal/mol (434.2 kJ/mol) as the C-H bond dissociation energy, compared to 99.8 kcal/mol (417.6 kJ/mol) in propane. As shown in Fig. 3, the transition-state-theory rate constant is an order of magnitude slower than from propane.

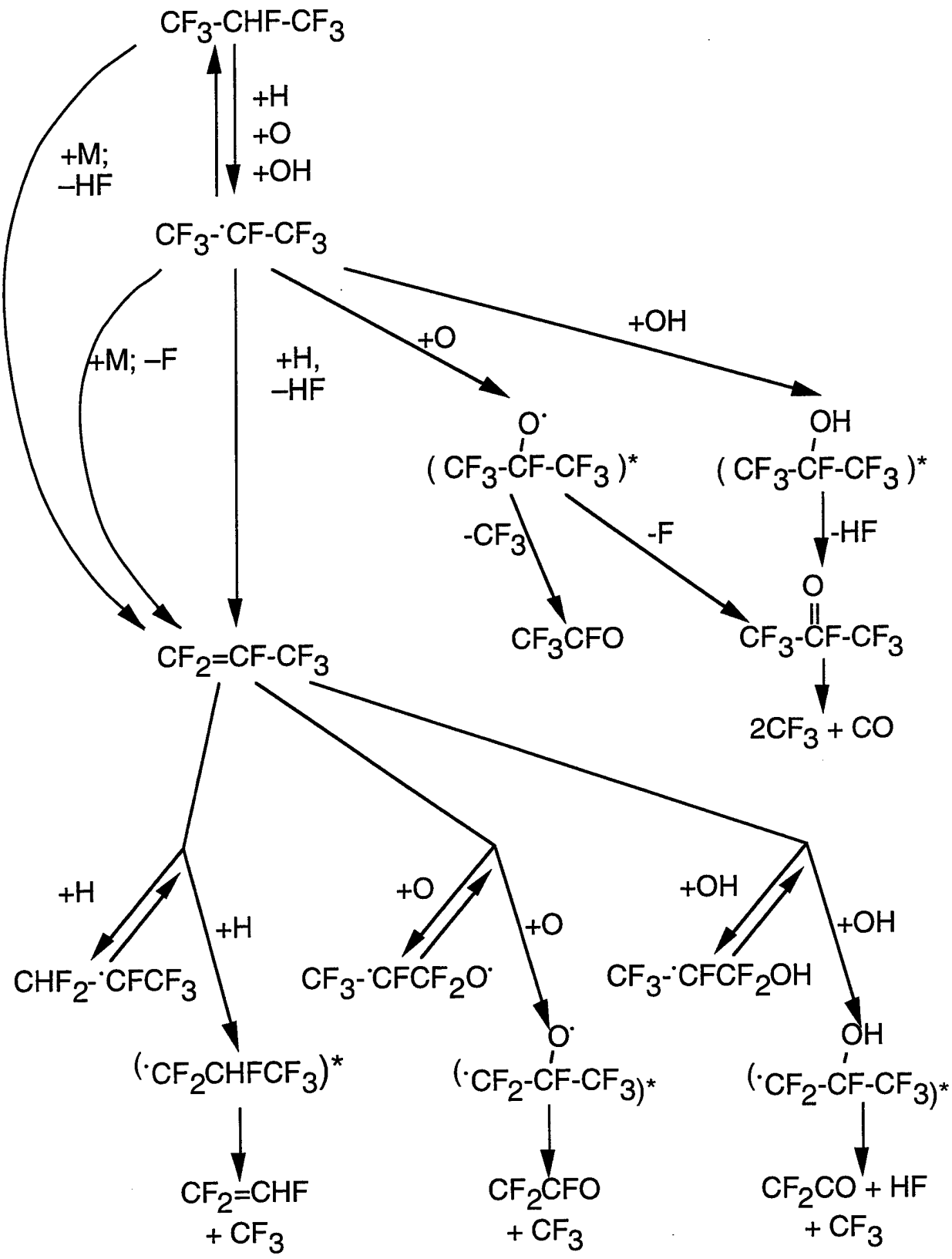

Fig. 2. Proposed C_3 mechanism.

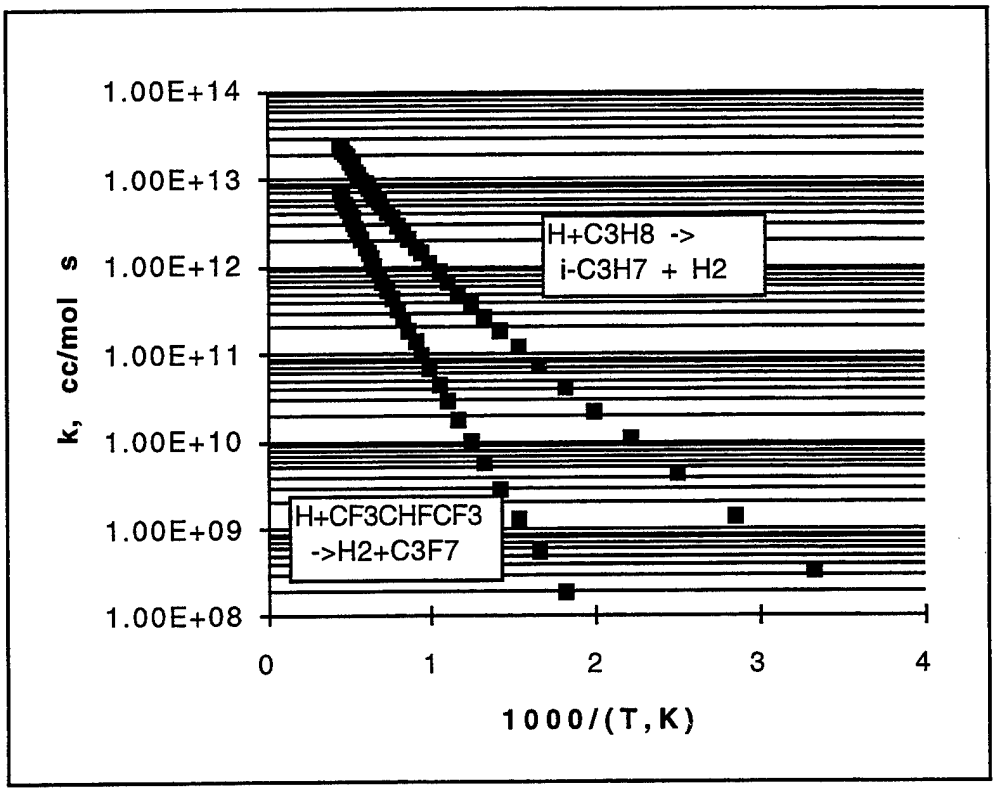

Fig. 3. Predicted secondary-H abstraction kinetics for H + CF_3CHFCF_3, compared to literature review for H + CF_2=$CFCF_3$.

Summary. The thermochemical properties $\Delta_f H^\circ_{298}$, S°_{298} , $C_p^\circ(T)$, and $G^\circ(T)$ were calculated for 9 species and 12 transition states. The longest periods of CPU time were 5:55:09 hours (SGI Power Indigo^2) for frequencies of the transition state for OH + CF_3CHFCF_3 → H_2O + CF_3CFCF_3 and 47:02:39 hours (WrightPatt Cray C90) for its MP4 calculations. Thermochemical properties for the stable and radical species were fitted to NASA-form polynomials, and rate constants from TST and Bimolecular Quantum-RRK calculations were were fitted to 3-parameter rate-constant expressions. In subsequent work, flame data from Naval Research Laboratory experiments will be used to test the mechanism.

Acknowledgments. Sponsorship of this research by the U. S. Naval Research Laboratory, under the direction of Dr. James W. Fleming and Dr. Ronald S. Sheinson, is gratefully acknowledged. Likewise acknowledged are the helpful comments of Drs. Fleming, Sheinson, and Bradley Williams.

Ab Initio Kinetics of the Thermal Dehydrohalogenation of Alkyl Halides

Karl K. Irikura and Wing Tsang

Physical and Chemical Properties DivisionChemical Science and Technology LaboratoryNational Institute of Standards and TechnologyGaithersburg, MD 20899
tel: (301) 975-2510; fax: (301) 975-3670
email: karl.irikura@nist.gov

High-level calculations of gas-phase kinetics are useful (1) to test the reliability of practical *ab initio* calculations for predicting both absolute and relative rate constants, (2) to guide and interpret experiments, and (3) to aid in the evaluation of experimental data. The unimolecular 1,2-dehydrohalogenation of small alkyl halides (reaction 1) were chosen for this

$$(R_1)(R_2)CX\text{-}CH_2(R_3) \xrightarrow{k(T)} (R_1)(R_2)C=CH(R_3)+HX \qquad (1)$$

study because (1) the forward and reverse reactions are important in a number of contexts, including that of the present conference, (2) experimentalists lack rules-of-thumb for estimating the rates of multicenter reactions, and (3) these systems have been experimentally characterized well enough to serve as benchmarks. In addition, these molecules are closed-shell, single-configuration, and small enough to expect *ab initio* calculations to be successful. In this ongoing project, the particular molecules studied to date are the ethyl halides (X = F, Cl, Br, I) and the *n*-propyl, *i*-propyl, and *t*-butyl halides (X = F, Cl).

The most similar prior work is by Toto et al.[1] In addition to reviewing the earlier literature, they did extensive calculations of many transition-state structures at modest levels of *ab initio* theory. They did not compute rate constants, but did consider multiply halogenated systems and discussed many trends.

In the present work, we use a modified Gaussian-2(MP2) method[2] in which the geometries and vibrational frequencies (scaled by 0.9467) are calculated at the frozen-core MP2/6-311+G(d,p) level. This extended basis set is more appropriate than the usual 6-31G(d) for describing the tenuous bonding in transition states. No effective core potentials are used, since all-electron basis sets perform somewhat better for thermochemical calculations.[3] High-pressure rate constants are calculated using transition-state theory (equation 2) and the rigid-rotor, harmonic-oscillator (RRHO) approximation. Reaction path degeneracies are included.

$$k(T) = \frac{k_B T}{h} \exp(-\Delta G^{\ddagger} / RT) \qquad (2)$$

Figure 1 provides both the experimentally-derived and *ab initio* values of the Arrhenius activation energy E_a. Although the calculations correctly reproduce the known trends, the absolute values are consistently too high. This would lead to very low rate constants but for the

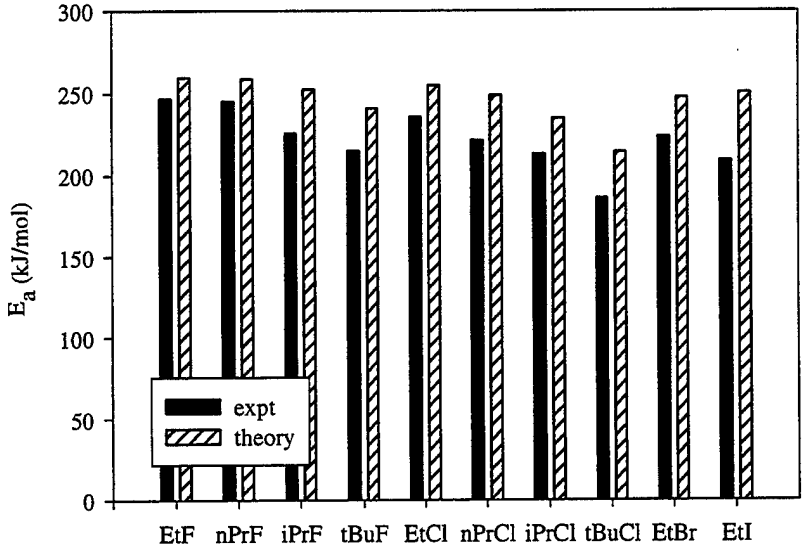

Figure 1. Experimental and calculated Arrhenius activation energies.

fact that the computed *A*-factors are also too high. As a result, the calculated rate constants generally agree reasonably well with experimental values. The computed rates and experimental Arrhenius fit for HCl elimination from ethyl and *t*-butyl chlorides are shown in Figure 2. The quantitative comparison is encouraging, since two important factors have yet to be included in the calculations: (1) proper treatment of the methyl rotors and (2) hydrogen-atom tunneling. Tunneling effects will also be probed by repeating the calculations for deuteriated isotopologues. If needed, the corresponding experiments will also be done.

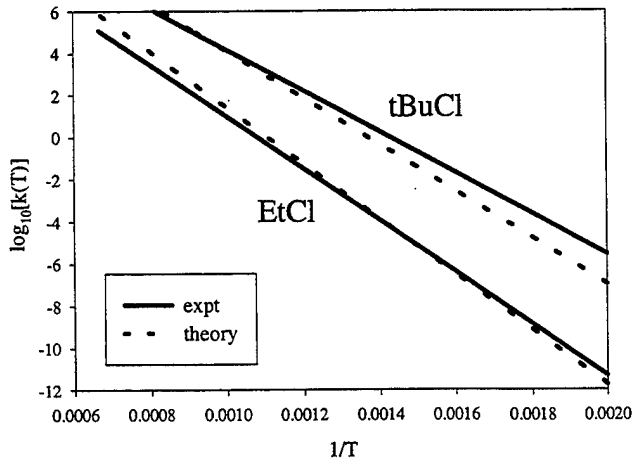

Figure 2. Experimental Arrhenius fit and calculated rate constants for ethyl chloride and t-butyl chloride decomposition.

It was observed in 1955[4] that the activation energy E_a is proportional to the heterolytic bond strength $D(R^+\text{-}Cl^-)$. As found earlier using qualitative Mulliken population analysis,[1] all the transition states involve substantial charge separation, which explains the observed correlation with heterolytic bond strengths. Inspecting the MP2/6-311+G(d,p) dipole moments confirms this picture. Although all the stable alkyl halides are computed to have a dipole moment of about 2 D, the moments of the transition states are 50% to 250% larger, increasing in the order F < Cl < Br < I and Et < nPr < iPr < tBu. We plan also to conduct a population analysis using Bader's AIM theory,[5] which is more robust than Mulliken analysis and provides additional information.

Ab initio calculations provide direct information about the transition state, and reveal a very long C_α-X bond and an acute C_α-C_β-H bond angle; the departing hydrogen appears to leap to the nearly dissociated halogen atom. Figure 3 shows the geometry of the transition state for the ethyl chloride reaction. The C_α-X distance increases as the corresponding alkyl cation becomes more stable, suggesting that the transition state is later. In contrast, the C_β-H distance decreases, the C_α-C_β distance increases slightly, and both carbons generally deviate more from planarity in the same series, suggesting an earlier transition state. We conclude that it is not helpful to correlate the polarity of the transition state with simple concepts of lateness or earliness.

Figure 3. Transition state for HCl elimination from ethyl chloride.

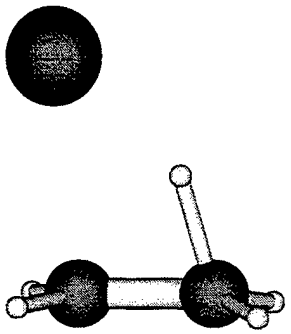

References

(1) Toto, J. L.; Pritchard, G. O.; Kirtman, B. *J. Phys. Chem.* **1994**, *98*, 8359-8370.

(2) Curtiss, L. A.; Raghavachari, K.; Pople, J. A. *J. Chem. Phys.* **1993**, *98*, 1293-1298.

(3) Hassanzadeh, P.; Irikura, K. K. *J. Phys. Chem. A* **1997**, *101*, 1580-1587.

(4) Maccoll, A.; Thomas, P. J. *Nature* **1955**, *176*, 392.

(5) Bader, R. F. W. *Atoms in Molecules: A Quantum Theory*; Clarendon: Oxford, 1990.

A Theoretical Study of the Two-Channel Hydrogen Abstraction by Cl and Br Atoms and Reverse Reactions

Jerzy Jodowski, Marie-Thérèse Rayez, Jean-Claude Rayez

Laboratoire de Physicochimie Theorique, URA503/CNRS, Universite Bordeaux I, 33405 Talence Cedex, France
tel: (33) 5 56 84 63 09; fax: (33) 5 56 84 66 45
email: rayez@cribx1.u-bordeaux.fr

Hydrogen atom reactions are frequently used in flow systems as the source of free radicals. However, in such reactions, often more than one reactive species are formed in competing reaction channels and may yield species of different reactivities. A good example for this is provided by the hydrogen abstraction reactions by H, F, Cl, Br or OH radicals from methanol:

$$CH_3OH + X \rightarrow CH_3O + HX \qquad X=H, F, Cl, Br, OH \text{ and } CH_3$$
$$\rightarrow CH_2OH + HX$$

The values of branching ratios, which are used as inputs in combustion and atmospheric modeling studies can have a fundamental influence on the outputs of model calculations. Beyond the determination of branching ratios, some aspects of reactivity have to be elucidated. In particular, the reaction with Cl is faster than expected for an almost thermoneutral reaction. Another aspect is the study of the reverse reactions and the variation of their rate constants with temperature. For example, CH_2OH + HCl and CH_2OH + Br have an opposite behavior when temperature varies.

All these behaviors can be understood with the help of the determination of the potential energy surfaces. Our calculations have shown that reactions with halogens involve the formation of loose complexes which decompose into products through barriers. On the contrary, reactions oh H, OH and CH_3 have been shown to behave like direct abstractions.

In this talk, the reaction mechanism of the reactions involving Cl and Br atoms are discussed in detail. All geometries of reactants, intermediate complexes and transition states were fully optimized using ab initio molecular orbital theory at the MP2/6-31G(d,p) and 6-311G(d,p) levels. When possible, energies were improved by using G2 method. Using the results of ab initio calculations as input data, a multichannel RRKM procedure has been settled in order to calculate rate constants and branching ratios.

This work is made in collaboration with the group of T. Berces (Budapest) where experimental determination of reaction rates and branching ratios have been done.

Inhibition of Hydrogen-Air Flames by CF_3Br

L. Truett, H. Thermann, D. Trees, K. Seshadri

Center for Energy and Combustion Research
Department of Applied Mechanics and Engineering Sciences
University of California San Diego, La Jolla CA 92093-0411
tel: (619) 534-3046; fax: : (619) 534-5345
email: ltruett@damkohler.ucsd.edu

This investigation examined the inhibition effectiveness of CF_3Br in a diluted hydrogen-air counterflowing diffusion flame. Numerical results were also computed using the fuel model of Peters and Rogg (1994) and the CF_3Br mechanisms of NIST (1996) and Westbrook (1983).

Extinction is a complex phenomenon where the characteristics of the chemistry and the flow must be taken into account. This relationship is represented by the Damkohler number where $D = \tau_f/\tau_c$. The characteristic chemical time, τ_c, depends on the reactants and the characteristic flow time, τ_f, is determined by the flow velocities. For the counterflowing configuration near the axis of symmetry, the strain rate, which is τ_f^{-1}, is well defined and is given by Seshadri and Williams (1975) as

$$a = \frac{2|v_2|}{L}\left(1 + \frac{|v_1|\sqrt{\rho_1}}{|v_2|\sqrt{\rho_2}}\right)$$

L: separation distance between ducts; v: velocity; ρ: density;
subscripts 1 and 2 represent fuel and oxidizer streams respectively

In all experiments the momentum flux $\left(|v_i|\sqrt{\rho_i}\right)$ of the reactants was balanced so that a stagnation plane was established in the center and the equation reduced to $\tau_f = a^{-1} = L/(4v_2)$.

Experiments were performed for 15%H_2 and 16%H_2 diluted in N_2 as the fuel stream and with various concentrations of CF_3Br added to the oxidizer stream. These fuel concentration were selected because they had similar uninhibited extinction strain rates to the CH_4-air flame. A flame was established for a predetermined concentration of CF_3Br and the strain rate was gradually increased until extinction occurred. Extinction was defined as the strain rate at which a flame was not stable for 10 seconds, even after relighting. The flow rates of the products were computed by custom software that also regulated all the mass flow controllers.

Figure 1 shows the mole fraction of CF_3Br at extinction as a function of strain rate for 15% and 16% H_2, and for comparison, recent data (Trees 1997) of a inhibited CH_4-air flame is also shown. The extinction data for the uninhibited H_2-air flames compare well with previous experiments (Trees 1994) on H_2-air flames. All three curves have large reduction in extinction strain rate for increased agent concentration showing CF_3Br to be an effective inhibitor. In Fig. 2 the results are normalized by dividing by the uninhibited extinction strain rate. It is noteworthy that the different fuels show similar reduction in extinction strain rate with the addition of CF_3Br. However, this may not be the case for higher concentrations of H_2.

A numerical simulation of the extinction conditions was performed using *FlameMaster* (Pitsch 1993) employing detailed chemical kinetics. The boundary conditions were consistent with those in the experiments and the initial radial component of velocity was set to zero (plug flow). The chemical-kinetic mechanism of Peters and Rogg was utilized for the fuel oxidation and results were computed for both the NIST and Westbrook mechanisms for CF_3Br inhibition. Only C_1 reactions were considered.
The numerical results for 16% H_2 are plotted in Fig. 3 showing that both mechanisms over-predict the inhibiting effect of CF_3Br. Also, the calculated uninhibited extinction strain rate is closer to the 15% H_2 experimental results. This could be due to small errors in the mass flow controllers. Figure 4 displays the calculated profiles of temperature and selected species in both the inhibited and uninhibited flames with the strain rate set to 150^{-1}. It clearly shows that the predicted temperature and radical concentrations are reduced for the inhibited case.

The temperature of the diluted H_2-air flame is several $100°K$ lower than that of the CH_4-air flame at the same strain rate. This could explain why the model over-predicts the inhibition effect for the H_2-air flame since the inhibition kinetics were optimized for the hydrocarbon flames. Further investigation is required to improve these models for the H_2-air flame.

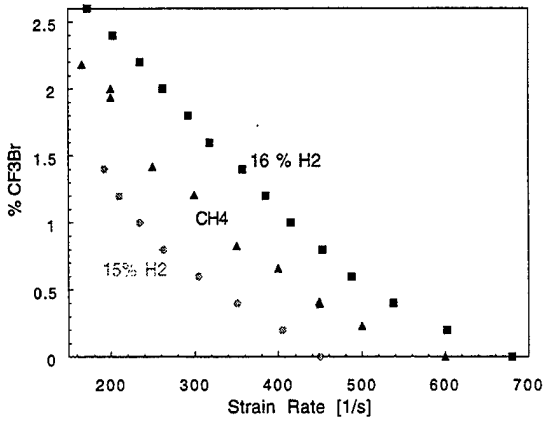

Fig. 1 Mole fraction of CF_3Br in the oxidizer stream at extinction as a function of strain rate

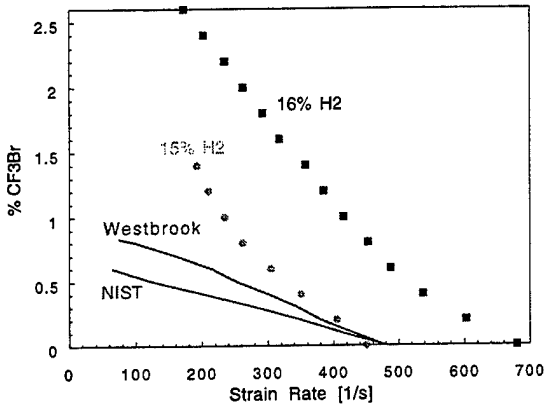

Fig. 3 Mole fraction of CF_3Br in the oxidizer at extinction as a function of strain rate. Numerical data calculated for 16%H_2 diluted in N_2.

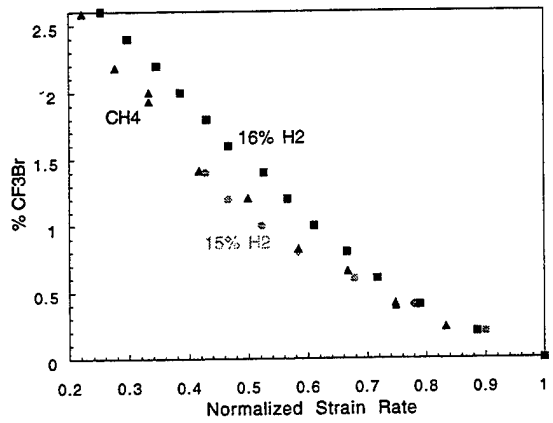

Fig. 2 Mole fraction of CF_3Br in the oxidizer stream at extinction as a function of strain rate normalized by the uninhibited extinction strain rate.

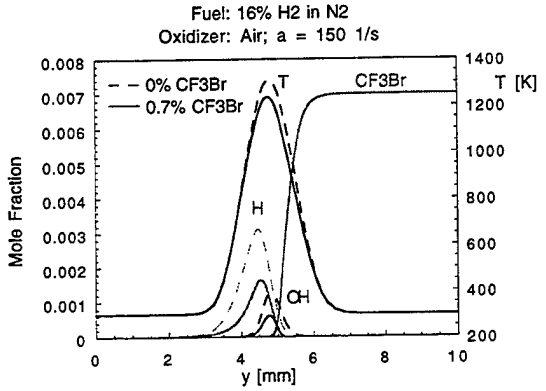

Fig. 4 Comparison of uninhibited and inhibited profiles for temperature and selected species.

Labile Bromine Fire Suppressants

Peter Haaland and John Huntington

Huntington Research and Engineering, San Jose, CA and Louisville, CO
tel: (303) 604-6526 ; fax: (303) 604-6457
email: haalanpd@rmi.net

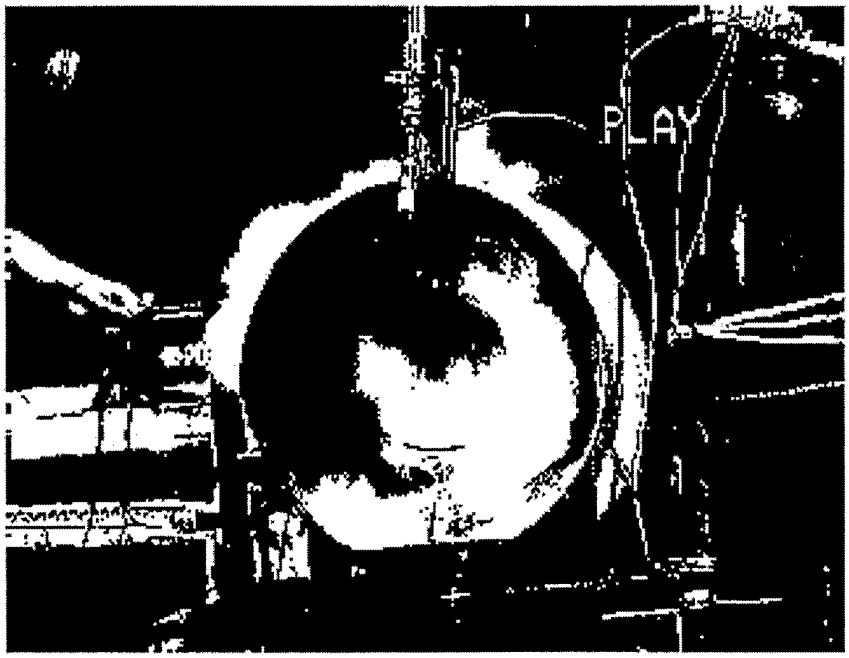

Uncombusted kerosene aerosol (smoke) is early evidence of 500kW fire suppression in an engine nacelle simulator. The image was recorded 33 milliseconds following injection of 10cc of PBr_3 in a 10 m/s airflow.

A new class of potent fire suppression materials (U.S. Patent 5,626,786) involving weakly bound (labile) bromine is described from both fundamental and applied perspectives. These materials act to suppress fires using the same chemical mechanisms as Halons 1301 and 1211, but they do so with superior weight and volume efficiency. In addition, they are rapidly hydrolyzed by atmospheric moisture to produce simple acids with neither ozone depletion nor global warming potentials. The chemical kinetics, toxicology, and mode of action for these materials will be described, as will their application to suppression of fires in jet engine nacelles and fuel-vapor laden enclosed spaces such as dry bays and the ullage of fuel tanks.

Reactions of Bromine Species Leading to Inhibition in: H_2, Methane and C2 Hydrocarbon Oxidation

Joseph W Bozzelli

Department of Chemical Engineering, Chemistry and Environmental Sciences, New Jersey Institute of Technology, Newark, NJ 07102
tel: (201) 596-3459; fax: (201) 802-1946
email: bozzelli@tesla.njit.edu

The halogenated compound CF_3Br, halon 1301, is currently and has been widely used and known as a flame inhibitor and fire suppression agent. It has been implemented into many fire protection systems dating back as far as the early 1940's. Despite the favorable, experimentally- observed flame suppression properties, the detailed chemistry effecting the inhibition in flames by this and similar compounds is not well understood. Notable research efforts in this regard were MB/MS experiments by Biordi, Lazzara and Papp in the 1970's, by Safieh, Vandooren and Van Tiggelen in 1982, and the benchmark modeling efforts of Westbrook in the early 1980's. That there has been very limited research on the chemistry of brominated fire retardants until the past several years, is due to their empirically known effectiveness and ease of availability, leaving little financial incentive for industry or government to study the processes. Recent developments leading to discovery that these bromides (and chlorides) promote degradation of the earth's ozone layer, and behave as greenhouse gases with implications for global warming, have lead to significant use restrictions. Safety benefits from use of flame retardants, and inhibitors as well as needs for inert (non or low flammability) solvents have led to a resurgence in research such as that of Zachariah et. al., and Berry et. al on these and other fluorinated hydrocarbons.
Detailed chemical reaction mechanisms for oxidation and combustion of bromine/hydrogen and bromine/hydrocarbon chemical systems containing up to 2 carbons, are used to evaluate important chain branching and inhibition (chain termination) pathways. The hydrocarbon mechanism includes extensive peroxy and hydroperoxy chemistry and provides insights into the chemical processes at moderate combustion temperatures where reactions of these species are important as well as at higher temperatures, where elimination reaction processes dominate the peroxy chemistry. Rate constants and pathways for the peroxy and new bromine reactions are determined from thermodynamic analysis of reaction pathways and principles of statistical mechanics applied to fundamental kinetic theory. Molecular and transition state properties are determined by *ab initio* and semi-empirical calculations, along with evaluations of experimental data. Pressure dependence is incorporated for reactions in the fall-off regime or at the low pressure limit.

Investigation on the Inhibiting Effect of CF_3I and Some Fluorinated Hydrocarbons

F. Battin-Leclerc

Department de Chimie-Physique des Reactions URA 328 CNRS, INPL-ENSIC and Universite de Nancy I, 1 rue Grandville-BP451-54001 NANCY Cedex, France
tel: (33) 3 83 17 51 25; fax: (33) 3 83 37 81 20
email: fredie@dcpr.ensic.u-nancy.fr

The major losses of stratospheric ozone over Antarctica which are observed each spring (the so-called *Ozone Hole*) and the indications of significant loss of ozone in the Arctic in winter are the most significant evidences of the ozone depletion problem. The role of halogenated compounds such as chlorofluorocarbons (CFCs) and halons in the ozone depletion has been confirmed; consequently, international agreements (the Montreal Protocol and its recent revisions) led to the phasing out of the production of halons in January 1994. Halons (mainly halon 1301 (CF_3Br) and halon 1211 (CF_2BrCl)) are still widely used for fire extinguishment for military and civilian applications

The European project SUBSTHAL has permitted to perform experimental and modelling studies of the effects of the addition of brominated compounds, perfluoroalkanes (FCs), hydrofluoroalkanes (HFCs) and hydrochlorofluorocarbons (HCFCs) on a model reaction (the oxidation of methane) in flames [3] (works performed by LCSR-Orleans), in flow reactors [1-2] and in shock tubes [4].

The modelling studies performed for the flame systems have shown a high sensitivity to the reactions of CF_2 radicals. A laser flash photolysis technique, using U.V. absorption, has been then used to study the kinetics of the self reactions and the reactions with O_2, H_2, CH_4 and C_2H_4 of CF_2 radicals between 296 and 873 K (works performed in AEA-Technology-Harwell) [5]. The CF_2 radicals were generated by photolysis at 193 nm of C_2F_4-N_2 mixtures and detected using its strong banded absorption spectrum around 250 nm.

The rate coefficients for the self reaction, derived at atmospheric pressure, have been shown to be at their high pressure limit and to exhibit a positive temperature dependence. These measurements combined with the high temperature shock tube data of K.P. Schug and H.Gg. Wagner [6] present a clear curvature of the Arrhenius plot and can be fitted by the following expression:

$$k_1 (T) = 2.3 \times 10^{-20} T^{2.2} \exp(480/T) \text{ cm}^3 \text{ molecule}^{-1} \text{ s}^{-1} \text{ for } T = 298\text{-}1400 \text{ K}.$$

No reaction was observed between CF_2 and any of the molecular reagents studied at temperatures up to 873K; but higher limits were derived. At 873K, the values are (in units of cm^3 $molecule^{-1}$ s^{-1}) $< 5 \times 10^{-19}$ for H_2, $< 3 \times 10^{-17}$ for O_2, $< 4 \times 10^{-19}$ for CH_4 and $< 2 \times 10^{-16}$ for C_2H_4.

Recent studies have shown that iodinated fluorocarbons (IFCs) would be as efficient fire extinguishing compounds as halons and some recent papers have indicated that CF_3I would have an O.D.P. close to zero since its residence time in the atmosphere is very short. We have then performed an experimental and theoretical study of the inhibiting effect of the addition of 1 to 5 % (related to the amount of methane) of CF_3I on methane oxidation in a perfectly stirred reactor for temperatures from 970 to 1150K [7]. A clear inhibiting effect was then observed (figure 1) :

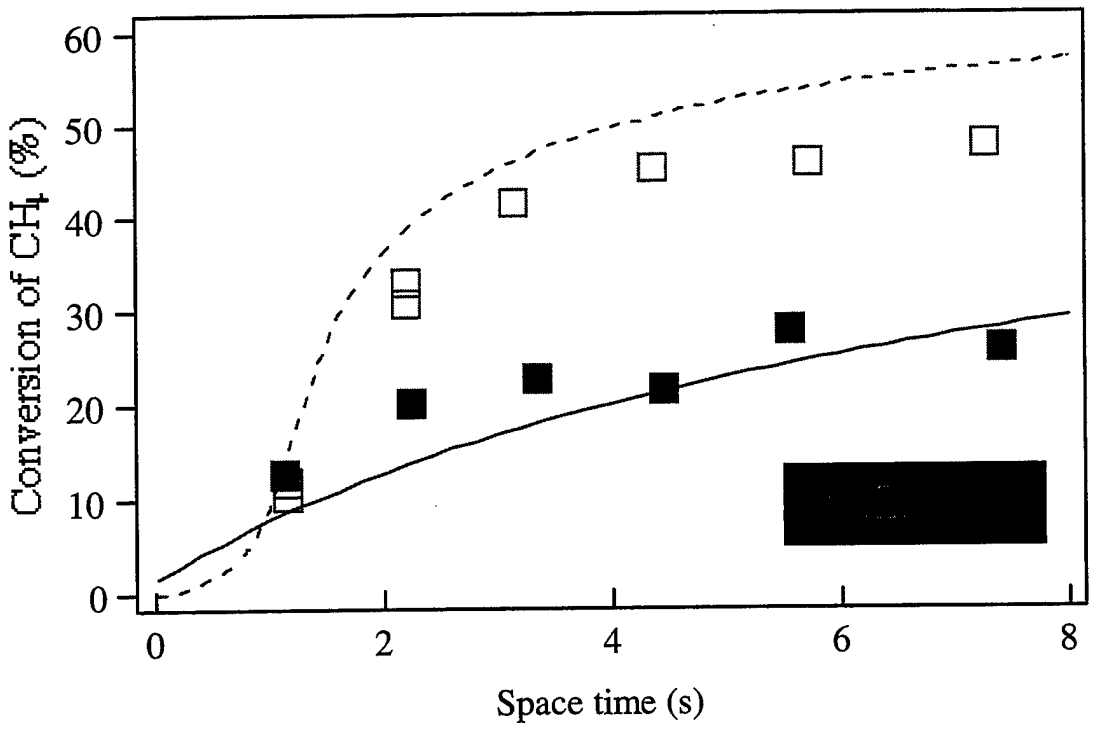

Figure 1: Conversions of CH_4 versus space time in the presence of 2 % CF_3I (T = 1070 K, Pressure = 1 bar, Mixtures : He : CH_4 : O_2 : (+ CF_3I) = 10 : 1 : 1 : (+0.02) (mol)).

Symbols represent experimental data and lines show computed profiles.

Methane oxidation and the influence of halogenated compounds on this reaction were modelled using a detailed reaction mechanism including the recent kinetic values for the reactions of iodinated compounds. The proposed mechanism was able to reproduce our experimental data.

Sensitivity analyses have led to a determination of the dominant steps accounting for the inhibiting effect of CF_3I. The inhibiting influence of CF_3I on methane oxidation seems to be mainly due to the two following steps,

$$I + CH_4 \quad => \quad HI + CH_3$$

and,

$$I + HO_2 \quad => \quad O_2 + HI \ .$$

These two steps form a cycle which acts as a termination reaction between HO_2 and CH_3 radicals to give CH_4 and O_2.

References

[1] Battin-Leclerc F., Côme G.M. and Baronnet F., Comb. Flame, 99:644 (1994).

[2] Walvarens B., Battin-Leclerc F., Côme G.M. and Baronnet F., Comb. Flame, 103:339 (1995).

[3] Battin-Leclerc F., Côme G.M., Baronnet F., Sanogo O., Delfau J.L. and Vovelle C., in *Halon Replacements: Technology and Science*, (A.W. Miziolek and W. Tsang eds), American Chemical Society Symposium Series book, 1995, p. 290.

[4] Baugé J.C., Glaude P.A., Pommier P., Battin-Leclerc F., Scacchi G., Côme G.M., Baronnet F. and C. Paillard, J. Chim. Phys., 94:460 (1997).

[5] Battin-Leclerc F., Smith A.P., Hayman G.D. and Murrells T.P., J. Chem. Soc., Faraday Trans., 92 (18):3305 (1996).

[6] Schug K.P. and Wagner H. Gg., Ber. Bunseng. Phys. Chem., 82:719 (1978).

[7] Battin-Leclerc F., P.A. Glaude, Côme G.M. and Baronnet F., Comb. Flame, 109:285 (1997).

Research funded in part by the European Commission, DG XII in the framework of the Environment Programme (SUBSTHAL - Contract n° EV5V-CT92-0230)

The Kinetics and Unusual Products of the Reactions of Oxygen Atoms with Alkyl Iodides

Rajiv J. Berry,[a] Ashutosh Misra,[b] Paul Marshall[b]

[a]*WL/MLBT, Wright-Patterson AFB OH 45433*
tel: (937) 255-2467; fax: (937) 255-9019
email: berryrj@ml.wpafb.af.mil

[b]*Department of Chemistry, University of North Texas, Denton, TX 76203*

Iodocarbons (e.g. CF_3I) are being considered as potential replacements for halon flame suppressants (e.g. CF_3Br, CF_2ClBr) in commercial and military applications since the production of halons is banned due to their high ozone depletion potential (ODP). CF_3I is as efficient a flame suppressant as halons, but has a much shorter atmospheric lifetime and hence a much lower ODP and global warming potential. CH_3I (formed by the recombination of CH_3 + I) has been identified as a key species responsible for the observed strong inhibition by CF_3I. Therefore, the reactions of CH_3I with species abundant in flames such as H, OH and O radicals are expected to play a significant role in the inhibition chemistry of CF_3I. We have recently reported Gaussian-2 (G2) computational results for the reaction of CH_3I with H and OH (1). A focus of that study was to predict the preference of H-abstraction versus I-abstraction. For CH_3I + H the I-abstraction channel leading to the formation of HI was computed to be the faster reaction while for CH_3I + OH the H-abstraction pathway was predicted to be more favorable. A subsequent study which combined flash-photolysis resonance fluorescence measurements on the rate constant for CH_3I + H with G2 calculations showed that the substitution pathway leading to the formation of CH_4 + I was a relatively slow reaction (2).

In contrast to the reactions of CH_3I with H and OH, the reaction of CH_3I with O (^3P) leads to a complex potential energy surface (PES) where numerous species are accessible due to inter-system crossing (ISC) from the triplet to the singlet surface. Experiments of Gilles *et al* (3) account for ~70% of the products which include CH_3 + IO (44%); CH_2I + OH (16%); CH_2O + I + H (7%); I + CH_3O (<3%); and CH_2O + HI (<5%). They also noted that this reaction was 5 orders of magnitude faster than CH_3Br + O. The PES for CH_3I + O as computed with the G2 method is shown in Figure 1. For comparison the PES of CH_3Br + O is overlaid such that the energy of the various products and intermediates is relative to an energy of 0 kJ/mol for the reactants. One can see that the singlet adduct CH_3IO is more stabilized than CH_3BrO. The lowest barrier pathway for CH_3IO leads to

hindered due to the relatively high activation barrier leading to CH_2-Br-OH. The CH_2-I-OH also can rearrange to the alcohol ICH_2OH which can undergo further chemistry leading to HI + CH_2O, I + CH_2OH, H + I + CH_2O, CHI + H_2O and HClO + H_2. These pathways are discussed in more detail elsewhere (4). A QRRK analysis that employed these results (200-2000 K range) gave good accord with the kinetic and product studies of Gilles et al (3).

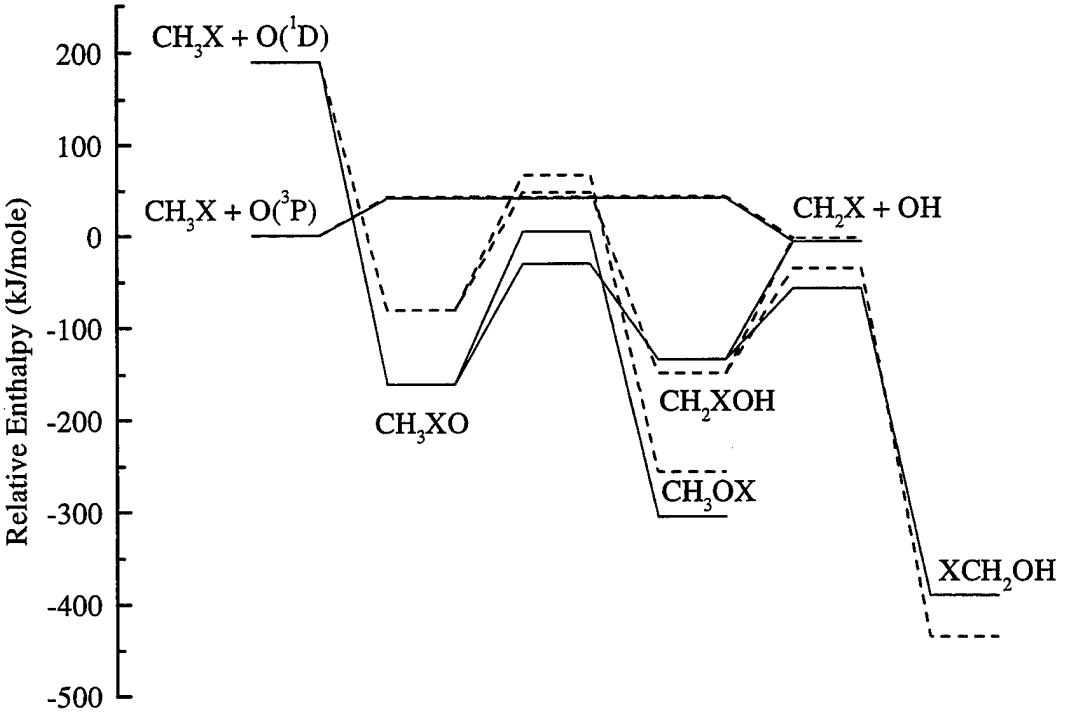

Figure 1. PES's for the reaction of $O(^3P)$ with CH_3X, X=Br (dashed) and X=I (solid)

PESs for the reaction of O with CH_3-CH_2I, CH_3-CH_2-CH_2I and CH_3-CHI-CH_3 were also explored computationally. Experimental results (3, 5) for the reaction of the alkyl iodides with O indicate that IO yields are reduced from 44% (CH_3I) to 11% (CH_3-CH_2I) while HOI production increases from 0% to 30%. The G2 PES for CH_3-CH_2I (Figure 2) shows that the low energy pathway leading to HOI production which occurs via addition/dissociation through a five-membered ring transition state. This pathway is also computed as the lowest energy path for the larger alkyl iodides.

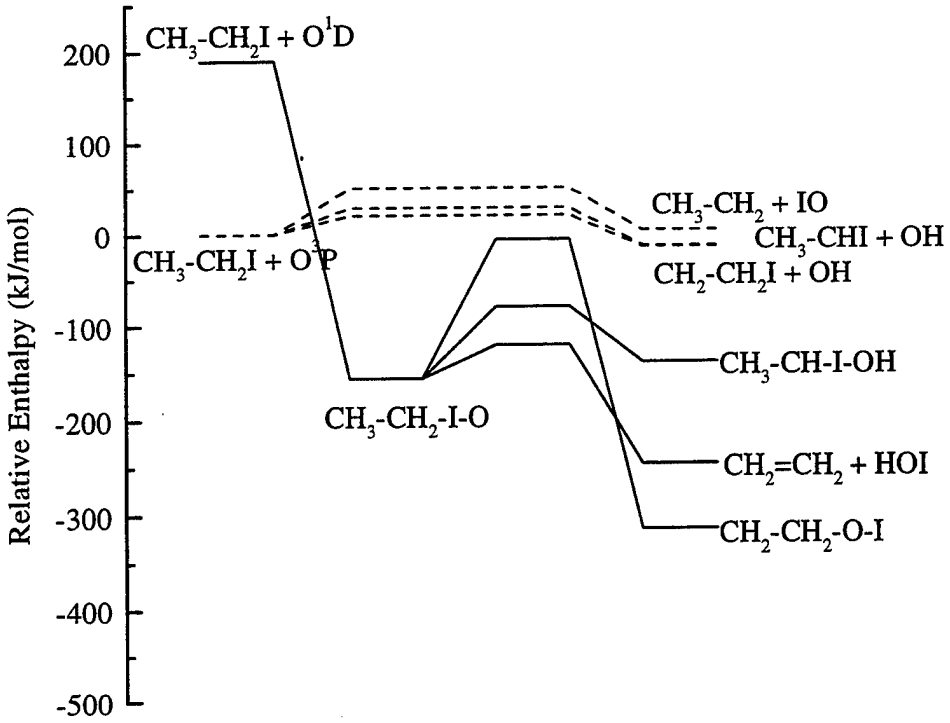

Figure 2. Singlet (solid) and Triplet (dashed) PESs for CH_3-CH_2I + O

References:

1. P. Marshall, A. Misra and R. J. Berry, *Chem. Phys. Lett.* **265**, 48, 1997.

2. J. Yuan, L. Wells and P. Marshall, *J. Phys. Chem.* **A101**, 3542, 1997.

3. M. K. Gilles, A. A. Turnipseed, R. K. Talukdar, Y. Rudich, P. W. Villalta, L. G. Huey, J. B. Burkholder, and A. R. Ravishankara, *J. Phys. Chem.* **100**, 14005, 1996.

4. A. Misra, R. J. Berry, and P. Marshall, *J. Phys. Chem.* in press.

5. J. J. Wang, D. J. Smith, and R. Grice, *J. Phys. Chem.* **A 101**, 3293, 1997.

The kinetics of elementary reactions of CF_3Br and CF_3I with H, OH, O and CH_3 radicals: experiments, ab initio calculations and implications for combustion chemistry

Paul Marshall,[a] Jessie Yuan,[a] Ashutosh Misra,[a] Leah Wells,[a] Samantha Hawkins,[a] Aneal Krishnan,[a] Ripal B. Nathuji[a] and Rajiv J. Berry[b]

[a]*Department of Chemistry, University of North Texas, Denton, Texas 76203*
tel: (817) 565-2294; fax: (817) 565-4318
email: marshall@unt.edu

[b]*WL/MLBT, Wright-Patterson AFB OH 45433*

CF_3Br is a typical halon fire extinguishing agent, and there have been several studies of its behavior in flames.[1-5] Halons are thought to damage the ozone layer and a potential replacement, in some applications, is CF_3I. A barrier to understanding the details of the mechanisms by which these agents suppress combustion has been a lack of thermochemical and kinetic data for bromine and iodine compounds. In this work ab initio molecular orbital theory and measurements of isolated elementary reactions are used to analyze several processes critical to the chemistry of these agents.
The kinetics of the reactions:

$$CF_3Br + H \rightarrow CF_3 + HBr \quad (1)$$
$$CF_3I + H \rightarrow CF_3 + HI \quad (2)$$
$$CF_3I + OH \rightarrow CF_3 + HOI \quad (3)$$
$$CF_3I + O \rightarrow CF_3 + IO \quad (4)$$

have been studied by means of the pulsed-photolysis time-resolved resonance fluorescence method to yield the following rate expressions:

$k_1 = (6.9 \pm 0.4) \times 10^{-11} \exp(-21.7 \pm 0.2 \text{ kJ mol}^{-1}/RT)$ cm^3 molecule^{-1} s^{-1} (295-860 K)
$k_2 = (6.8 \pm 0.2) \times 10^{-11} \exp(-4.0 \pm 0.1 \text{ kJ mol}^{-1}/RT)$ cm^3 molecule^{-1} s^{-1} (295-730 K)
$k_3 = (1.0 \pm 0.2) \times 10^{-11} \exp(-12.7 \pm 0.6 \text{ kJ mol}^{-1}/RT)$ cm^3 molecule^{-1} s^{-1} (280-440 K)
$k_4 = (1.7 \pm 0.1) \times 10^{-11} \exp(-2.6 \pm 0.1 \text{ kJ mol}^{-1}/RT)$ cm^3 molecule^{-1} s^{-1} (295-715 K)

(all errors $\pm 1\sigma$ and represent statistical uncertainties only)

The results are in good accord with earlier measurements made at around room temperature or below, and considerably extend the upper range towards combustion conditions. The potential energy surfaces for reactions 1-4 have been characterized at the Gaussian-2 level of theory,[6,7] which reveals that they fall into three classes. Reactions 1 and 2 proceed over a clear energy barrier and have been modeled using transition state theory. The results agree well with our measurements. The k_1 measurements and calculations show that the k_1 expression[1] commonly used for modeling flame suppression by halons is incorrect. Reaction 3 has no computed energy barrier beyond the endothermicity. The measured activation energy can therefore be employed to obtain $D_fH_{298}(HOI) = (-70 \pm 7)$ kJ mol^{-1}, which agrees with our ab initio value. Reaction 4 proceeds via a bound CF_3IO intermediate which has been characterized computationally, and quantum RRK calculations indicate that under combustion conditions the major products will be CF_3 + IO. Preliminary computed rate constants for reactions of the HOI and IO products will be also be discussed briefly. The reactions involving methyl, another important radical in hydrocarbon flames,

$$CF_3Br + CH_3 \rightarrow CF_3 + CH_3Br \quad (5)$$

$$CF_3I + CH_3 \rightarrow CF_3 + CH_3I \quad (6)$$

have been analyzed at the G2 level. Transition state theory results agree well with literature data for k_5 and k_6 over the approximate range 360-500 K,[8,9] and resolve a discrepancy between earlier flame[1] and lower temperature determinations of k_5. Recommended rate constant expressions for combustion modeling are

$k_5 = 4.6 \times 10^{-19} T^{2.05} \exp(-3990/T)$ cm^3 molecule^{-1} s^{-1}

$k_6 = 8.3 \times 10^{-19} T^{2.18} \exp(-1870/T)$ cm^3 molecule^{-1} s^{-1}

The new data for reactions 1-6, together with literature information about unimolecular decomposition, have been employed in flame models to assess their relative importance. It is found that attack by atomic hydrogen is the major pathway for destruction of both CF_3Br and CF_3I in a methane flame.

References

1. J. C. Biordi, C. P. Lazzara and J. F. Papp, J. Phys. Chem., 82, 125 (1978).
2. C. K. Westbrook, Combust. Sci. Tech., 34, 201 (1983).
3. F. Battin-Leclerc, G. M. Come and F. Baronnet, Combust. Flame, 99, 644 (1994).
4. V. Babushok, T. Noto, D. R. F. Burgess, A. Hamins and W. Tsang, Combust. Flame, 107, 351 (1996).
5. A. R. Masri, B. B. Dally, R. S. Barlow and C. D. Carter, Combust. Sci. Tech., 113/114, 17 (1996).
6. L. A. Curtiss, K. Raghavachari, G. W. Trucks and J. A. Pople, J. Chem. Phys., 94, 7221 (1991).
7. M. N. Glukhovtsev, A. Pross, M. P. McGrath and L. Radom, L. J. Chem. Phys., 103, 1878 (1995).
8. D. M. Tomkinson and H. O. Pritchard, J. Phys. Chem., 70, 1579 (1966).
9. H. Sidebottom and J. Treacy, Int. J. Chem. Kinet., 16, 579 (1984).

Kinetic Modeling of Hydrogen Combustion Suppression by CF_3I

Andrew McIlroy

Combustion Research Facility, MS 9051 Sandia National Laboratory, Livermore, CA 94551
tel: (510) 294-3054; fax: (510) 294-2276
email: amcilr@ca.sandia.gov

Hydrogen fire suppression is interesting from both practical and scientific viewpoints. Hydrogen fires have proven difficult to extinguish by conventional means; halons, which have superior performance in suppressing hydrocarbon fires, have only modest performance for hydrogen fires. Yet a high performance hydrogen fire suppressant would have many practical applications. Space launch vehicles use hydrogen for fuel, oil refineries use hydrogen in cracking, and hydrogen would be an excellent general use fuel from an environmental standpoint. All of these areas would benefit from an efficient means of extinguishing or preventing hydrogen fires. From a scientific viewpoint, hydrogen fire suppression is an attractive area for study because the hydrogen combustion models are well developed and quite simple. The hydrogen combustion sub-mechanism is a critical part of all hydrocarbon combustion mechanisms; thus, any fire suppressant that is effective against hydrogen fires should also be very effective against hydrocarbon fires. CF_3I has shown promise as a high-performance halon replacement in some applications. Recent calculations have produced new rate constants for several of the key iodine reactions needed for a CF_3I combustion mechanism. These rate constants are used in a one-dimensional laminar premixed flame model of $H_2/O_2/CF_3I$ combustion. Calculations are performed varying CF_3I concentration, flame stoichiometry, and total pressure. Trends are predicted for macroscopic variables such as flame speed and temperature, and the chemical mechanism is analyzed in detail. The calculations show good agreement with a limited set of low-pressure flame measurements. Catalytic reaction cycles are identified that have the potential to inhibit combustion. However, the overall suppression effect of CF_3I on hydrogen flames is found to be modest.

Numerical Modeling Results for Iron-Pentacarbonyl Inhibited Flames[1]

M. D. Rumminger[2], D. Reinelt[3], V. Babushok, and G. T. Linteris

Building and Fire Research Laboratory , National Institute of Standards and Technology, Gaithersburg MD 20899, USA
tel: (301) 975-5721; fax: (301) 975-4052
email: marc.rumminger@nist.gov

Iron pentacarbonyl ($Fe(CO)_5$) is an extremely efficient flame inhibitor, yet its inhibition mechanism has not been described. The flame-inhibition mechanism of $Fe(CO)_5$ in premixed and counterflow diffusion flames of methane, oxygen and nitrogen is investigated. A gas-phase inhibition mechanism involving catalytic removal of H atoms by iron-containing species is presented. For premixed flames, numerical predictions of burning velocity are compared with experimental measurements at three equivalence ratios (0.9, 1.0, and 1.1) and three oxidizer compositions (0.20, 0.21, and 0.24 oxygen mole fraction in nitrogen). For counterflow diffusion flames, numerical predictions of extinction strain rate are compared with experimental results for addition of inhibitor to the air and fuel stream. The numerical predictions agree reasonably well with experimental measurements at low inhibitor mole fraction, but at higher $Fe(CO)_5$ mole fractions the simulations overpredict inhibition. The overprediction is suggested to be due to condensation of iron containing compounds since calculated supersaturation ratios for Fe and FeO are significantly higher than unity in some regions of the flames. The results lead to the conclusion that inhibition occurs primarily by homogeneous gas-phase chemistry.

[1] Official contribution of the Nattional Institute of Standards and Technology; not subject to copyright in the United States
[2] National Research Council/NIST postdoctoral fellow
[3] Currently with BASF Aktiengesellschaft, 67056 Ludwigshafen, Germany

CHEMICAL LIMITS TO FLAME INHIBITION RELATIVE EFFECTIVENESS OF METALLIC COMPOUNDS

V. Babushok, W. Tsang, G. T. Linteris, D. Reinelt

Physical and Chemical Properties Division (CSTL) and Fire Science Division (BFRL), National Institute of Standards and Technology, Gaithersburg, MD 20899, USA
tel: (301) 975-5109; fax: (301) 975-3670
email: babushok@oxazine.nist.gov

INTRODUCTION. The search for replacements of halon 1301 as a fire suppressant is of a current concern. This paper describes some recent work carried out in our laboratory in support of this effort. The original impetus for this paper was to develop a better understanding of the mechanism of fire inhibition by iron carbonyl. It has been known for some time and confirmed recently [1-3] that iron carbonyl in the hundreds of ppm levels, has the same effect as conventional retardants in the percent level. At the levels of concern, the effectiveness of $Fe(CO)_5$ can only arise from chemical effects. In the course of this work it became apparent that with iron carbonyl one may be approaching the natural limit to the amount of inhibition that can be caused by chemical effects. The present discussion will be therefore presented within this framework. In addition, this provides a basis for discussing the comparative analysis of relative suppression potential of metal-containing additives on flame propagation in gaseous systems. We will therefore also present some results based on published experimental determinations.

MECHANISMS FOR FLAME INHIBITION. The suppression of combustion through chemical inhibition arises from the lowering of the concentration of reactive radicals through scavenging reactions with the retardant. Inherent in this picture is not only the reaction of the radical with the scavenging species but also the regeneration of the latter, so that there is an amplifying effect [4]. Thus, effective inhibition mechanisms contain two important types of reactions: reactions scavenging chain carriers and those regenerating an inhibitor agent. A variety of analogous processes have been invoked to cover the action of chemicals such as HBr, NO, SO_2 etc. In all cases they involve catalytical cycles leading to the destruction of chain carriers.

These mechanisms illustrate the type of reactions that are needed for inhibition. The nature as well as the rate of the scavenging reaction is also of importance. In the case of bromine, it is a chain propagation step. Regeneration reactions can take the form of chain propagation ($Br + CH_2O = HCO + HBr$) or termination processes ($CH_3 + I + M = CH_3I + M$, $I + HO_2 = HI + O_2$). Generalizing from the above, we can write the simplest effective mechanism for inhibition in terms of the following two reactions: $X + In\ (+M) = InX\ (+M)$ and $X + InX = X_2 + In$, where X is the major chain carrier and In is the inhibiting species. Both scavenging and regeneration reactions are termination processes. Further simplification can

be brought about by noting that at atmospheric pressure, rates of termolecular reactions are usually much slower than for bimolecular processes. Therefore, the more effective cycle will be a cycle with bimolecular scavenging of chain carrier or X + In = InX. Obviously, the inhibitor must be inactive with respect to the other species in the system. Then if one assigns a collisional rate constant for these processes obviously any decrease in the calculated flame velocity will be the maximum achievable.

KINETIC MODELS AND CALCULATIONAL PROCEDURE. The Premix code of CHEMKIN Library was used in these calculations. The inhibitor efficiency was determined by modeling of its influence on the laminar burning velocity of premixed methane/air and hydrogen/air mixtures. The following cases are considered:

a. "Perfect" inhibitor model. H-atoms are scavenged and regenerated by the inhibitor in termination reactions with H, OH and O. For simplicity we assume that the rate constants are equal and they were varied from 10^{13} - $5x10^{14}$ $cm^3mol^{-1}s^{-1}$.

b. Model with inhibitor intermediate. This represents a means of increasing the effectiveness of the termolecular H + In + M = InH + M scavenging reaction by the two step reaction sequence [5]: In + CO (H_2O) + M = InCO (InH_2O) + M and H + InCO (InH_2O) = InH + CO (H_2O).

c. Iron pentacarbonyl inhibition model.

d. H-atom recombination model. The model includes only the overall reaction of H atom recombination with the inhibitor species as recombination catalyst. The overall rate constant, obtained experimentally in [6] for Cr atom as third body and assumed to be independent on temperature was used.

e-f. CF_3Br inhibition model and NO catalytical cycle were used for comparison purposes.

RESULTS AND DISCUSSION. Table 1 contains a summary of the results of calculations of the concentrations required to achieve 30% and 50% decreases in the flame velocity. Particularly interesting is the close match between the experimental results for $Fe(CO)_5$ and the "perfect" inhibitor model. In contrast and in accord with experimental observations CF_3Br is much less effective.

The concentrations of H, O and OH are related by partial equilibrium relationships in the flame zone. Thus, changing concentration of one species leads to changes in those for the other reactive components. Scavenging of various chain carriers does not lead to great changes in flame velocity. Thus the scavenging of H atoms is only 1.5 times more effective than that for O atoms. The S_u reductions when only H atom is scavenged and scavenging of all chain carriers (H,O,OH) are 19.5 and 23.5 cm/s respectively (methane flame, 100 ppm additive).

The regeneration properties of an inhibitor can be characterized a regeneration coefficient or the effective number of catalytical cycles involving the inhibitor in a flame zone [7]. The calculated regeneration coefficient for 100 ppm of "perfect" inhibitor is about 104.

Regeneration coefficients for HBr and HI are 7 and 3 for methane flame with 1% CF_3Br and CF_3I additives respectively. Thus a "perfect" inhibitor is one which is more effective in regenerating itself.

Modeling results for $Fe(CO)_5$ model indicate an underestimate of the experimental observations. It is clear that a reasonable adjustment of the rate constants can bring results into agreement. The use of overall reaction of H atom recombination on metallic atoms leads to approximately the same results as for iron pentacarbonyl. It is interesting that H atom recombination leads to a faster saturation than $Fe(CO)_5$ model due to quadratic dependence of scavenging rate on H atom concentration.

RELATIVE INHIBITION EFFECTIVENESS OF METALLIC COMPOUNDS. A relatively large volume of experimental data on the influence of different additives on burning velocities, flammability limits, extinction strain rates and others, for different fuel compositions can be found in literature. Probably the more reliable and representative data are the burning velocity measurements. For the purposes of this work the experimental data on influence of different additives on burning velocity of air/hydrocarbon mixtures are considered. As a first step the data on inhibitor influence on burning velocity have been collected and systemized.

The ranking of metallic inhibitors was established from measured burning velocity decrease brought about through addition of suppressants. It is assumed that there exist "some similarity" in influence of inhibitors on different hydrocarbon flames and for different values of equivalence ratios (i.e., ranking and relative influence are the same). The literature data are treated on a molar base and reduced to a "single" fuel system - stoichiometric methane/air mixture at ambient conditions, i.e., all experimental data are scaled by single fuel mixture composition. Data were estimated by using as benchmarks - burning velocities obtained for the same inhibitors in different systems. Where available the data used were obtained for relatively small concentration range of additives and in the range for burning velocity decreases down to 30%.

The considered compounds are mostly liquids or solids. The experimental results obtained for such compounds are also treated on the molar base. Analyzed experiments were carried out for fine mists or finely divided powders of inhibitors.

Figure 1 contains a summary of our preliminary results and includes metallic and nonmetallic compounds. Approximately 60% of presented results are based on "direct" experiments and the remaining 40% were deduced by estimates based on data obtained for "other conditions" (fuel system, an equivalence ratio). Figure 1 also provides a comparison of relative efficiency for different flame suppressants. The data are presented in the order of increasing of inhibitor efficiency. They show that metallic compounds containing Fe, Pb, and Cr are the most effective. Next in effectiveness are alkali compounds containing Rb, K and Na.

CONCLUSIONS. There is a natural limit to the extent that neutral ground state chemistry can contribute to flame inhibition. This is apparently in the 10 to 100 ppm level of additive for pronounced effect on the combustion processes. The experimental results for the metal systems suggest that they are very close to this limit. Thus it is not likely that one can obtain much more efficient inhibitors. An important consequence is that for these metal systems, it is highly unlikely that surface processes are making contributions. Concentration of particles must be lower than that of gas phase species.

Results on ranking of metallic flame suppressants indicate that the high effectiveness of metallic compounds is primarily due to the presence of a metallic atom in the molecule of inhibitor compound. The organic ligands may not be of primary importance. There is considerable support for a gas phase mechanism of inhibition by metallic compounds. Condensation processes set a limit to the concentration of metallic species in the gas phase. Therefore, a decrease of metallic inhibitor influence is observed with increasing concentration. Two limitations are observed for chemical influence: 1) saturation of chemical influence [7], and 2) saturation due to condensation processes. Thus, we have a "natural" limit for quantity of "super" agents in a gas phase for practical applications. It may be necessary to use several agents to arrive at the desired flame suppression.

References

1. Lask, G., Wagner, H., Gg. 8-th (Int.) Symp. on Combustion, 1960, pp.432-438.
2. Bonne, U., Jost, W., and Wagner, H.Gg. Fire Research Abstracts and Reviews, 4:pp.6-18 (1962).
3. Reinelt, D., Linteris, G.T. 26th Symposium (Int.) on Combustion, 1996.
4. Day, M.J., Stamp, D.V., Thompson, K., Dixon-Lewis, G. 13-th Int.Symp.on Combustion, 1971, pp.705-711.
5. Iya, K.S., Wollowitz, S., Kaskan, W.E. 15-th Symposium (Int.) on Combustion, 1975, pp.329-336.
6. Bulewicz, E.,M., Padley, P., J. 13th Symposium (Int.) on Combustion, 1971, pp.73-80.
7. Noto, T., Babushok, V., Hamins, A., Tsang, W. Combustion and Flame, 1997, in press.

Table 1.

Inhibitor Concentration Required for 30 and 50 % Decreasing of Burning Velocity for Different Models and Experimental Data. Stoichiometric Air/Methane Flame, 1 atm

Model and Experimental Data	Parameter	Inhibitor, ppm	
		30 %	50 %
Perfect inhibitor model	$5x10^{13}$ 10^{14} $2x10^{14}$	100 50 30	200 110 60
Inhibitor-reaction intermediate (10^{16}, 10^{14})	InCO InH_2O	2700 700	3500 1000
$Fe(CO)_5$ model		400	800
Overall rate of H recombination		200	750
CF_3Br model		5000	10000
NO cycle		60000	> 60000
Experiment, [2] $Fe(CO)_5$ additive*		120	200
Experiment, [3] $Fe(CO)_5$ additive*		70	130

* The data are obtained by linear extrapolation from experimental results.

Figure 1. Additive Effectiveness for Various Elements

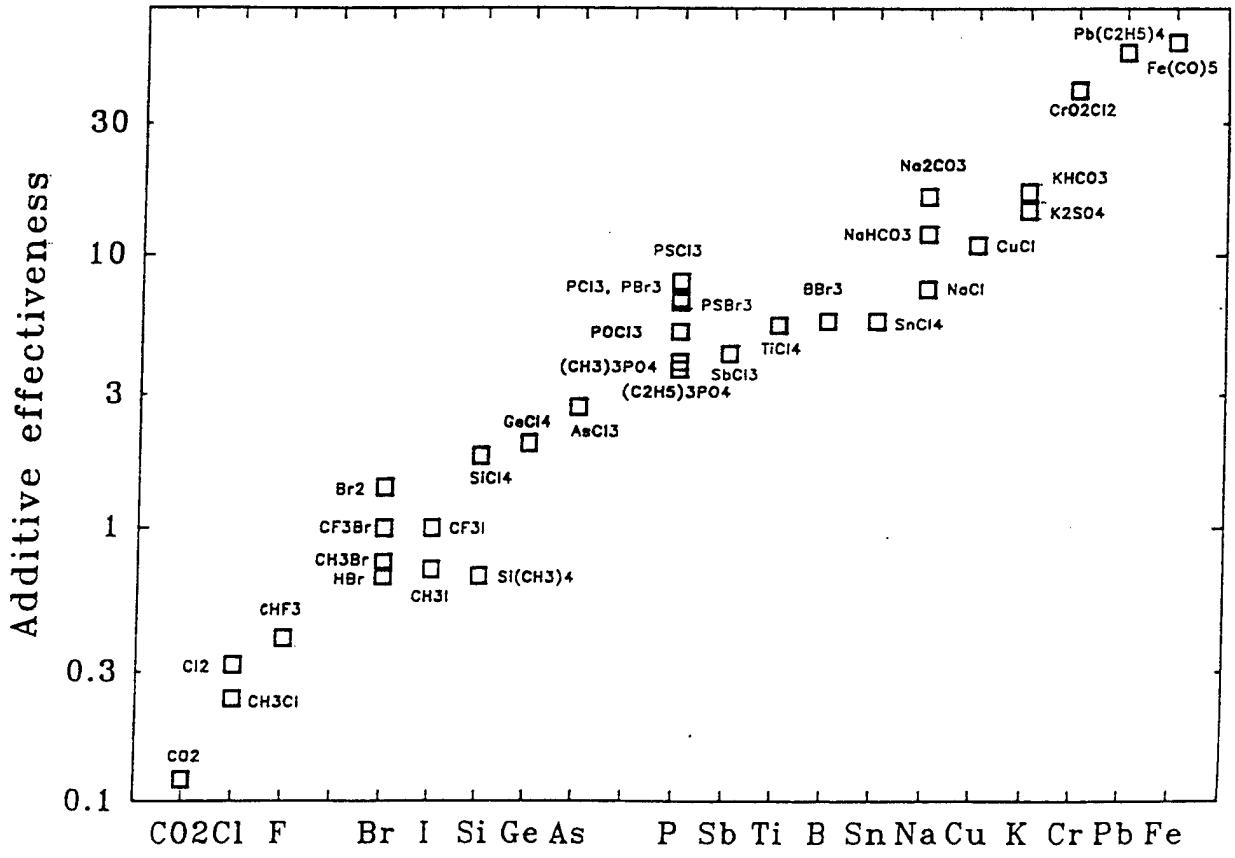

Predicting Kinetics, Dynamics, and Mechanisms of Gas-phase Polyatomic Reactions from First Principles: A Practical *Ab Initio* Direct Dynamics Methodology

Thanh N. Truong

Department of Chemistry, University of Utah, Salt Lake City, UT 84112
tel: (801) 581-4301; fax: (801) 581-8433
email: truong@mercury.chem.utah.edu

The need for accurate rate constants is growing rapidly as advances in the areas of computational fluid dynamics and process simulation require more accurate kinetic models. For this reason, predicting rate constants has been a major goal of theoretical chemistry. However, it also has been a challenge particularly for polyatomic reactions for the following reasons. The conventional approach of reactive dynamical calculations using either the full quantal dynamics, classical or semiclassical trajectory method, or variational transition state theory (VTST) requires the availability of an accurate analytical potential energy function (PEF). Developing such a potential energy function is not a trivial task and is a major obstacle for the dynamical study of a new reaction despite the steady improvement in computer speed. This is because; i) the explicit functional form for a potential energy function is somewhat arbitrary and mostly depends on the investigator's intuition, ii) fitting this functional form to a set of *ab initio* energy points and any available experimental data is tedious and yet does not guarantee convergence or correct global topology, iii) the number of energy points needed grows geometrically with the number of geometrical internal coordinates. As the system size increases, this task becomes much more complex if it can still be accomplished at all. Thus, developments of new methodologies for studying dynamics, kinetics and mechanisms of large polyatomic reactions are of great interest.

Direct dynamics methods such as those being developed in our lab [1]offer a viable alternative for studying chemical reactions of complex systems. In the direct dynamics approach, all required energies and forces for each geometry that is important for evaluating dynamical properties are obtained directly from electronic structure calculations rather than from empirical analytical force fields.

We focus only on our recent contributions to the development of *ab initio* direct dynamics methods in which no experimental data other than physical constants were used for calculating thermal rate constants of gas-phase polyatomic reactions. The dynamical method is based on full VTST theory plus multi-dimensional semiclassical tunneling corrections. Potential energy information needed includes geometries, energies, gradients, and Hessians at the stationary points and along the minimum energy path. In our approach, these quantities are obtained directly from *ab initio* electronic structure

calculations, thus no fitting is involved. For quantitative predictions of kinetic properties, the potential energy surface must be adequately accurate. If such information is to be calculated from a sufficiently accurate level of *ab initio* molecular orbital theory, the computational demand can be substantial. In this case, these methods are only useful for small systems such as the $OH + H_2$ hydrogen abstraction reaction, and thus they stop short of our goal. To alleviate this difficulty, we have introduced three new advances. First is a focusing technique or an adaptive grid method in which more computational resources are spent on regions that are most sensitive to the dynamics and less resources elsewhere. This allows one to obtain an optimal accuracy with a minimum computational cost at a given level of theory. Second is the use of a computationally less demanding electronic structure method, density functional theory (DFT), for the computationally most expensive step required for rate calculations namely calculations of Hessians along the minimum energy path. We found that the hybrid Becke half-&-half exchange with Lee-Yang-Parr correlation (BH&H-LYP) functional yields geometries and frequencies along the reaction coordinate in excellent agreement with accurate QCISD calculations. Enegetics information sometimes required more accurate *ab initio* single-point calculations. The third advance is the energy interpolation technique that allows a minimum number of such single-point calculations. These advances are parts of the TheRate program[13] which is available to any interested research group.

To illustrate the applicability, accuracy and versatility of this direct *ab initio* dynamics approach, we present different applications. A more detailed discussion is given to the hydrogen abstraction $CH_4 + H <\!\!\longrightarrow CH_3 + H_2$ reaction. It is because this reaction has served as a prototype reaction involving polyatomic molecules and has played an important role in the theoretical and experimental developments of chemical kinetics. In addition, it has an intrinsic importance to combustion kinetics and is of fundamental interest to organic reaction mechanisms. For this reason, ample experimental rate data is available for comparison. Also this reaction is small enough so that accurate *ab initio* MO calculations can also be performed to test the accuracy of DFT methods. Other applications such as for the $H + HCF_3$ and $Cl + CH_4$ reactions will be discussed briefly.

Finally, we present our recent work on the development of rate theory for reaction class. The reactions in a class have the same reactive moiety thus share similiarities in the shape of the potential energy surfaces. By exploring such similarities, we propose to transfer several reaction path information of the parent reaction, the smallest one in the class, in calculations of reaction rates of larger reactions belonging to that class. This significantly reduces the computational cost. Accuracy of this methodology is examined.

References

[1]G. C. Schatz, *Rev. Mod. Phys.* **61,** 669 (1989).

[2]*Potential Energy Surfaces and Dynamics Calculations*, Vol. , edited by D. G. Truhlar (Plenum, New York, 1981).

[3]D. G. Truhlar, M. S. Gordon, and R. Steckler, *Chem. Rev.* **87,** 217 (1987).

[4]T. N. Truong, *J. Chem. Phys.* **100,** 8014 (1994).

[5]T. N. Truong and W. T. Duncan, *J. Chem. Phys.* **101,** 7408 (1994).

[6]T. N. Truong and T. J. Evans, *J. Phys. Chem.* **98,** 9558 (1994).

[7]T. N. Truong, *J. Chem. Phys.* **102,** 5335 (1995).

[8]R. Bell and T. N. Truong, *J. Chem. Phys.* **101,** 10442 (1994).

[9]W. T. Duncan and T. N. Truong, *J. Chem. Phys.* **103,** 9642 (1995).

[10]L. R. Bell and T. N. Truong, *J. Phys. Chem.* , in press (1997).

[11]R. L. Bell, D. L. Taveras, T. N. Truong, and J. Simons, *Int. J. Quantum Chem.* **63,** 861 (1997).

[12]T. N. Truong, W. T. Duncan, and R. L. Bell, in *Chemical Applications of Density Fucntional Theory*, Vol. 629, edited by B. B. Laird, R. B. Ross, and T. Ziegler (American Chemical Society, Washington DC, 1996), p. 85.

[13]T. N. Truong and W. T. Duncan, TheRate. More information is available on the web at http://www.chem.edu/mercury/therate/therate.html., *Revision* 1.0, (Univeristy of Utah, Salt Lake City, 1996)

Computer tools for complex reactions modelling

Guy-Marie Côme

Département de Chimie Physique des Réactions, CNRS, INPL-ENSIC,
Université H. Poincaré, 1, rue Grandville, NANCY, FRANCE
tel: (33) 3 83 17 50 06; fax: (33) 3 83 37 81 20
email: come@dcpr.ensic.u-nancy.fr

Reaction models of hydrocarbon combustion are needed for simulating laboratory and field-scale experiments on chemical inhibition, vessel inerting, and fire extinguishing by halon replacements.

A flowchart of NANCY system for creating detailed reaction models is shown in Figure 1. The C_0-C_1-C_2 reaction base includes 781 elementary reactions involving as reactants 42 molecules and free radicals containing up to two carbon atoms. The generation of detailed primary mechanisms is achieved by means of generic reactions (Figure 2), which are activated or not, according to kinetic rules defined by the chemist: the system works as an expert. Primary products having the same molecular formula and the same functional groups are lumped into one single species. A lumped secondary mechanism is generated using the rules summarized in Figure 3: the reactants are the lumped primary products, and the secondary products are species of the C_0-C_2 reaction base. Thermochemical data of molecules and free radicals are estimated by means of a software (THERGAS) based on BENSON's method. Kinetic data are computed either using BENSON's thermochemical kinetics or by means of quantitative structure-reactivity relationships. The reaction model and the associated numerical data are provided in a format ready for use for CHEMKIN simulations.

In order to reduce the size of the detailed primary mechanism, a lumping of primary free radicals can be achieved as shown in Figure 4. Lumped rate constants are computed by means of quasi-stationary state approximation.

Our system has been validated against experimental results obtained for paraffins and iosparaffins ranging from methane to decane. Work in progress is oriented towards cyclanes reactions.

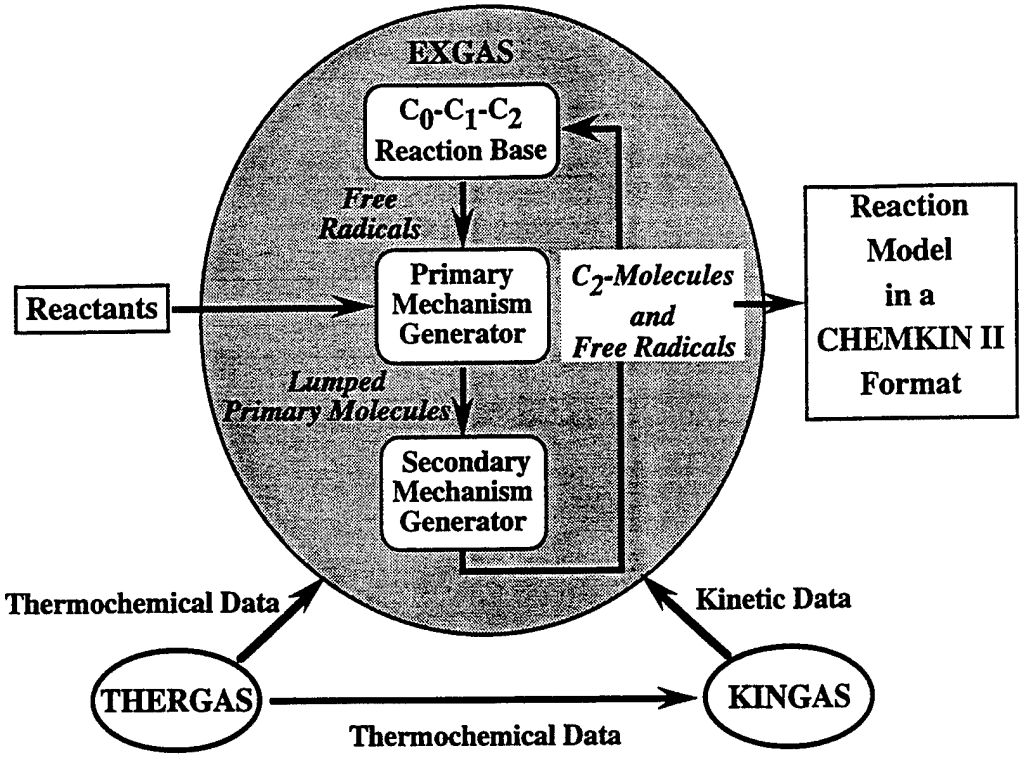

Fig. 1 - Flowchart of NANCY System

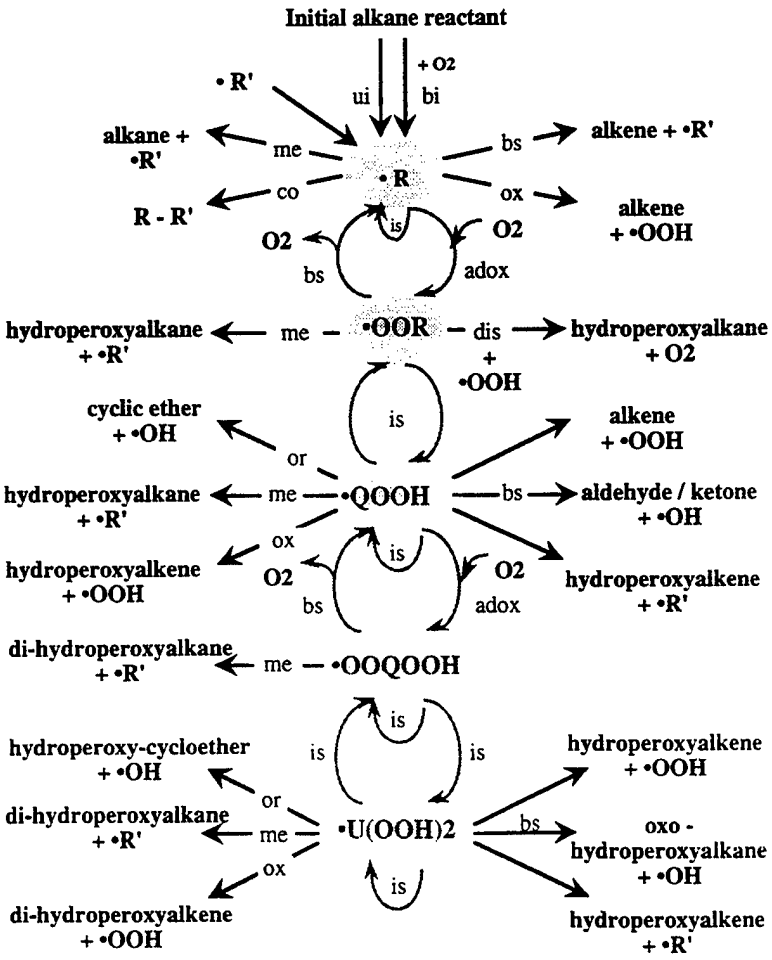

Fig. 2 -Primary mechanism

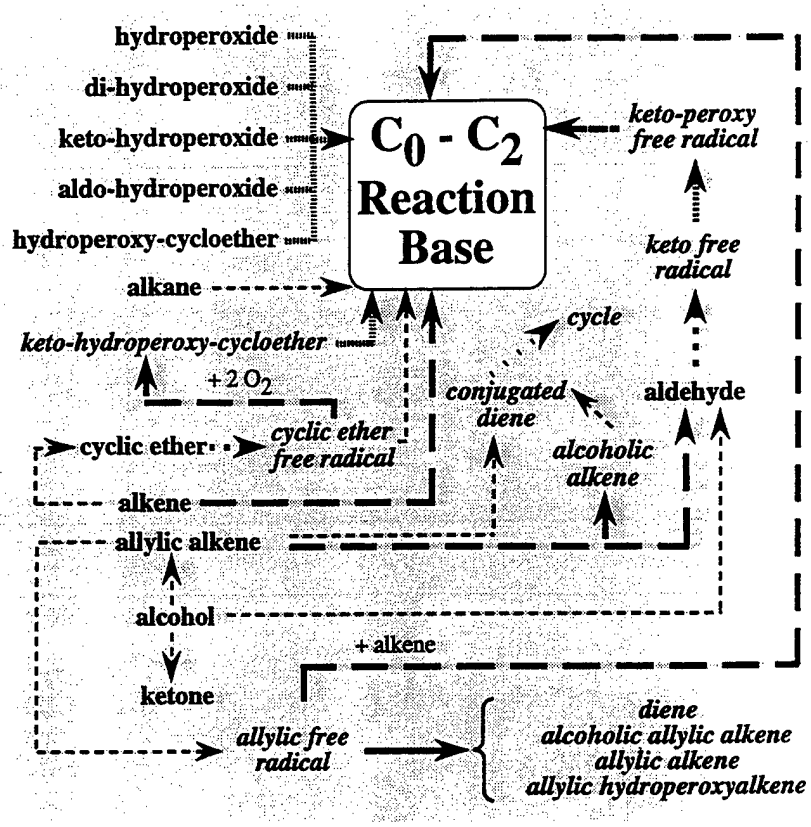

Fig.3 - Secondary mechanism

$$\cdot XY + O2 \xrightarrow{k1} \cdot O{-}O{-}XY$$

$$\dot{X}Y + O2 \xrightarrow{k2} \overset{O-O\cdot}{XY}$$

$$XY\cdot + O2 \xrightarrow{k3} XY_{O-O\cdot}$$

$$XY^{\cdot} + O2 \xrightarrow{k4} XY{-}O{-}O\cdot$$

$$\cdot C8H17 + O2 \xrightarrow{kL} \cdot (O{-}O)C8H17$$

$$kL = \frac{\Sigma\, ri\, ki}{\Sigma\, ri}$$

ri : quasi - stationary state rate of i^{th} reaction

Fig.4 - Lumped primary reactions

IV. D. Conclusions: Current Status and Future Directions

1. There has been considerable progress in experimental and computational characterization of elementary reaction rate constants and thermochemistry needed for modeling the behavior of flame suppressants. There is generally good agreement between both approaches and the combination of the two will be required to optimize the performance of the new generation of fire suppressants. Discarded agents (CF_3Br) and discounted agents (CF_3I) should still be studied to pin down mechanisms of action and their limitations.

2. Present computational approached are sufficiently accurate to yield thermochemical and kinetic data useful for preliminary modeling of combustion inhibition. However, more efficient methods must be developed for predicting rate constants for reactions without barriers, such as radical recombinations. Chemically activated association /decomposition accounts for much of halogen chemistry in flames (*e.g.* $H + C_2F_5$ ® $HF + C_2F_4$ *via* chemically activated C_2HF_5). Entrance channels and competing exit channels are frequently radical combinations, but full evaluation of rate constants by variational transition state theory is not yet a routine calculation. We must develop a proper treatment of anharmonic modes in quantum chemistry predictions of thermochemistry. The most prominent problem remaining for accurately predicting thermochemistry is the treatment of hindered internal rotors: identification, asymmetries, and barriers to rotation. Work reported at this meeting by Bernie Schlegel appears to be a big step towards fixing this problem, which presently can cause serious problems in entropy, specific heat, and rate constant predictions.

3. Newly developed theoretical methods offer the opportunity for computations at chemical accuracy. These methods will provide an important supplement to experiments. The bond energy and enthalpy requirements for the ideal hydrogen trap should be determined and compared to the properties of all available materials. Among the halogens, molecules that deliver Br appear to be close to this ideal. Nevertheless, Valeri Babushok's analysis made the point persuasively that homogeneous catalytic cycles can only reduce the radical pool down to an equilibrium mixture, which is still adequate at high temperatures to carry on combustion. Radical traps and temperature reducers are then more clearly necessary parts of the solution. Metal atom catalysis and stable high heat capacity agents appear promising. Petersson suggested that FeBr3 might combine the advantages of PBr_3 with those of $Fe(CO)_5$.

4. Many species and reactions remain to be characterized, especially for understanding high-efficiency next-generation suppressants based on metallic and labile-bromine compounds. Joe Bozzelli emphasized the need for additional data on both the thermochemistry of flame components and the temperature dependence of the rate constants for the chemical reactions.

5. Global reaction mechanisms are becoming increasingly sophisticated. Sensitivity analysis must be applied to identify the most important steps. The coupling of chemical reactions with fluid flow is critical for consideration of 'real life' applications. More detailed comparisons must be made between theory and experiment regarding the spatial composition and temperature variations for flames, so that improved computer models can be developed. Reduction schemes must be applied to chemical mechanisms to obtain practical models for analysis of complex flow patterns.

6. Innovative delivery systems will probably be as important as the new fire suppressants.

7. It is becoming more and more obvious that evaluation of practical efficiency, health effects, and environmental effects must be tied in at an earlier stage. Communications with project managers must be improved so that the agents we develop are in fact suitable for the intended use. Engineers and scientists must learn to collaborate more extensively. A variety of fire suppressants, each optimized for a specific application would provide optimum protection for Air Force personnel. Toxicity screening must be moved to an earlier stage of development.